

DISSERTATION

MEIOTIC RECOMBINATION AND SYNAPSIS IN
WILD-TYPE AND ASYNAPTIC MUTANTS OF
TOMATO (*SOLANUM LYCOPERSICUM*)

Submitted by

Huanyu Qiao

Department of Biology

In partial fulfillment of the requirements

For the Degree of Doctor of Philosophy

Colorado State University

Fort Collins, Colorado

Fall 2010

Doctoral Committee:

Department Chair: Daniel Bush

Advisor: Lorinda Anderson

Co-advisor: Stephen Stack

Pat Bedinger

Rajinder Ranu

ABSTRACT

MEIOTIC RECOMBINATION AND SYNAPSIS IN WILD-TYPE AND ASYNAPTIC MUTANTS OF TOMATO (*SOLANUM LYCOPERSICUM*)

Recombination nodules (RNs) and synaptonemal complexes (SCs) are meiosis-specific structures that play important roles in crossing over. During pachytene, RNs mark crossover sites along SCs. MLH1, a mismatch repair protein, promotes crossing over and is a component of most RNs. In wild-type tomato, each bivalent has one, two or three crossovers (=chiasmata), and the number and distribution of these crossovers is affected by crossover interference (the tendency for one crossover to reduce the likelihood of another crossover nearby). Although the phenomenon of genetic interference was discovered nearly one hundred years ago, its molecular basis is still unknown. SCs occur between pairs of homologous chromosomes (bivalents) during prophase I and consist of two parallel rod-like lateral elements held together by transverse fibers. Each lateral element is associated with the two sister chromatids of one of the homologous chromosomes. Cohesin complexes consisting of four proteins (SMC1, SMC3, SYN1/REC8 and SCC3) are found in lateral elements and link sister chromatids together. My research addressed the question of how synapsis (SC formation) is related to the frequency and control of crossing over using tomato, particularly the *as1* meiotic mutant, as a model system. Meiocytes from tomato plants homozygous for the mutation *as1* do not complete chromosome synapsis and have

few chiasmate bivalents, resulting in unbalanced chromosome segregation and sterility. We found a severe delay of prophase I in the *asI* mutant compared to wild-type tomato using an *in vivo* BrdU labeling method, which may be related to the asynaptic phenotype. The asynapsis and delay in the *asI* mutant are not likely to be due to a defect in the early steps of recombination, since the frequency and distribution of early recombination proteins (MRE11, RAD50, and RAD51) are similar in wild-type and in the *asI* mutant. EM immunolabeling demonstrated that MLH1, a late recombination protein, is present in a subset of RNs in *asI*, an observation similar to that in wild-type. However, RNs in *asI* are larger than those in wild-type. Previous work by other researchers showed a normal level of crossovers in several genetic intervals of the *asI* mutant, which was unexpected based on the high degree of asynapsis observed at the cytological level. To evaluate crossing over in the *asI* mutant, we examined the immunolabeling patterns of MLH1 foci that mark crossover sites. In *asI* meiocytes, we observed that most MLH1 foci were associated with SC segments between two homologous chromosomes. We found that the number of MLH1 foci per micrometer is higher in the *asI* mutant compared to wild-type. In addition, interference between MLH1 foci was lower in the mutant than in wild-type tomato. The weakened genetic interference in the *asI* mutant may be due to a defect of the medium of interference, since early events of the recombination pathway in *asI* seem normal, and MLH1 foci representing crossovers, the last step of the recombination pathway, are still present in the mutant. A good candidate to transmit interference is the cohesin complex that makes up a part of lateral elements. Compared to wild-type, we observed reduced immunofluorescence for the cohesins SMC1, SYN1, and SCC3, but not SMC3 in the *asI* mutant. Although we do not yet know the specific mutation of *asI* in tomato, we have shown that the asynaptic phenotype is accompanied by alterations in cohesin proteins in AE/LEs and in the

distribution of MLH1 foci compared to wild-type. To our knowledge, this is the first report of an association between cohesin proteins and crossover interference regulation in any organism. This discovery represents a significant advance in our efforts to understand the molecular basis of crossover interference.

ACKNOWLEDGEMENTS

I thank my uncles, my aunt, my sister, my cousins, and my friends for encouraging my education. I especially thank my loving parents for moral and financial support throughout my undergraduate and graduate school. I am deeply indebted to Dr. Lorinda Anderson and Dr. Stephen Stack for their guidance, encouragement, and friendship. I also owe a great debt of gratitude to the members of my graduate committee and my lab members. I would not be able to succeed without their support. This work was supported by a grant to Dr. Lorinda Anderson from the National Science Foundation (MCB-064344).

TABLE OF CONTENTS

CHAPTER 1 GENERAL INTRODUCTION.....	1
<u>Meiosis and Sex</u>	1
<u>Homologous Chromosome Pairing and the Bouquet</u>	3
<u>Synaptonemal complex</u>	6
<u>Recombination nodules</u>	17
<u>DNA Double-Strand-Break (DSB) Repair Model for Meiotic Recombination</u>	19
<u>Correspondence between recombination-related proteins and recombination nodules</u>	27
<u>Crossover interference</u>	28
<u>Models for crossover interference</u>	30
<u>Tomato as a model system for cytogenetic study of meiotic recombination</u>	33
<u>Tomato meiotic mutants</u>	34
<u>Project outline</u>	38

CHAPTER 2 SEQUENTIAL LOADING OF COHESIN PROTEINS DURING PROPHASE I IN TOMATO PRIMARY MICROSPOROCTES.....	40
<u>Introduction</u>	40
<u>Materials and Methods</u>	44
<u>Results</u>	45
<u>Discussion</u>	56
CHAPTER 3 <i>In vivo</i> BrdU LABELING METHOD TO STUDY THE MEIOTIC TIME- COURSE IN TOMATO POLLEN MOTHER CELLS.....	63
<u>Introduction</u>	63
<u>Materials and Methods</u>	65
<u>Results</u>	69
<u>Discussion</u>	75
CHAPTER 4 ALTERED INTERFERENCE AMONG MLH1 FOCI IS ASSOCIATED WITH CHANGES IN COHESIN PROTEINS IN TOMATO MEIOTIC MUTANT <i>asl</i>	79
<u>Introduction</u>	79
<u>Materials and Methods</u>	83
<u>Results</u>	85
<u>Discussion</u>	108

CHAPTER 5 GENERAL DISCUSSION.....	119
<u>Findings and significance of this study</u>	119
<u>A model for crossing over and genetic interference in tomato</u>	120
<u>Directions for further research</u>	122
REFERENCES.....	123

CHAPTER 1:

GENERAL INTRODUCTION

I. Meiosis and Sex:

Meiosis is a process in which one round of DNA replication is followed by two successive cell divisions to produce four genetically different, haploid, daughter cells. In the first division (Meiosis I), the chromosome number is reduced from diploid to haploid when homologous chromosomes separate. This unique, reductional division occurs only during Meiosis I. The second division (Meiosis II) is essentially the mitotic division of a haploid cell when sister chromatids separate. In animals, one (egg) or all (sperm) of the meiotic products will become gametes. In plants, the haploid cells resulting from meiosis form spores that will divide to form multicellular mega-gametophytes and micro-gametophytes that contain eggs and sperm, respectively. During sex (fertilization), gametes fuse to form a new diploid cell called a zygote. The zygote will divide by mitosis and grow and develop into a new individual.

Meiosis and sex alternate as two complementary processes in the life cycles of most multicellular eukaryotes. The two processes generate genetically distinct individuals within a population due to three important factors: crossing over, independent assortment and fertilization. Crossing over is the exchange of DNA fragments between two homologous chromosomes and results in a change of the genetic composition of the chromosomes compared to the parents. Crossing over is also important to link the two homologs to ensure reductional segregation of homologous chromosomes at anaphase I. Without at least one crossover, the two homologous chromosomes may segregate to the same pole, leaving one daughter cell with two

copies of the chromosome while the other daughter cell has no copies of it. This process, called non-disjunction, leads to unbalanced chromosome sets as in Down syndrome (trisomy 21).

Another source of genetic variability is independent assortment of homologous chromosomes (also called Mendel's Second Law). Independent assortment refers to the fact that each pair of homologous chromosome align at the metaphase I plate and then separates from its partner at anaphase I without regard to how the other pairs of homologs separate. Independent assortment is even more important than crossing over for changing the genetic makeup of cells. Finally, the random nature of fertilization, *i.e.*, which sperm fertilizes which egg, also contributes to genetic variation. Genetic variability among individuals in a population is an important factor in the ability of the population to adapt to changing environmental conditions. Individuals with favorable genetic combinations are more likely to survive and leave more offspring than individuals with less favorable combinations. Thus, the population evolves in response to environmental changes.

Events that occur during Prophase I are responsible for the exceptional nature of meiosis I. Prophase I is divided into five substages that are defined based on changes in chromosome behavior and morphology (Moses 1968; John 1990). More recently, the molecular events occurring during these stages have begun to be deciphered (Roeder 1997; Zickler and Kleckner 1998; Villeneuve and Hillers 2001; Page and Hawley 2003). The first stage of Prophase I is leptotene (leptos = fine, tene = thread, Greek), and individual chromosomes begin to condense into long thin threads. A protein core, called an axial element (AE), is present between the two sister chromatids of each chromosome. During leptotene, meiotic recombination begins with the programmed formation of numerous DNA double strand breaks (DSBs) throughout the genome. DSB formation is important to facilitate alignment between homologous chromosomes in many

organisms including budding yeast, animals, and plants (Zickler and Kleckner 1999; Page and Hawley 2004). Zygotene (zygon = couple, Greek) comes next. During zygotene, a special structure called the synaptonemal complex (SC) begins to form between paired homologous chromosomes (= bivalents) in a process called synapsis. The SC is an evolutionarily conserved, proteinaceous structure (Moses 1968; Zickler and Kleckner 1999; Page and Hawley 2004) that will be discussed in more detail below. The next stage, pachytene (pachy = thick, Greek), is defined as the stage when homologous chromosomes are completely synapsed with an SC along their entire length. Several important steps of meiotic recombination occur during zygotene and pachytene including resolution/repair of each DSB either as a non-crossover (the large majority) or a crossover. Pachytene is followed by diplotene (diplos = double, Greek). The SC begins to come apart during diplotene in a process called desynapsis. The two homologous chromosomes remain together at crossover sites that are now visible as chiasmata, but the two homologs separate elsewhere along their length. Chromosomes continue to shorten progressively through all these substages to the last substage of prophase I, diakinesis, when the chromosomes are the shortest before nuclear envelope breakdown. Kinesis means movement in Greek.

Pairing, synapsis, and crossing over between homologous chromosomes are unique events that make prophase I longer and more complicated than mitotic prophase. These events also establish physical links between bivalents that are required for correct segregation of homologous chromosomes during anaphase I.

II. Homologous Chromosome Pairing and the Bouquet

Chromosomes pair with their homologous counterparts before synapsis and SC formation. An outstanding question of meiosis is how do homologous chromosomes recognize each other? At least two types of homologous pairing can be distinguished in different

organisms, recombination-dependent and recombination-independent (Page and Hawley 2003). This distinction is most obvious in *spo11* mutants. Spo11 was first discovered in budding yeast and it is a meiosis specific enzyme that generates DSBs through a topoisomerase II-like transesterification reaction (Keeney et al. 1997; Bergerat et al. 1997; Keeney 2001). Programmed DSB formation by Spo11 marks the initiation of meiotic recombination in most organisms. Mutation of *SPO11* causes synaptic defects in a number of organisms including fungi (Giroux et al. 1989; Loidl et al. 1994; Celerin et al. 2000), mammals (Baudat et al. 2000), and plants (Grelon et al. 2001). However, mutations of *SPO11* do not disrupt meiotic synapsis in two invertebrates, *Drosophila melanogaster* and *Caenorhabditis elegans* (McKim et al. 1998; Dernburg et al. 1998; McKim and Hayashi-Hagihara 1998). Possibly, meiotic pairing in these species is related to the side-by-side alignment of homologous chromosomes in somatic cells from *Drosophila* (Page and Hawley 2003). Bhalla and Dernburg (2008) have also suggested that bouquet formation and interaction between heterochromatic regions of bivalents during meiosis may be sufficient to allow stable interaction and pairing between homologous chromosomes in these organisms. It is possible that the bouquet and heterochromatin interactions are involved in homologous chromosome alignment in all organisms, but if so, DSB formation is critical for the final establishment of homologous synapsis in recombination-dependent organisms (Bhalla and Dernburg 2008). Supporting this hypothesis are observations that *spo11* mutants in budding yeast and *Coprinus cinereus* still retain some homologous pairing associations even though synapsis is disrupted (Loidl et al. 1994; Celerin et al. 2000). Other DNA processing steps after DSB induction such as end resection involving proteins of the MRE11 complex (MRE11, RAD50 and XRS2/NBS1) and single end invasion (SEI) are also important for pairing and synapsis in recombination-dependent organisms (Alani et al. 1990; Nairz and Klein 1997;

Gerecke and Zolan 2000; Peoples et al. 2002; Peoples-Holst and Burgess 2005; Cherry et al. 2007). Mutation of the *PHS1* gene also causes abnormal chromosome associations in maize and Arabidopsis due to a defect in importing Rad50 protein into nuclei (Pawlowski et al. 2004; Ronceret et al. 2009). Although recombination and synapsis are clearly inter-related in many organisms, significant questions remain as to the mechanisms by which chromosomes pair and synapse homologously during meiosis.

The bouquet has also been suggested to have a role in homologous chromosome alignment (Moses 1968; Scherthan and Schönborn 2001; Hamant et al. 2006). The name bouquet refers to the similarity in appearance of a bouquet of cut flowers to the configuration of chromosomes. The bouquet forms at the leptotene/zygotene transition when the ends of all the chromosomes become attached to the inner surface of the nuclear envelope then cluster together in one part of the nucleus. Actin is required for the telomere clustering (Scherthan et al. 1996; Cowan and Cande 2002; Cowan et al. 2002; Scherthan et al. 2008). Synapsis between homologous chromosomes usually begins near telomeres, and the bouquet may promote synapsis by bringing all telomeres together in a small region of the nucleus and making it easier for homologs to find one another (Moses 1968; Loidl et al. 1994). Indeed, experimental evidence supporting this idea has come from studies of *ndj1/tam1* (*nondisjunction 1; telomere-associated meiotic protein 1*) mutants in budding yeast and *pam1* (*plural abnormalities of meiosis 1*) mutants in maize (Conrad et al. 1997; Chua and Roeder 1997; Golubovskaya et al. 2002). *Ndj1* is a meiosis-specific, telomere-associated protein. A null mutation of *ndj1* disrupts both attachment and clustering of telomeres and is associated with a delay in AE and SC formation (Conrad et al. 1997; Chua and Roeder 1997; Trelles-Stricken et al. 2000). A reduction in crossover interference has also been observed in these mutants. In the maize *pam1* mutant,

telomere attachment and clustering occur at the leptotene/zygotene transition, but instead of a single, tight cluster of telomeres as observed in wild type cells, the *pam1* mutant has only small clusters of telomeres and a loose bouquet (Golubovskaya et al. 2002). Both incomplete and non-homologous synapsis have been observed in the *pam1* mutant, indicating the important role of the bouquet in efficient homologous synapsis (Harper et al. 2004). However, the presence of a bouquet does not guarantee homologous chromosome pairing and synapsis as observed for haploid rye (that forms SCs even though there is no homolog present - Santos and Jimenez 1994), *spo11* and *rad50S* mutants in budding yeast (Trelles-Sticken et al. 2005) and asynaptic *as1* and *asb* mutants in tomato (Havekes et al. 1994) still have bouquets. In addition, dipterans, like *Drosophila*, do not form a bouquet, perhaps related again to the pairing of homologs in somatic cells (McKee 2004). The link between bouquet formation and homologous chromosome pairing therefore remains unclear (Scherthan et al. 2008).

III. Synaptonemal complex

The synaptonemal complex (SC) was originally identified in spermatocytes from crawfish and vertebrates by Moses (1956) and Fawcett (1956). Since then, the SC has been observed in almost all prophase I cells from sexually reproducing organisms with only a few exceptions including fission yeast (*Schizosaccharomyces pombe*), *Aspergillus nidulans* and male *Drosophila melanogaster* (Zickler and Kleckner 1999). The SC is a highly conserved physical structure, although its molecular components are less well conserved (Zickler and Kleckner 1999; Page and Hawley 2004).

The SC is a proteinaceous, ladder-like structure composed of three parts: two lateral elements (LEs), a central element (CE), and transverse filaments (TFs) that connect the lateral

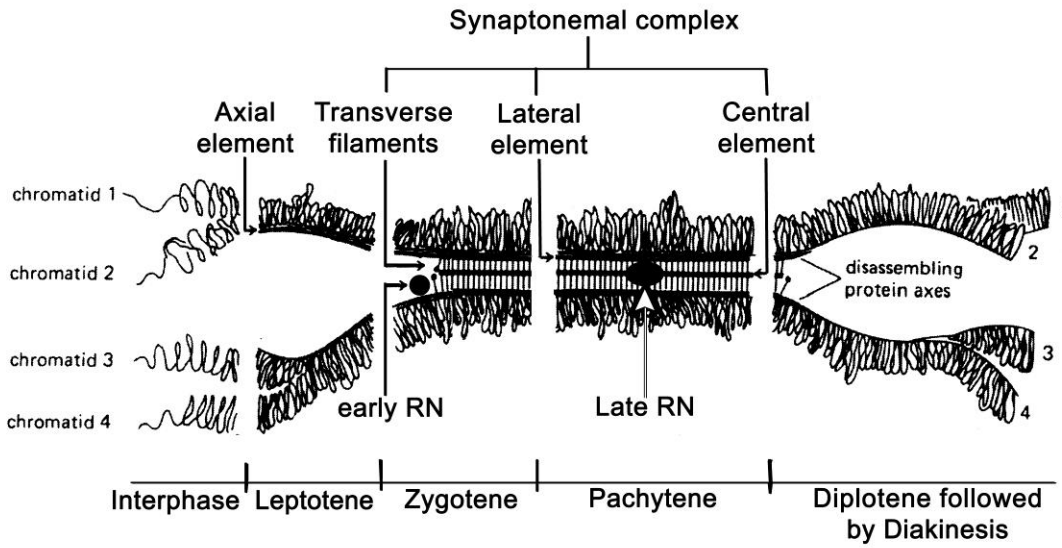


Figure 1a. Diagram of meiotic stages shows synaptonemal complex behavior [modified after (Heyting 1996)].

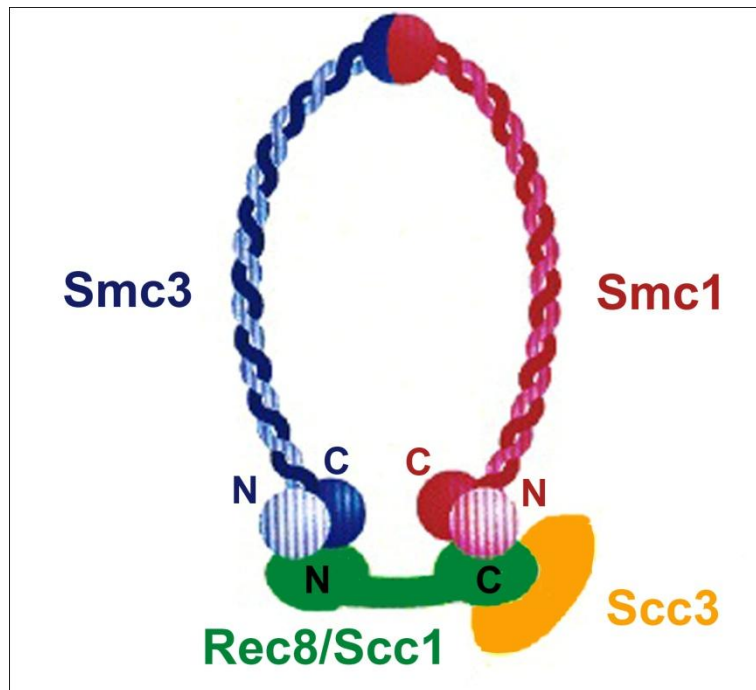


Figure 1b. Model of sister chromatid cohesion complex [modified after (Petronczki et al. 2003)].

and central elements (Figure 1a). Prior to SC formation, the lateral elements are called axial elements (AEs). At leptotene, an AE forms between each pair of sister chromatids and extends along the length of each homologous chromosome. At the onset of zygotene, the central element and transverse filaments begin to polymerize between AEs of two homologous chromosomes. TFs lie perpendicular to and connect the longitudinally-oriented lateral elements and central element. After SCs zipper up along the whole bivalent length, meiotic cells enter the stage of pachytene.

Some of the protein components of SCs and proteins that interact with SC components have been identified in several organisms (Table 1).

A. Axial (lateral) element components

1. Cohesin proteins

Proteins that are involved in sister chromatid cohesion (SCC) play an important role in AE formation. Sister chromatid cohesion during meiosis involves four protein components: SMC1, SMC3, REC8, and SCC3 (Nasmyth 2002; Petronczki et al. 2003; Nasmyth and Haering 2009). Two of the proteins, SMC1 and SMC3, belong to the structural maintenance of chromosomes (SMC) group of proteins that function in chromosome dynamics (Jessberger et al. 1998; Jessberger 2002). SMC proteins have two coiled-coil domains separated by a hinge domain and globular domains at N- and C-termini (Figure 1b). Each SMC protein folds back on itself at the hinge and the two coiled-coil domains interact and form an extended 45-nm rod-like structure while the N- and C-terminal domains interact to form a globular ATPase “head” opposite the hinge. In a cohesin complex, SMC1 and SMC3 proteins interact at their hinge domains to form a V-shaped heterodimer. The non-SMC cohesin proteins, REC8 (a member of the kleisin family of proteins) together with SCC3, link the heads of SMC1 and SMC3 to close

Table 1. List of known SC protein components with naming variations (by species/group).

SC component	Proteins	Species studied in and alternative names
Axial Element Proteins: 1. Cohesin components	1. SMC1	Eukaryotes
	Meiosis-specific variant SMC1 β	Mammals
	2. SMC3	Eukaryotes
	3. SCC1	Eukaryotes (Grasshopper = Rad21)
	Meiosis-specific variant REC8	Yeasts, plants, animals Arabidopsis = SYN1/DIF1 Rice =RAD21-4 Maize = AFD1
	4. SCC3	Eukaryotes (Grasshopper = SA1)
	Meiosis-specific variants	<i>S. pombe</i> = Rec11 Mammals = STAG3
2. Non-cohesin components	Red1, Hop1	Budding Yeast
	SCP2/SYCP2, SCP3/SYCP3	Mammals
	HIM3, HTP1, HTP2, HTP3	<i>C. elegans</i>
	C(2)M	Drosophila
	Hop1-like proteins:	
	ASY1, PAIR2	Arabidopsis, rice
	HORMAD1, HORMAD2	mammals
Transverse filament (TF) proteins:	Zip1	Budding yeast
	C(3)G	Drosophila
	SYP1, SYP2, SYP3	<i>C. elegans</i>
	SCP1/SYCP1	Rat/Mouse
	ZYP1	Arabidopsis
	ZEP1	Rice
Central element (CE) proteins:	SYCE1, SYCE2, TEX12	mouse
	Corona (CONA)	Drosophila

the open-V shape of the SMC heterodimers and form a ring (Nasmyth 2001; Petronczki et al. 2003; Losada and Hirano 2005; Onn et al. 2008; Skibbens 2009).

The cohesin ring structure is thought to be important for enclosing the two sister chromatids to provide sister chromatid cohesion, but there is still debate about how cohesins interact to accomplish this function (Onn et al. 2008; Nasmyth and Haering 2009). REC8 is a meiosis-specific cohesin that replaces SCC1 used in mitotic cohesion (Watanabe and Nurse 1999). Other meiosis-specific cohesins that have been identified include SMC1 β that is found only in mammalian meiotic cells (Hodges et al. 2005; Novak et al. 2008; Adelfalk et al. 2009) and STAG3 (=REC11) that is present in mammalian (and *S. pombe*) meiotic cells (Prieto et al. 2001; Kitajima et al. 2003).

Cohesin proteins are essential for the normal formation of AEs and for SC formation (Jessberger 2002; Schubert 2009; Nasmyth and Haering 2009). In all species examined so far, cohesin proteins load first to form a meiotic chromosome core, followed by addition of meiosis-specific AE proteins (such as SYCP2, SYCP3, Red1, HIM3) to form the functional AE (Klein et al. 1999; Pelttari et al. 2001; Pasierbek et al. 2001; MacQueen et al. 2002; Colaiácovo et al. 2003; Eijpe et al. 2003; Hamant et al. 2006; Golubovskaya et al. 2006; Colaiácovo 2006). Mutations of REC8 are not lethal (unlike the other cohesins), so REC8 function has been examined in several organisms (Hamant et al. 2006; Onn et al. 2008; Peters et al. 2008; Nasmyth and Haering 2009). Mutation of REC8 causes defects in AE assembly, SC formation, and meiotic sister chromatid cohesion (Hamant et al. 2005; Brar et al. 2006; Onn et al. 2008; Peters et al. 2008; Brar et al. 2009; Nasmyth and Haering 2009), except in *C. elegans* where two additional REC8-like kleisins, COH-3 and COH-4, act together with REC8 and all three must be mutated to get AE defects (Severson et al. 2009; Wood et al. 2010). REC8 plays a key role in

many unique aspects of meiosis including roles in chromosome pairing, synapsis, recombination, and chromosome morphogenesis (Brar et al. 2009). REC8 has many phosphorylation sites that are important for the differing functions of REC8 in these various aspects of meiosis (Brar et al. 2009). REC8 also has an important role in the two-step release of cohesion that is unique to meiosis (Brar et al. 2006). During metaphase I – anaphase I, cohesion between sister chromatids is removed along chromosome arms when separase cleaves REC8. However, cohesins remain between sister centromeres because shugoshin (SGO) protects REC8 from cleavage (Kitajima et al. 2004; Hamant et al. 2005; Watanabe 2005). The centromeric cohesion keeps the two sister chromatids together as one unit so that homologous chromosome separate at anaphase I.

2. Non-cohesin proteins

In contrast to cohesin proteins, non-cohesin components of LEs are poorly conserved (Page and Hawley 2004), and, aside from their importance for SC formation, comparatively little is understood about their roles in meiotic pairing and recombination.

a. Mammals:

The first proteins to be identified as components of AEs/LEs were SCP2 and SCP3 that occur in mammals (Heyting et al. 1985; Heyting et al. 1987; Moens et al. 1987; Offenberg et al. 1991; Smith and Benavente 1992; Lammers et al. 1994; Dobson et al. 1994; Offenberg et al. 1998; Yuan et al. 1998; Schalk et al. 1999; Tarsounas et al. 1999b; Yuan et al. 2000; Yuan et al. 2002; Kouznetsova et al. 2005; Yang et al. 2006; Winkel et al. 2009). The original names of SCP2 and SCP3 have since been changed to SYCP2 and SYCP3 (presumably because of a naming conflict with sterol carrier protein, Liebe et al. 2004). Both are meiosis-specific proteins (Heyting et al. 1989; Heyting 1996), and both have coiled-coil domains near the C-termini of the proteins (Lammers et al. 1994; Dobson et al. 1994; Offenberg et al. 1998; Schalk et al. 1999).

SYCP3 is a 30 kD protein that can interact with itself through the C-terminal coiled-coil as demonstrated by its ability to self-assemble into fibers when it is expressed in cultured mammalian cells (Tarsounas et al. 1997; Yuan et al. 1998; Ollinger et al. 2005). SYCP3 is also highly phosphorylated during meiosis, and additional phosphorylation occurs at the early to middle pachytene transition, although the function of the phosphorylation patterns is still not known (Lammers et al. 1995). SYCP3 has an important role in attaching AEs to the chromosomes (Pelttari et al. 2001). SYCP2 is a much larger protein (173 kD) (Offenberg et al. 1998; Schalk et al. 1999). The coiled-coil domain of SYCP2 interacts with SYCP3 (Yang et al. 2006), and SYCP2 and SYCP3 form filaments together when the two proteins are co-expressed in cultured mammalian cells (Pelttari et al. 2001). However, SYCP2 is not capable of self-assembly in the same system (Pelttari et al. 2001). SYCP2 also interacts with the C terminus of the mammalian TF protein, SYCP1 (Winkel et al. 2009). The biochemical evidence plus cytological immunolocalization of SYCP2, SYCP3, and SYCP1 during prophase I indicate that SYCP2 links transverse filaments to axial elements in mammalian SCs (Offenberg et al. 1998; Schalk et al. 1999; Pelttari et al. 2001; Winkel et al. 2009).

Mutations of *SYCP2* or *SYCP3* result in defects in AE formation, SC formation (synapsis), bouquet release, and chromosome compaction (Yuan et al. 2000; Pelttari et al. 2001; Liebe et al. 2004; Kolas and Cohen 2004; Yang et al. 2006). For reasons that are not yet understood, mutation of either protein results in sterility in males (often due to apoptosis of pachytene spermatocytes) but only reduced fertility in females (Kolas and Cohen 2004). In female mice that lack SYCP3 protein, axial elements do not form although cohesin cores do form, and crossing over and interference are similar to that of wild-type female mice (de Boer et

al. 2007). Therefore, chromosome alignment and recombination are not dependent on intact AEs, at least in females.

Other AE-associated proteins in mammals include two proteins that possess HORMA domains (Hop1, Rev7, and Mad2) - HORMAD-1 and HORMAD-2 (Wojtasz et al. 2009; Fukuda et al. 2010). The HORMA domain may recognize certain chromatin states, such as those associated with DSBs, and act to recruit other proteins that are involved in cell cycle checkpoints, chromosome synapsis, and DNA repair (Aravind and Koonin 1998). In mammals, HORMAD-1 and HORMAD-2 preferentially associate with AEs of unsynapsed chromosomes (leptotene and zygotene), and the formation of SC (*i.e.*, the polymerization of SYCP-1) leads to the displacement of HORMADs from AE/LEs. After diplotene begins, HORMAD proteins reassociate with desynapsed LEs, but HORMADs are mostly absent from chromosomes by the beginning of diakinesis (Wojtasz et al. 2009; Fukuda et al. 2010). TRIP13 protein [related to budding yeast Pch2, a protein involved in the synapsis checkpoint at pachytene in both yeast and *C. elegans* (San-Segundo and Roeder 1999; Bhalla and Dernburg 2005; Wu and Burgess 2006)] is required for the depletion of HORMADs that accompanies synapsis (Wojtasz et al. 2009). Thus, mammals, like yeast, appear to have a synapsis surveillance system that utilizes HORMAD proteins (similar to *C. elegans* and plants, see below).

b. Budding yeast

Red1 and Hop1 are two AE components discovered in budding yeast (Rockmill and Roeder 1988; Hollingsworth et al. 1990). Hop1 dissociates from synapsed chromosomes before late pachytene, while Red1 remains along the bivalents (Smith and Roeder 1997). Hop1 physically interacts with Red1 and Mek1, a meiosis-specific, serine/threonine kinase (Rockmill and Roeder 1991; Hollingsworth and Ponte 1997; Niu et al. 2005). Hop1 and Red1 also help to

ensure interhomolog recombination by inhibiting DSB repair between sister chromatids (Niu et al. 2005; Niu et al. 2007; Carballo et al. 2008; Lin et al. 2010). Red1, Hop1, and Mek1 are all critical for forming SCs (Rockmill and Roeder 1988; Rockmill and Roeder 1990; Rockmill and Roeder 1991; Hollingsworth and Ponte 1997; Smith and Roeder 1997; Niu et al. 2005). AEs but not SCs form in *hop1* mutants (Loidl et al. 1994) while both AE and SC formation are defective in *red1* mutants (Rockmill and Roeder 1990). In *mek1* mutants, short stretches of SCs form, but full length SCs cannot be detected (Rockmill and Roeder 1991). Meiotic recombination is reduced but not completely eliminated in these three mutants (Rockmill and Roeder 1990; Rockmill and Roeder 1991). Hop1 and Red1 are also involved in the pachytene checkpoint by monitoring the progress of recombination and chromosome synapsis and interacting with Pch2 (Bailis and Roeder 2000; Brar et al. 2009).

c. C. elegans

Four HORMA domain proteins with important meiotic roles have been identified in *C. elegans*: HIM-3 and HTP-1, HTP-2 and HTP-3 [him three paralogs; (Zetka et al. 1999; MacQueen et al. 2005; Colaiácovo 2006; Goodyer et al. 2008; Martinez-Perez et al. 2008)]. Each of these proteins is a component of AEs and remains associated with chromosome axes until the metaphase I – anaphase I transition. The association of HIM-3 with AEs is dependent on REC8 and HTP-3 (Zetka et al. 1999; Goodyer et al. 2008), and HTP-3 links DSB formation with homolog pairing and crossing over through its interactions with MRE11/RAD50 and HIM-3 (Goodyer et al. 2008). HTP-1/2 proteins are involved in a major remodeling of the chromosome axis that occurs after crossing over (Martinez-Perez et al. 2008). HTP1/2 proteins (that are similar enough to be recognized by the same antibody) are initially distributed uniformly between bivalents, but after crossing over, HTP1/2 are lost from the portion of the bivalent that

remains synapsed and are enriched on the part of the bivalent that becomes desynapsed (Martinez-Perez et al. 2008). The boundary between HTP1/2 enriched and SYP-1 enriched portions of the bivalent are located close to (and perhaps at) the position of the single crossover typically observed for each *C. elegans* chromosome (Martinez-Perez et al. 2008; Bhalla et al. 2008). The reorganization of HTP1/2 is dependent on crossing over and is the most obvious cytological example of a change in chromosome axis organization in response to crossing over that has been observed in any organism. The reorganization may also provide a single defined position (the end of the chromosome enriched for SYP-1 protein) to act as the centromere for meiotic segregation of holokinetic *C. elegans* chromosomes and could be one reason why crossing over in *C. elegans* is limited to a single crossover. The change in axis organization has also been proposed to be involved in crossover interference (Martinez-Perez et al. 2008).

d. *Plants*

HORMA-domain proteins that have been identified in plants include ASY1 in *Arabidopsis* and *Brassica* and PAIR2, the ASY1 ortholog in rice (Armstrong et al. 2002; Nonomura et al. 2004; Nonomura et al. 2006). Morphologically normal AEs form in mutants of both *ASY1* and *PAIR2*, but SCs do not form (*i.e.*, there is no synapsis). Each protein is closely associated with AEs, but their patterns through prophase I vary in male wild-type meiocytes (pollen mother cells = PMCs) in the different plant species. For example, ASY1 is associated with AE/LEs from leptotene through pachytene, begins to dissociate from chromosomes at the beginning of diplotene, and is completely removed from chromosomes by late diplotene (Armstrong et al. 2002). In comparison, PAIR2 associates with AEs in leptotene and zygotene, but PAIR2 is depleted from areas of synapsis (SC) in zygotene and pachytene nuclei. This pattern is similar to that of HORMAD-1 and -2 in mammals (above). Small amounts of PAIR2

protein are retained at sister centromeres at diakinesis in wild-type rice plants, but *pair2* mutants have no defects in the sister chromatid cohesion or centromere behavior at anaphase I (Nonomura et al. 2006).

B. *Transverse Filament proteins*

Transverse filament (TF) proteins share very limited homology at the amino acid sequence level among different organisms, but their secondary and tertiary structures exhibit striking similarity [Table 1; (Page and Hawley 2004; de Boer and Heyting 2006; Wang et al. 2010)]. All possess a long coiled-coil domain in the middle of the protein with globular domains at both N- and C-termini. Biochemical and genetic studies indicate that two TF proteins interact through their coiled-coil domains to form a homopolymer with both N- and C- termini in parallel orientation (Page and Hawley 2004). In the SC, two pairs of homodimers then interact through their N-termini (*i.e.*, head-to-head) to bridge the space between the cores of homologous chromosomes with the C-termini of TF proteins close to the LEs. This orientation has been confirmed by EM immunolocalization in budding yeast (Dong et al. 2000), mammals (Schmekel et al. 1996; Liu et al. 1996), and *Drosophila* (Anderson et al. 2005). The C-terminal segment of TF proteins is required for anchoring the TFs to LEs as confirmed by deletion mutations of Zip1 and C(3)G (Tung and Roeder 1998; Jeffress et al. 2007). In *Drosophila*, C(2)M may be the link between the TF protein C(3)G and LE proteins (Manheim and McKim 2003; Anderson et al. 2005) while in mammals, SYCP2 links the TF protein SYCP1 and the AE protein SYCP3 (Winkel et al. 2009). In addition, Ser/Thr-pro (S/T-P) motifs on carboxyl termini of TF proteins indicate that they can bind DNA (Heyting 1996), and SYCP1 protein purified from testicular extracts can bind to chromatin (although at a lower level than either SYCP2 or SYCP3 (Yang et al. 2006)).

In most organisms, transverse filaments consist of a single protein, such as SCP1/SYCP1 in mammals, Zip1 in budding yeast, C(3)G in *Drosophila*, ZYP1 in *Arabidopsis*, and ZEP1 in rice (de Boer and Heyting 2006; Wang et al. 2010). However, in *C. elegans*, three proteins, SYP1, SYP2, and SYP3, make up TFs (de Boer and Heyting 2006; Smolikov et al. 2007).

C. Central Element Proteins

The original model for TF protein interaction suggested that the longitudinal central element may originate from the interaction of the N-terminal globular domains of TF proteins (Liu et al. 1996; Dong and Roeder 2000; Page and Hawley 2004). However, high resolution EM tomography showed that the CE structure of an insect also included pillar-like protein structures that were unlikely to be formed simply from TF N-terminal interactions (Schmekel and Daneholt 1995). Subsequent work has demonstrated the presence of three additional CE components (SYCE1, SYCE2, and TEX12) in mouse (Costa et al. 2005; Hamer et al. 2006; Bolcun-Filas et al. 2007; Hamer et al. 2008). These three proteins interact with each other and with the N-terminal domain of the TF protein SYCP1. SC formation is disrupted in *TEX12*^{-/-} and *SYCE2*^{-/-} mutants in which synapsis is initiated but not completed (Bolcun-Filas et al. 2007; Hamer et al. 2008). Another likely CE protein, Corona (CONA), has been identified in *Drosophila* (Page et al. 2008). CONA colocalizes with the TF protein C(3)G and is required for the assembly of C(3)G into mature SC. CONA is not similar in sequence or structure to mammalian CE proteins.

IV. Recombination nodules (RNs)

Densely stained bodies observed by electron microscopy along SCs in female *Drosophila* were hypothesized to have a role in crossing over and named recombination nodules (RNs) by Carpenter (1975). Subsequent work has confirmed and extended this initial report (Zickler and Kleckner 1999; Page and Hawley 2004; Anderson and Stack 2005).

RNs are protein complexes with ellipsoidal shape that are associated with AEs and SCs. There are two types of RNs, early (ENs) and late (LNs), that have been observed in various organisms (Anderson and Stack 2005). ENs appear at leptotene and remain associated with AEs and SCs until early pachytene, when most ENs are lost from SC. LNs appear in pachytene and persist into diplotene. There is evidence that a subset of ENs become LNs (Plug et al. 1998; Anderson and Stack 2005).

In addition to differences in the time of their appearance, ENs also differ from LNs in frequency, size and shape, location, and potential functions (Zickler and Kleckner 1999; Page and Hawley 2004; Anderson and Stack 2005). The number of ENs per cell is typically several hundred (and up to several thousand in species with large genomes like lily), while the number of LNs is typically only 1-3 per SC (or about 20-30 per cell for most model species). The size and shape of ENs are quite variable from ~50 X 50 nm to ~ 250 X 290 nm while LNs have a more regular ellipsoidal shape and size of 50 X 100 nm. A small number of ENs are associated with asynapsed axial elements during leptotene, and additional ENs are added at synaptic forks (the intersection between synapsed and unsynapsed segments) when SCs are assembling. However, ENs do not bind to intact SC segments (Anderson et al. 2001). ENs occur in higher frequencies in euchromatic than in heterochromatic SC segments (Anderson et al. 2001; Stack and Anderson 2002). In comparison, LNs are observed only on SCs and are not associated with AEs. Each SC has at least one LN, and LN numbers and positions on SCs closely match those estimated from chiasmata and linkage maps (Sherman and Stack 1995; Zickler and Kleckner 1999; Anderson et al. 2003; Anderson and Stack 2005). LNs are common in euchromatin, rare in heterochromatin, and essentially absent from kinetochores and telomeres (Sherman and Stack 1995; Anderson et al. 2003). Different molecular components have been immunolocalized to

ENs and LNs. RAD51/DMC1, two closely related RecA-like proteins, have roles in comparing two DNA strands for sequence homology, and both proteins have been localized in ENs (Anderson et al. 1997; Moens et al. 2002; Anderson and Stack 2005). Other proteins that have early roles in recombination have also been observed associated with AE/SC in zygotene nuclei such as BLM, RPA, and MSH4/5 (Moens et al. 2002; Moens et al. 2007). One protein involved in promoting crossovers, MLH1, has been localized to LNs (Moens et al. 2002; Lhuissier et al. 2007; Moens et al. 2007). Both LNs and MLH1 foci show interference similar to genetic crossover interference (Anderson and Stack 2005; de Boer et al. 2006; Lhuissier et al. 2007; Falque et al. 2009). To summarize, ENs are thought to be involved in early events in recombination and perhaps also in recognition and alignment of homologous chromosomes (Anderson and Stack 2005) while LNs are thought to mark sites on chromosomes where DSBs have been converted into crossovers (= chiasmata) (Zickler and Kleckner 1999; Anderson and Stack 2005).

V. DNA Double-Strand-Break (DSB) Repair Model for Meiotic Recombination

Much progress has been made in elucidating the molecular events that lead to crossovers between homologous chromosomes (Figure 2). Several DNA intermediates have been isolated using special electrophoretic techniques and many proteins involved in DSB formation, end processing, and repair to form crossovers (CO) or non-crossovers (NCO) have been identified (Hunter and Kleckner 2001; Börner et al. 2004). Many of the proteins involved in meiotic recombination are also involved in DNA repair in somatic tissues, as one might expect if meiotic recombination evolved from DNA repair (Zickler and Kleckner 1999). However, some proteins are meiosis-specific (as discussed below), and others (no doubt) have yet to be discovered.

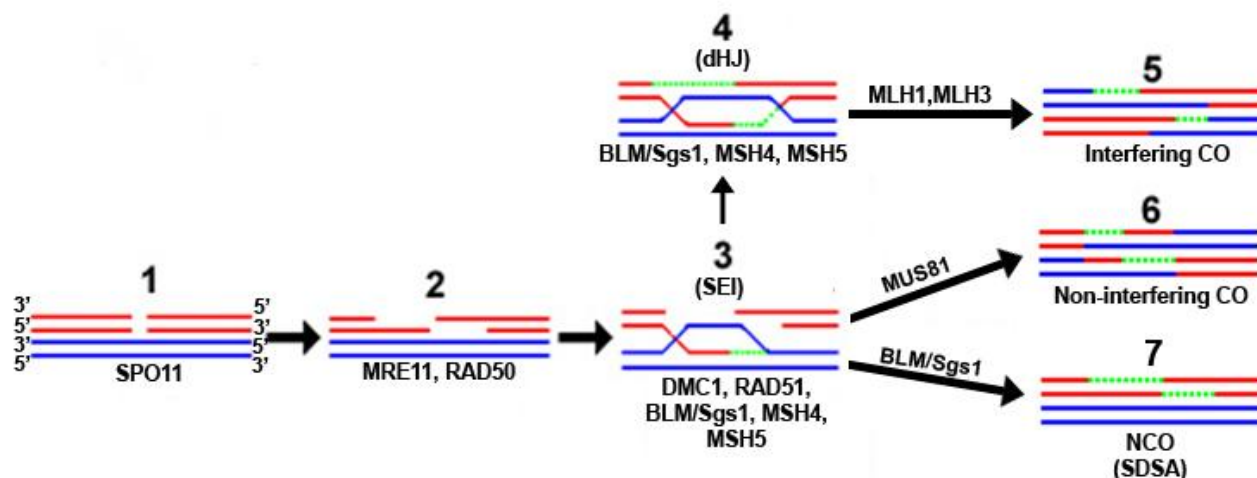


Figure 2. DSB repair model for meiotic recombination. The DNA helices of two non-sister chromatids from homologous chromosomes are shown (red and blue lines). Newly synthesized DNA is shown in green. (1) Spo11 homodimer generates a DSB, and one Spo11 protein remains covalently bound at each 5' end of the DSB. Resection of the 5' end begins with removal of Spo11 (together with an attached oligonucleotide) by the Mre11 complex and other enzymes. (2) Resection of the 5' ends continues, resulting in overhanging 3' ends that invade the DNA helix of a non-sister chromatid to form a single-end invasion (SEI) complex (3). The invasion process is facilitated by two RecA-like recombinases, Rad51 and Dmc1. After the SEI forms, a DSB may be repaired as a crossover (CO, 4-6) or a non-crossover (NCO, 7). Crossovers may be either interfering (4-5) or non-interfering (6). Interfering COs arise from double Holliday junctions (dHJs, 4) and involve the Mlh1/Mlh3 complex (5). In this pathway, the displaced D-loop (3) interacts with the 3' tail of the DSB on the other homolog by a process called second end capture. Subsequent DNA synthesis and ligation give rise to a dHJ. Theoretically, dHJs can be resolved as CO or NCO, but in budding yeast, dHJs lead predominantly, perhaps even exclusively, to COs. Non-interfering COs (6) are generated in the Mus81 pathway and may arise through resolution of single HJ or aberrant joint molecules. In the NCO pathway (7), synthesis dependent strand annealing (SDSA) repairs DSBs without reciprocal exchanges. In the SDSA pathway, the free 3' tail dissociates from the non-sister chromatid, reanneals to the original chromatid, and is repaired by new DNA synthesis. Figure modified after Cohen et al. (2006).

Protein	Meiotic function
SPO11	induces DSBs
MRE11 and RAD:	5' end resection
DMC1 and RAD51:	formation of D-loop when scanning non-sister chromatid for DNA sequence homology
BLM (mammalian) or Sgs1 (yeast):	unwinding Holliday junctions (anti-crossover activity)
MSH4 and MSH5:	molecular role not yet clear but ultimately involved in commitment to crossover
MLH1 and MLH3:	interference type crossovers
MUS81:	non-interference type crossovers

a. Programmed induction of DNA DSBs by SPO11

Meiotic recombination initiates with the programmed induction of DSBs by Spo11 protein (Keeney et al. 1997; Lichten 2001). Spo11 is a member of a novel family of type II-like topoisomerases, and Spo11 generates DSBs by a topoisomerase-like transesterification reaction rather than by endonucleolytic hydrolysis (Keeney 2001; Cole et al. 2010). In most organisms, there is only one copy of *SPO11*, and the protein acts as a homodimer to make DSBs (Keeney and Neale 2006). However, many plant species have three SPO11 genes, SPO11-1 and SPO11-2 that act together as a heterodimer to make DSBs and SPO11-3 that has a role in endoreduplication (Stacey et al. 2006). After generating DSBs, SPO11 remains covalently bound to the 5' end of each DNA strand and must be removed before the DSB can be repaired as a CO or NCO (Neale et al. 2005; Cole et al. 2010).

SPO11 is required for homologous synapsis in many organisms including fungi, mammals and plants (Giroux et al. 1989; Celerin et al. 2000; Baudat et al. 2000; Romanienko and Camerini-Otero 2000; Grelon et al. 2001; Keeney 2001). However, SPO11 activity is not required for chromosome pairing and SC assembly in two invertebrates, *Drosophila* and *C. elegans* (McKim et al. 1998; Dernburg et al. 1998; McKim and Hayashi-Hagihara 1998).

b. Role of MRE11 (MRN) complex

The MRE11 complex (MRN) complex includes three proteins, MRE11, RAD50 and NBS1/Xrs2, and has an important and evolutionarily conserved role in sensing and repairing DSB in somatic and meiotic cells (Bannister and Schimenti 2004; Assenmacher and Hopfner 2004; Borde 2007). During meiosis, the MRE11 complex is required for Spo11-dependent DSB formation (in some but not all organisms), for subsequent resection of the 5' ends, and for removal of covalently attached Spo11-oligonucleotide complexes from DSB sites (Borde et al.

2004; Neale et al. 2005). The MRE11 complex also has roles in DNA replication, telomere maintenance, genomic stability and checkpoint signaling (Borde 2007).

MRE11 and RAD50 are highly conserved proteins while NBS1 (Xrs2 in budding yeast) is less well conserved (Assenmacher and Hopfner 2004). The core of the MRE11 complex is Rad50, a member of the SMC family of proteins, and each Rad50 protein has two long coiled-coil sections that fold back on each other to form a rod with a zinc hook on one end and a globular structure on the other end composed of the N- and C-termini (that together form an ATP binding cassette). The two ATPase motifs of RAD50 interact with MRE11 and NBS1 protein together binds to DNA molecules (de Jager et al. 2001; Borde 2007). The zinc hook promotes interactions between MRE11 complexes, which enables them to tether two or more DNA molecules (Wiltzius et al. 2005).

The meiotic role of the MRE11 complex has been analyzed in several organisms. In general, *mre11*, *rad50*, and *nbs1/xrs2* null mutants have defects in meiotic homologous chromosome pairing, AE and/or SC assembly and crossing over (Alani et al. 1990; Merino et al. 2000; Gerecke and Zolan 2000; Gallego et al. 2001; Bleuyard et al. 2004; Borde 2007; Waterworth et al. 2007). In Arabidopsis, chromosome fragmentation occurs after SC breakdown in *mre11*^{-/-} mutants because Spo11-induced DSBs are not repaired (Puizina et al. 2004). Thus, unlike budding yeast, MRE11 is not required for the formation of DSBs by SPO11 in plants (Keeney and Neale 2006). In contrast, an *mre11* null mutant in *C. elegans* synapses normally, but no crossovers are formed (Chin and Villeneuve 2001). Analysis of the meiotic role of the MRE11 complex in mammals is complicated by the fact that these proteins are essential for viability (D'Amours and Jackson 2002). To avoid this problem, hypomorphic mutants of NBS1 and MRE11 (that correspond to the human disorders of Nijmegen Breakage Syndrome and

Ataxia-Telangictasia-Like Disorder) have been generated in mice (Cherry et al. 2007). The *mre11* and *nbs1* hypomorphic mutants have defects in the temporal progression of meiotic prophase, incomplete and aberrant synapsis, abnormal persistence of DNA repair proteins, and alterations in both the frequency and placement of MLH1 foci (a marker for crossing over). Surprisingly, the number of MLH1 foci decreased in females but increased in males, an observation unexpected for a defect in a recombination-related protein.

Other evidence indicates that MRE11 and RAD50 may not always work together in a complex. For example, MRE11 can associate with DNA (chromatin) transiently without RAD50, and MRE11 can function independently in DNA repair-related activities (Usui et al. 1998; Furuse et al. 1998; Borde et al. 2004; Borde 2007). Mutants of *mre11* affect vegetative growth in Arabidopsis more than *rad50* mutations, also indicating MRE11 complex-independent functions that may also apply to meiosis (Gallego et al. 2001; Puizina et al. 2004).

Immunolabeling studies in plant meiocytes also show a difference in localization patterns between Mre11 and Rad50. Many MRE11 foci were observed associated with chromosome cores in tomato and Arabidopsis at leptotene – zygotene stages (Lohmiller et al. 2008). In comparison, fewer and larger RAD50 foci are observed at the same stages of meiosis, and RAD50 and MRE11 foci often do not colocalize even though they both associate with meiotic chromosome axes (H.Q., L.L. and L.K.A. - unpublished data). Therefore, MRE11 and RAD50 proteins are likely to have independent functions as well as functions in the MRE11 complex during meiosis.

c. RAD51 and DMC1 recombination proteins

RAD51 and *DMC1* (*disrupted meiotic cDNA 1*) are two RecA homologs in eukaryotes that are important for meiotic recombination (Shinohara et al. 1992; Bishop et al. 1992; Sung et

al. 2000). RecA is a bacterial protein that coats single-strand DNA (ssDNA) to form a nucleoprotein filament that is capable of scanning double-strand DNA for sequence homology and facilitating homologous DNA-DNA interactions and DNA strand exchange (West 1992; Heyer 1994). *RAD51* and *DMC1* share 45% identity by alignment and are highly conserved among most eukaryotes (Bishop et al. 1992; Masson and West 2001; Shinohara and Shinohara 2004). However, *DMC1* is absent from *Drosophila melanogaster* and *C. elegans*, model species in which DSB are not required for homologous chromosome alignment and SC formation (Villeneuve and Hillers 2001; Masson and West 2001; Shinohara and Shinohara 2004).

RAD51 is essential for both meiotic and mitotic recombination (Shinohara and Shinohara 2004). *rad51* mutants are embryo-lethal in vertebrates, apparently due to the important role of Rad51 in repairing DNA damage during replication (Bannister and Schimenti 2004; Pawlowski and Cande 2005). However, *rad51* is not required for somatic growth in other species, including plants (Li et al. 2004; Bannister and Schimenti 2004; Pawlowski and Cande 2005; Li et al. 2007). Arabidopsis *rad51* mutants are defective in homologous pairing, exhibit extensive chromosome fragmentation, and both male and female are sterile (Li et al. 2004). In comparison, maize *rad51* mutants have some nonhomologous synapsis, limited chromosome fragmentation, and complete male (but not female) sterility (Li et al. 2007). Li et al. (2007) speculated that these differences between Arabidopsis and maize *rad51* mutants could be related to a suggestion by Pawlowski et al. (2004) that maize, but not Arabidopsis, has a backup DNA repair mechanism that acts later in meiosis to mend chromosome breaks. RAD51 foci are considered to mark DSB sites (Hayashi et al. 2007), and several maize asynaptic mutants exhibit reduced frequency and altered nuclear distribution of Rad51 foci (Pawlowski and Cande 2005). The severity of the synaptic defects was generally correlated with the degree of disruption of

RAD51 foci, so the reduction in RAD51 foci may reflect an alteration in the control of DSBs by SPO11.

DMC1 is a meiosis-specific protein that is required for normal meiosis and crossing over in most eukaryotes [except *Drosophila* and *C. elegans* as noted earlier (Shinohara and Shinohara 2004)]. Mutation of DMC1 results in synaptic defects and sterility in budding yeast, plants, and animals (Bishop et al. 1992; Yoshida et al. 1998; Pittman et al. 1998; Doutriaux et al. 1998).

RAD51 and DMC1 have overlapping functions in meiotic recombination (Masson and West 2001). Cytological evidence showing colocalization of RAD51 and DMC1 foci in meiotic nuclei also supports the interaction of these two proteins (Bishop 1994; Tarsounas et al. 1999a), and both proteins are thought to be components of early recombination nodules (Anderson et al. 1997; Tarsounas et al. 1999a). However, double mutants of *rad51 dmc1* in budding yeast are more defective in recombination than *rad51* and *dmc1* single mutants (Bishop 1994; Schwacha and Kleckner 1997). In addition, Dmc1 has more of a role in promoting inter-homolog recombination while Rad51 is more likely to facilitate recombination between sister chromatids, especially in the absence of AE proteins such as Red1 (Schwacha and Kleckner 1997; Hunter and Kleckner 2001). These differences in function may be related to differences in structure. RAD51 makes right-handed nucleoprotein filaments that are similar in structure to those formed by bacterial RecA protein (Ogawa et al. 1993; Egelman 2001) while DMC1 rather forms a ring of eight subunits around the ssDNA (Masson et al. 1999; Passy et al. 1999). There is also evidence that RAD51 and DMC1 can assemble independent complexes in budding yeast and mice (Tarsounas et al. 1999a; Shinohara and Shinohara 2004). Thus, although RAD51 and DMC1 are similar in structure and at least partially redundant in function, they also have distinct roles to play during meiosis.

d. Role of MLH1 protein in promoting crossing over

Several proteins that are involved in somatic DNA mismatch repair (MMR) are also required for meiotic recombination (Hassold 1996; Kolodner and Marsischky 1999; Buermeyer et al. 1999; Svetlanov and Cohen 2004; Hoffmann and Borts 2004). These proteins are named for their similarities to MutS and MutL, DNA mismatch repair proteins in *E. coli* and include MSH4 and MSH5 (Mut-S homolog) and MLH1 and MLH3 (Mut-L homolog). Two heterodimers, MSH4/MSH5 and MLH1/MLH3, are especially important in promoting interhomolog crossing over in budding yeast, plants and animals (Villeneuve and Hillers 2001). In another departure from the “normal” pathway of meiosis, *MSH4/MSH5* is not present in the *Drosophila* genome. In budding yeast, Mlh1 and Mlh3 are thought to function after double Holliday junction (dHJ) formation in DSB repair pathway to promote crossovers (Hunter and Borts 1997; Wang et al. 1999). Similarly, although synapsis is normal, null mutants of *MLH1* or *MLH3* in mammals and plants are sterile because crossing over is virtually eliminated in the mutants resulting in irregular disjunction at anaphase I (Edelmann et al. 1996; Baker et al. 1996; Jackson et al. 2006; Dion et al. 2007). Immunogold labeling revealed that MLH1 protein is a component of LNs in mice and tomato (Moens et al. 2002; Lhuissier et al. 2007). Like LNs, the distribution of MLH1 foci is correlated with SC length, and MLH1 foci show crossover interference (Anderson et al. 1999; de Boer et al. 2006). Because MLH1/3 marks crossover sites, the distribution of MLH1 foci can be used to analyze crossover interference in cytological way (de Boer et al. 2006). Crossover interference is a phenomenon in which one crossover reduces the likelihood of another crossover nearby. MLH1 and MLH3 foci in meiotic cells mark about 90% of crossovers in mammals (Lipkin et al. 2002; Marcon and Moens 2003; Guillon et

al. 2005) and more than 70% of crossovers in plants (Jackson et al. 2006; Lhuissier et al. 2007; De Muyt et al. 2009).

VI. Correspondence between recombination-related proteins and recombination nodules

Many of the recombination proteins discussed above are expected to be components of early and/or late recombination nodules (Zickler and Kleckner 1999; Anderson et al. 2005). One of the expected characteristics of such EN/LN components is focal immunofluorescent signals along or around chromosomal axes at early prophase I, which are in numbers and patterns similar to ENs and/or LNs. Such patterns have been observed for several proteins including SPO11 (Phillips et al. 2008), MRE11 (Lohmiller et al. 2008), RAD51 (Bishop 1994; Terasawa et al. 1995; Anderson et al. 1997; Franklin et al. 1999), DMC1 (Bishop 1994), RPA, BLM, MSH4 (Moens et al. 2002) and MLH1/3 (Moens et al. 2002; Jackson et al. 2006; Lhuissier et al. 2007). In some cases, immunogold labeling at the EM level has verified the presence of the proteins in ENs or LNs (Anderson et al. 1997; Marcon and Moens 2003; Lhuissier et al. 2007). However, sometimes focal signals that are closely associated with SC components do not correspond to ENs. For example, in tomato, only about 10% of the MRE11 foci observed by LM correspond to ENs by EM immunolabeling, and similar results have been observed for RAD50 in tomato (Lohmiller et al. 2008) (H.Q. and L.A., unpublished results). Thus, the appearance of a focal signal associated with AEs/SCs is not sufficient evidence to verify that a protein is an EN or LN component. Surprisingly, some proteins that appear as focal fluorescent signals in one species do not show a focal pattern in another species. For example, MRE11 and RAD50 appear as foci in tomato but as a diffuse nuclear signal in mice (Eijpe et al. 2000b; Lohmiller et al. 2008). Whether these are true differences in function or are simply due to technical issues are not yet

clear. However, it is clear that much remains to be determined about ENs and LNs and their protein components in different species.

Similarly, little is known about the relationship between ENs and RNs. One popular idea that has some experimental support is that a small number of ENs are somehow “selected” to develop into LNs and the other ENs are removed by the mechanism of crossover interference (Stack and Anderson 1986a; Plug et al. 1998; Zickler and Kleckner 1999; Agarwal and Roeder 2000; Moens et al. 2002; Anderson and Stack 2005). The “selection” process for crossovers may occur very early, perhaps concurrent with or even preceding SC formation [based primarily on evidence from budding yeast (Bishop and Zickler 2004)]. If some ENs become LNs, then one expectation is that some recombination-related proteins would be shared by both ENs and LNs. Two proteins that share this characteristic are MSH4 and RPA that co-localize with RAD51/DMC1 and MLH1, respectively, EN and LN protein components (Plug et al. 1998; Santucci-Darmanin et al. 2000; Moens et al. 2002; Neyton et al. 2004).

Not all ENs are equally likely to become LNs. There is a general tendency for crossing over to be higher in distal regions of chromosomes from plants and animals (Bishop and Zickler 2004; Anderson and Stack 2005). Synapsis usually begins in distal parts of chromosomes, and ENs would be able to bind here before more proximal regions that synapse later (Stack and Anderson 2002; Anderson and Stack 2005). Perhaps, the longer association of ENs in distal regions facilitates the maturation of some ENs to LNs in these regions.

VII. Crossover interference

Crossover interference was first described in *Drosophila* (Muller 1916; Hillers 2005; Falque et al. 2009; Berchowitz and Copenhaver 2010) and refers to the observation that the occurrence of one crossover decreases the probability of other crossovers nearby. Crossover

interference can be measured in different ways. First, the classical approach to measure interference is to use linkage maps with at least three markers covering two adjacent intervals. The observed frequency of a crossover in each interval (double crossover) is divided by the frequency of expected double crossovers (*i.e.*, if there were no interference) to yield the coefficient of coincidence (COC). Interference is defined as one minus COC.

$$\text{COC} = \frac{[\# \text{ observed double crossovers}]}{[\# \text{ expected double crossovers}]}$$

$$\text{Interference (I)} = 1 - \text{COC}$$

When $I = 0$, there is no interference between crossovers, and when $I = 1$, there is complete interference between crossovers.

Another method to calculate crossover interference is to use cytogenetic markers like chiasmata or late recombination nodules that mark all crossover sites (Laurie and Hultén 1985; Sherman and Stack 1995; Anderson and Stack 2005) or MLH1 foci that mark most crossover sites (Anderson et al. 1999; Froenicke et al. 2002; de Boer et al. 2006; Lhuissier et al. 2007). Each method has advantages and disadvantages. The positions of chiasmata are often difficult to measure precisely because of the variability in chromosome compaction at diplotene-diakinesis when chiasmata are easiest to see. In addition, individual chromosomes are almost impossible to identify without the use of fluorescence in situ hybridization (FISH). The combination of both techniques has been useful in examining crossing over in *Arabidopsis* and cotton (Reyes-Valdés et al. 1996; Armstrong and Jones 2003). LNs provide high-resolution cytogenetic maps, but LNs can be visualized only by electron microscopy, a comparatively difficult technique that limits the number of observations that can be made. MLH1 foci cytogenetic maps are lower resolution than LNs but higher resolution than chiasmata. However, only 70-95% of all crossovers are

detected using this procedure. Recently, a new approach using MLH1 immunolabeling in combination with squashes of diakinesis-metaphase I chromosomes (chiasmata) has been used to investigate crossing over in *Arabidopsis* and allotriploid and allotetraploid hybrids of *Brassica* (Leflon et al. 2010; Chelysheva et al. 2010).

Measuring interference using cytogenetic data requires a different approach than genetic data. Distances (in μm or as a percentage of SC length) between adjacent crossovers are used to estimate interference using a statistical gamma model that provides the best fit to the observed data (de Boer et al. 2006; Falque et al. 2009). The equation for the gamma model is $f(x|l,v) = (l^v x^{v-1} e^{-lx}) / \Gamma(v)$ where X is the inter-event distance, l is the rate of occurrence, and v is the level of interference. When $v = 1$, there is no interference. When $v > 1$, positive interference is detected and increasing values of v indicate more interference. The gamma model has been applied to calculate crossover interference among MLH1 immunofluorescence foci in mice, humans, and tomato (Lhuissier et al. 2007; de Boer et al. 2007; Lian et al. 2008) and among LNs in maize (Falque et al. 2009).

VIII. Models for crossover interference

Several models have been proposed to explain the biological basis of crossover interference [recently review by (Berchowitz and Copenhaver 2010)]. Three of the most popular models (polymerization, mechanical stress, and counting) are reviewed below. While each model has certain attractive features, none fully explains crossover interference. (Note that the gamma model described above is a mathematical method to evaluate the presence and intensity of crossover interference and is distinct from the following models that attempt to explain how crossover interference is established in meiotic cells.)

a. *Polymerization model*

The polymerization model that has been developed in greatest detail is that of King and Mortimer (1990). In that paper, they suggested that early recombination structures (possibly represented by ENs) are randomly distributed along AEs. At some of these sites, polymerization (originally thought to be formation of central element) begins and progressively extends in both directions along the chromosome axes (most probably along with SC formation).

Polymerization prevents additional ENs from binding to chromosome cores and also ejects bound ENs. Ejected ENs are either degraded or bound to polymer-free AEs where they can initiate polymerization. Polymerization at each site continues until another polymer is contacted or the centromere or telomere is reached. In the model, early synaptic initiation sites develop into crossover sites (LNs), and the interference signal that is conferred by polymerization is strongest close to initiation sites and gradually decreases away from these sites with polymer growth. The model explains how both crossover interference and crossover assurance (at least one crossover per bivalent) can be tied together (Martini et al. 2006). A computerized simulation fit existing crossover data from *Drosophila* and budding yeast (King and Mortimer 1990). While this model has several attractive features, the polymer, *i.e.* the source of the interference signal, has not been identified. Several lines of evidence indicate that polymerization of the SC by central element formation is not the source of the interference signal (de Boer et al. 2007; Shinohara et al. 2008). However, other possible sources of the “polymerization” signal have been suggested such as modification of cohesions or other AE components by phosphorylation, methylation, acetylation, or ubiquitination (Berchowitz and Copenhaver 2010).

b. Mechanical stress model

(Kleckner et al. 2004) proposed a stress model in which mechanical forces associated with chromosome structure play a critical role in governing chromosome functions such as crossing over. In this model, expansion and compression of chromatin generates mechanical stress along each chromosome, and stress builds until a CO is achieved. The CO relieves stress locally in a bidirectional way, which prevents other crossovers from occurring nearby. Aside from a lack of a mechanism to explain how stress is generated, the stress model also does not explain how crossovers generated by through the MLH1-type interference pathway would reduce stress but crossovers generated by the MUS81-type non-interference pathway would not. Also, as pointed out by (Berchowitz and Copenhaver 2010), it is difficult to understand how one or two crossovers could relieve stress on a chromosome while the earlier presence of hundreds of DSBs would allow stress to build. On the other hand, a number of studies have found a close link between proteins that are involved in establishing or maintaining chromosome axis structure (such as PCH2, HTP-3, DPY-28, HIM-3, SMC1 β) and crossover distribution and interference (Zetka et al. 1999; Jessberger 2002; Tsai et al. 2008; Goodyer et al. 2008; Zanders and Alani 2009; Joshi et al. 2009; Mets and Meyer 2009).

c. Counting model

Foss et al. (1993) proposed a model based on the concept that successful COs are separated (= crossover interference) by a certain number of NCO events, and the NCO number is fixed for each organism. Unlike the other two models in which chromosome structure is closely associated with interference, the counting model is based solely on genetic parameters. One advantage of the counting model is that it can explain the large variation of interference strength among organisms (Stahl et al. 2004; Berchowitz and Copenhaver 2010), and it is the only model

in which adding non-interfering COs actually helps the model fit better (Copenhaver et al. 2002; Stahl et al. 2004; Lam et al. 2005a; Berchowitz and Copenhaver 2010). Recently, the counting model was tested in *S. cerevisiae* using a series of *spo11* hypomorphic mutants that reduce the frequency of DSBs to 20%, 30%, and 80% of wild-type (Martini et al. 2006). The counting model predicts that reduced levels of DSBs that are precursors of both COs and NCOs would result in proportionally reduced frequencies of COs and NCOs. However, the predicted result was not observed. Instead, (Martini et al. 2006) found that CO levels were maintained at the expense of NCOs, a phenomenon they called crossover homeostasis. Another problem of the counting model is the lack of a molecular mechanism (Berchowitz and Copenhaver 2010).

In summary, substantial progress is being made in defining the proteins and molecular events of recombination, but even basic aspects of how crossover frequency and distribution is controlled remain mysterious.

IX. Tomato as a model system for cytogenetic study of meiotic recombination

Tomato (*Solanum lycopersicum*) is native to South America and was probably domesticated in Central America (Spooner et al. 2005). All members of the tomato clade are diploid ($n = 12$) although rare tetraploid forms occur (Spooner et al. 2005). Tomato is a model plant for genetic, developmental, and pathologic studies with advantages that include extensive germplasm collections, numerous mutants (natural, induced, and transgenic), routine transformation technology, a dense linkage map, many cDNA and genomic libraries, a small genome that has been recently sequenced, relatively short life-cycle, and ease of growth and maintenance (Tanksley and McCouch 1997; Mueller et al. 2009).

We chose to use cherry tomato as model to investigate meiotic recombination for several reasons. First, cherry tomatoes grow and bloom in the greenhouse all year. Second, using

spreads of SCs, ENs and LNs can be distinguished at the EM level based on a number of morphological characteristics (Stack et al. 1993; Anderson and Stack 2002; Anderson and Stack 2005). In contrast, it's difficult if not impossible to identify ENs in SC spreads from yeast, mammals, or birds using only morphology (Dresser and Giroux 1988). Third, representative dicot, monocot, and lower vascular plants behave similarly regarding EN distribution and general synaptic behavior (Anderson et al. 2001). Thus EN and LN distribution patterns from tomato apply to other plants. Fourth, a detailed tomato RN (=LN) map is available (Sherman and Stack 1995). The RN map is useful in order to study the LNs with reference to different recombination pathways and genetic interference. Fifth, antibodies to a number of tomato recombination-related and SC proteins have been prepared, and most antibodies against Arabidopsis proteins also can be used for tomato spreads (Lohmiller et al. 2008). While Arabidopsis is an excellent model for meiotic studies in plants (Ma 2006), SC spreads are more difficult to make, and ENs and LNs have been observed by EM only from sectioned primary microsporocytes, making their study much more difficult (Albini 1994; Armstrong et al. 2002; Ma 2006). Therefore, tomato provides a good cytological model to examine the molecular events of recombination within the cytological framework of RNs and SCs.

X. Tomato meiotic mutants

A number of tomato mutants that reduce fertility have been identified (Emmanuel and Levy 2002; Menda et al. 2004), but only seven mutants (*as1-as6*, *asb*) that specifically affect meiosis have been examined using genetic and/or cytological methods (Soost 1951; Moens 1969; Havekes et al. 1994; Havekes et al. 1997). All seven are spontaneous, recessive, non-allelic mutations, and all have various levels of meiotic asynapsis except *as5* (Table 2). The *as5* mutation should more properly have been defined as a desynaptic mutation because synapsis is

complete, but crossovers are not maintained. Without crossovers, bivalents from *as5* plants fall apart to univalents that do not segregate properly when SCs breakdown in diplotene. The synaptic defects in the other mutants also affect meiotic recombination and segregation, resulting in reduced fertility. We will review the phenotypes of two of the mutants (*as1* and *asb*).

The asynaptic mutants *as1* and *asb* possess generally similar cytological characteristics. First, chromosomes pair, and the pairing is probably homologous because of the similar lengths of the AEs involved (Havekes et al. 1994). SC assembly is initiated, but only short segments of SC are formed in each mutant. The average percentage of synapsis (total length of LE per total AE/LE length for each set) is about 25% for *as1* and about 6% for *asb*, and the amount of synapsis observed in different sets varies for each mutant [4 - 70% for *as1* and 0 - 17% for *asb*; (Havekes et al. 1994)]. Second, the average number of pachytene bivalents (including chromosome pairs with even partial synapsis) is correlated with the average number of metaphase I bivalents in *as1* and *asb* mutants. Pachytene and metaphase I cells average about 6-7 bivalents per cell in *as1* and about 3 bivalents per cell for *asb* compared to 12 in wild-type cells (Havekes et al. 1994). This result indicates that even partially synapsed homologs have at least one crossover that is sufficient to hold the bivalent together at metaphase I (Havekes et al. 1994). Soost (1951) obtained a similar average of ~ 7 diakinesis bivalents per cell in *as1* (range of 1-12). The high number of metaphase I univalents (average ~ 5 pairs per cell) that would be free to move independently to either pole at anaphase I would result in a high proportion of genetically unbalanced gametes and low fertility, the character that first brought these plants to the attention of researchers. Both *as1* and *asb* produce almost no viable pollen (Soost 1951; Moens 1969). However, crosses between *as1* or *asb* using wild-type pollen yielded fruits with only about a 50% reduction in seeds compared to wild-type fruits (Soost 1951; Moens 1969), indicating that

Table 2. Characteristics of two tomato asynaptic mutants [data from (Havekes et al. 1994; Havekes 1999)].

Mutant	Average synapsis (%)	Average No. of Bivalents		RN observation	Possible protein defect
		Pachytene	Metaphase		
<i>asb</i>	6.1 ± 5.8	3.2 ± 2.4	3.2 ± 1.4	ENs were found between aligned axial elements	RAD50, RAD51, and DMC1
<i>asl</i>	25.0 ± 18.9	6.4 ± 3.4	7.3 ± 1.7	ENs were found between aligned axial elements	RAD50, RAD51, and DMC1
Wild type	100	12	12	LN's are present on SCs	---

males are more deleteriously effected by *asI* or *asb* mutations than females. Third, both early and late RNs were observed in SC spreads from both mutants (Havekes et al. 1994; Havekes 1999). LNs were studied in more detail in *asb*, and (Havekes 1999) observed that most bivalents had only a single SC segment that had at least one LN. These results are consistent with the correspondence between the numbers of pachytene and metaphase I bivalents noted earlier. They also observed that longer SC segments often had multiple LNs. Overall, the frequency of LNs per μm SC was about two-fold higher in *asb* mutants than in wild-type (Havekes 1999). Soost (1951) observed that some bivalents from *asI* plants lag at the metaphase I plate and do not separate easily, a behavior that could indicate the presence of many crossovers on those bivalents. Large numbers of crossovers may be more difficult to resolve at anaphase I in order to allow timely chromosome separation.

Both Soost (1951) and Moens (1969) examined crossing over in *asI* and *asb* mutants using genetic markers on chromosome 2 (although the markers were originally thought to be on chromosome 1 by Soost (1951)). In both studies, the asynaptic plant was used as the female parent. Soost (1951) observed a small increase in the frequency of crossing over between two markers in the *asI* mutant. However, the increase was not statistically significant, and he was not able to examine genetic interference because only two markers were evaluated. Moens (1969) evaluated crossing over between three markers. For *asI*, he found essentially the same overall genetic distance for each interval as observed in control plants (Interval 1 = 12 cM for both control and *asI*; Interval 2 = 16 cM for control and 19 cM for *asI*). However, the frequency of double crossovers was 10 times higher in the *asI* mutants ($22/1360 = 1.6\%$) than in the backcross control ($1/607 = 0.16\%$) corresponding to lower genetic interference in the *asI* mutant than in control plants (interference = 0.3 versus 0.9, respectively). For the *asb* mutant, crossing

over was elevated in both genetic intervals compared to control plants (Interval 1 = 12 cM for control and 18 cM for *asb*; Interval 2 = 16 cM for control and 36 cM for *asb*). Like *as1*, the frequency of double crossovers was higher in the *asb* mutants ($40/640 = 6.2\%$) compared to the backcross control ($15/1516 = 1\%$) and genetic interference was lower in the *asb* mutant than in the control [interference = 0.3 versus 0.5, respectively; (Moens 1969)]. Moens (1969) also took advantage of heteromorphic satellites of the NOR of chromosome 2 and found that chromosome 2 synapsed only about half the time in the *as1* mutant. Therefore, the higher frequencies of double crossovers in recovered offspring from *as1* were observed amidst a background of greatly reduced chromosome pairing and synapsis. While gamete selection for increased pairing and recombination in order to produce viable progeny could skew the observed genetic crossover frequencies, this factor would not be sufficient to explain the higher double crossover frequency and reduced interference observed (Moens 1969). Moens (1969) suggested that the process of genetic exchange was itself altered in these mutants, a suggestion supported by later observations that long SC segments from *asb* mutants often had higher numbers of LNs than observed in wild-type (Havekes et al. 1999). Therefore, *as1* and *asb* have defects in crossover control as well as in synapsis, but the exact cause of the defect in either mutant is unknown.

XI. Project outline

Numerous studies have revealed a close correspondence between patterns of synaptic initiation and crossing over in a number of different organisms, and, although little is understood about crossover interference, interference may be imposed during synaptic initiation, at least in budding yeast (Zickler and Kleckner 1999; Fung et al. 2004; Bishop and Zickler 2004). The tomato asynaptic mutants *as1* and *asb* provide an opportunity to investigate the relationship between synapsis, crossing over and interference in a higher plant. Spreads of SCs from tomato

are superior in demonstrating synaptic patterns at both the LM and EM levels, and tomato is one of the few plants in which patterns of ENs and LNs have been examined in detail (Stack and Anderson 1986a; Stack and Anderson 1986b; Sherman et al. 1992; Sherman and Stack 1992; Sherman and Stack 1995; Anderson et al. 2001; Anderson and Stack 2002; Chang et al. 2007; Lohmiller et al. 2008). Since the earlier work on tomato asynaptic mutants (Soost 1951; Moens 1969; Havekes et al. 1994; Havekes 1999), new molecular approaches have been developed to examine the role of different proteins in synapsis and meiotic recombination. In this work, we take advantage of these new methods, particularly immunolocalization, to examine in more detail the relationship between synapsis, crossing over, and genetic interference in tomato asynaptic mutants, particularly *as1*.

CHAPTER 2:

SEQUENTIAL LOADING OF COHESIN PROTEINS DURING PROPHASE I IN TOMATO PRIMARY MICROSPOROCTES

Sister chromatid cohesion (SCC) is essential for faithful chromosome segregation in both mitosis and meiosis. In budding yeast, mitotic sister chromatid cohesion is established by a complex of four cohesin proteins (SMC1, SMC3, SCC1, and SCC3) (Onn et al. 2008; Peters et al. 2008; Nasmyth and Haering 2009; Uhlmann 2009). SMC1 and SMC3 belong to the structural maintenance of chromosomes (SMC) group of proteins that function in chromosome dynamics (Jessberger et al. 1998; Jessberger 2002). SMC proteins have two coiled-coil domains separated by a hinge domain and two globular domains at the N- and C-termini. Each SMC protein folds back on itself at the hinge which allows the two coiled-coil domains to interact and form an extended 45-nm rod-like structure. This folding allows the N- and C-terminal domains to interact to form a globular ATPase “head” opposite the hinge. In a cohesin complex, SMC1 and SMC3 proteins interact at the hinge domains to form a V-shaped heterodimer. The non-SMC cohesin proteins, SCC1 (a member of the kleisin family of proteins) together with SCC3, link the heads of SMC1 and SMC3 to close the open-V shape of the SMC heterodimers and form a ring (Nasmyth 2001; Losada and Hirano 2005; Onn et al. 2008; Skibbens 2009). The ring-structure of the cohesin complex is important to its role in sister chromatid cohesion, and one popular model suggests that the two sister chromatids are held together within the large ring formed by the four cohesin proteins (Nasmyth and Haering 2009). However, the exact interaction of the cohesin complex with the two sister chromatids is still a matter of debate (Guacci 2007; Onn et al. 2008; Surcel et al. 2008; Skibbens 2009).

Cohesin proteins are highly conserved among eukaryotes [although the nomenclature of the proteins is rather confused – (Onn et al. 2008; Peters et al. 2008)]. Prokaryotes also have an SMC protein that functions in chromosome dynamics although the SMC protein acts as a homodimer. The high level of evolutionary conservation in cohesin protein form and function has led some to suggest that cohesin-mediated chromosome structure is more ancient than histone-based nucleosome structure (Peters et al. 2008).

Cohesin complexes associate with DNA in a highly regulated manner through the mitotic cell cycle in eukaryotes (Nasmyth and Haering 2009; Uhlmann 2009). Sister chromatid cohesion is established at S-phase when cohesins load onto chromatin, and SCC is maintained through metaphase. At anaphase, separase cleaves SCC1, breaking the cohesin rings and allowing sister chromatid separation (Nasmyth and Haering 2009). Not all cohesin complexes are involved in SCC, however. Cohesin complexes also load onto DNA at stages other than S-phase, but these “non-cohesive” cohesins appear to be involved in responses to DNA damage and/or transcription functions (Waizenegger et al. 2000; Onn et al. 2008; Uhlmann 2009; Skibbens 2009).

During meiosis, SCC is important both for homologous chromosome separation at meiosis I and sister chromatid separation at meiosis II (Petronczki et al. 2003). SCC along chromosome arms is essential to maintain chiasmata that join homologous chromosomes and to establish monopolar orientation of sister kinetochores at metaphase I (Maguire 1978; Maguire 1995) (van Heemst and Heyting 2000; Chelysheva et al. 2005). At anaphase I, the action of separase cleaving SCC1 causes the release of cohesion along chromosome arms as well as chiasma resolution, allowing homologous chromosomes to separate (Kudo et al. 2006; Kudo et al. 2009). However, sister chromatids remain together at centromeres because the protein

Shugoshin (SGO) protects the cohesin complex in this region from separase (Hamant et al. 2005; Nasmyth and Haering 2009). At anaphase II, the remaining sister centromere cohesion is released to finally yield four haploid, unreplicated nuclei. Thus, SCC is released by separase in two phases during meiosis compared to one phase during mitosis.

Several meiosis-specific cohesin proteins have been identified in different organisms, which are important for adaptations of chromosome behavior through the two-step meiotic division. REC8 is a meiosis-specific kleisin that replaces its mitotic orthologue SCC1 and was first identified in budding yeast (Klein et al. 1999). REC8 orthologs have since been identified in many different groups including invertebrates, mammals and plants (Molnar et al. 1995; Parisi et al. 1999; Watanabe and Nurse 1999; Dong et al. 2001; Manheim and McKim 2003; Schleiffer et al. 2003; Bannister et al. 2004; Golubovskaya et al. 2006; Zhang et al. 2006; Peters et al. 2008; Nasmyth and Haering 2009). REC8 and its protection at centromeres by SGO are required for accurate implementation of the two-step meiotic division. In mammals, two meiosis-specific proteins, SMC1 β and STAG3, can replace SMC1 and SCC3 orthologs, respectively (Pezzi et al. 2000; Revenkova et al. 2001; Revenkova and Jessberger 2006). SMC1 β has been found to be important in chiasma stabilization (Hodges et al. 2005), telomere protection (Adelfalk et al. 2009), and chromatin loop organization (Novak et al. 2008) while STAG3 plays a specialized role in sister arm cohesion during meiosis (Prieto et al. 2001). So far, no meiosis-specific proteins comparable to SMC1 β has been found in other organisms, and only one meiosis-specific ortholog of STAG3, *S. pombe* REC11, has been found (Hirano 2002; Peters et al. 2008; Schubert 2009).

During meiosis, cohesin proteins are found in protein cores called axial elements (AEs) that form between sister chromatids during leptotene (Zickler and Kleckner 1999; van Heemst

and Heyting 2000; Page and Hawley 2004). During zygotene, homologous chromosomes synapse, and transverse filaments connect the two AEs of homologous chromosomes. Once synapsed, attached AEs are called lateral elements. The two lateral elements (LEs), together with transverse filaments and a central element that runs parallel between the two LEs, forms a meiosis-specific structure called the synaptonemal complex (SC). One SC runs along the length of each pair of homologous chromosomes during pachytene when synapsis is complete. At diplotene, desynapsis begins, and the two LEs are held together at only a few sites where crossing over has occurred and where chiasmata form.

While the SC is an evolutionarily conserved structure, the function of the SC in the unique events that occur during meiosis (including homologous synapsis and recombination) is still under debate (Page and Hawley 2004). Because cohesins are an integral part of SC structure, investigating the behavior of cohesin proteins during the early stages of meiosis may shed light on SC function. Such immunolocalization studies have been undertaken in mammals and grasshoppers, but the results are difficult to compare because different proteins were examined in the studies (Eijpe et al. 2000a; Eijpe et al. 2003; Valdeolmillos et al. 2007). Here, we have examined the dynamics of four cohesin proteins [SMC1, SMC3, SCC3, and REC8=SYN1=DIF1; (Schubert 2009)] in early meiotic prophase I of tomato microsporocytes using immunolocalization. While the tomato genome has been sequenced (Mueller et al. 2009), the genome has not yet been fully analyzed for cohesin genes. For comparison, the Arabidopsis genome contains only one copy each of the cohesin genes *SMC1*, *SMC3* and *SCC3* and four paralogs of the *SCC1* gene (*SYN1-4*), only one of which (*SYN1/REC8*) is meiosis-specific (Schubert 2009). Given that the Arabidopsis genome has a more recent polyploidization event than tomato (The Arabidopsis Genome Initiative 2000; Ku et al. 2000; Stack et al. 2009), it is

likely that tomato is similar to Arabidopsis in the number and types of cohesin genes and the lack of meiosis-specific variants (such as SMC1 β and STAG3 that occur in mammals). Tomato SC spreads are optimal for examining cohesin protein behavior with respect to synapsis using both light and electron microscopy.

MATERIALS AND METHODS

Plants

Wild type tomato (*Solanum lycopersicum* var. cherry, accession LA4444) seeds were planted and grown in a greenhouse with temperature control. All the plants were used before they were 3 months old.

Antibodies

Antibodies against tomato SMC3, SMC1, and MLH1 proteins were raised in rabbits and used in previous studies (Lhuissier et al. 2007; Lohmiller et al. 2008). To facilitate colocalization studies of different cohesins, we also used antibodies to tomato SMC1 that had been raised in chicken (Lohmiller et al. 2008). Rabbit antibodies to Arabidopsis cohesin proteins SYN1/REC8 and SCC3 were used as in previous studies (Cai et al. 2003; Chelysheva et al. 2005).

SC spreads, immunocytochemistry, image and data analysis

SC spreads were prepared using a hypotonic bursting technique (Lohmiller et al. 2008; Stack and Anderson 2009). SC spreads were labeled with anti-AtSCC3 serum (1:1000), anti-SISMC3 serum (1:200 for LM and 1:1200 for EM), anti-AtREC8/AtSYN1 serum (1:5000), and/or affinity-purified antibodies to SISMC1 protein (1:25). Secondary antibodies included goat anti-chicken tetramethyl rhodamine iso-thiocyanate (TRITC; Jackson Labs; diluted 1:100)

and goat anti-rabbit 488 (Molecular Probes; diluted 1:500). DAPI (4', 6-diamidino-2-phenylindole; 10µg/ml in water) was used to counterstain SC spreads, and Vectashield (Vector Laboratories) was used to mount coverslips. Labeled chromosome spreads were imaged using a Leica 5000 fluorescence microscope equipped with a grayscale CCD camera and IP Lab (ver. 4) software (Lohmiller et al. 2008). Each fluorochrome was imaged using the same settings and exposure times for every SC spread. Grayscale images were assigned artificial colors in IP Lab. The signal intensity of each image was uniformly adjusted to increase contrast and reduce background using the level command of Adobe Photoshop 7. Color images for each SC set were merged using Photoshop 7. The immunogold labeling procedure for electron microscopy was similar to that used for immunofluorescence except that SCs were prepared using a sucrose-spreading procedure, secondary antibodies were conjugated to 6 nm gold particles, and SCs were post-stained with uranyl acetate (Lohmiller et al. 2008; Stack and Anderson 2009). SC spreads were examined and photographed in an AEI801 electron microscope, micrographs were scanned at 1200 dpi, and images were assembled in Photoshop 7.

RESULTS

Antibody assessment

Immunolocalization of SMC1, SMC3, REC8, and SCC3 cohesin proteins revealed that each protein was present in AEs and LEs of SCs from leptotene into diplotene (Figures 1, 2, 3). For each cohesin, the fluorescence signal was discontinuous, and the intensity of the signals varied along the chromosomes as reported earlier by (Lhuissier et al. 2007; Lohmiller et al. 2008). However, the punctate signal of SCC3 was more discontinuous than for any of the other three cohesin proteins, a pattern that may be related to the high level of background observed for

this particular antibody when used in tomato [although not in *Arabidopsis* chromosome spreads (Chelysheva et al. 2005)]. Even though all of the cohesin signals were discontinuous, the linear nature of the AE/LEs was evident, and patterns of synapsis and desynapsis in zygotene and diplotene nuclei, respectively, could be discerned.

In addition to the discontinuous labeling of cohesins along AE/LEs, we also noted that SMC1 does not fully co-localize at similar signal intensities with any of the other cohesins at any stage of prophase I (Figures 1-3), in contrast to current models for the interaction of SCC proteins (Nasmyth and Haering 2009). To check whether this result was due to interference of the two primary antibodies during simultaneous labeling, we incubated SC spreads with one of the primary antibodies followed by the appropriate secondary antibody, captured images, then incubated the same spreads with the second antibody series and captured a second set of images (Figure 4). In all single and sequential labeling combinations of SMC1 with SMC3 or REC8, we observed discontinuous labeling of AE/LEs. We also found fluorescence intensities and exposure times for each protein, which were like those when simultaneous labeling was performed. These results show that the lack of complete cohesin protein colocalization is due to biological factors and is not a consequence of the immunolabeling procedure.

Electron microscopic (EM) immunogold localization of SMC3 revealed that the cohesin label was specific for AE/LEs (Figure 5). In addition, the gold particles were present in clusters similar to the discontinuous focal immunofluorescence pattern observed by LM (Figure 2). Similar discontinuous immunogold labeling of AE/LEs has been observed at the EM level for SMC1 in tomato (Stack and Anderson 2009).

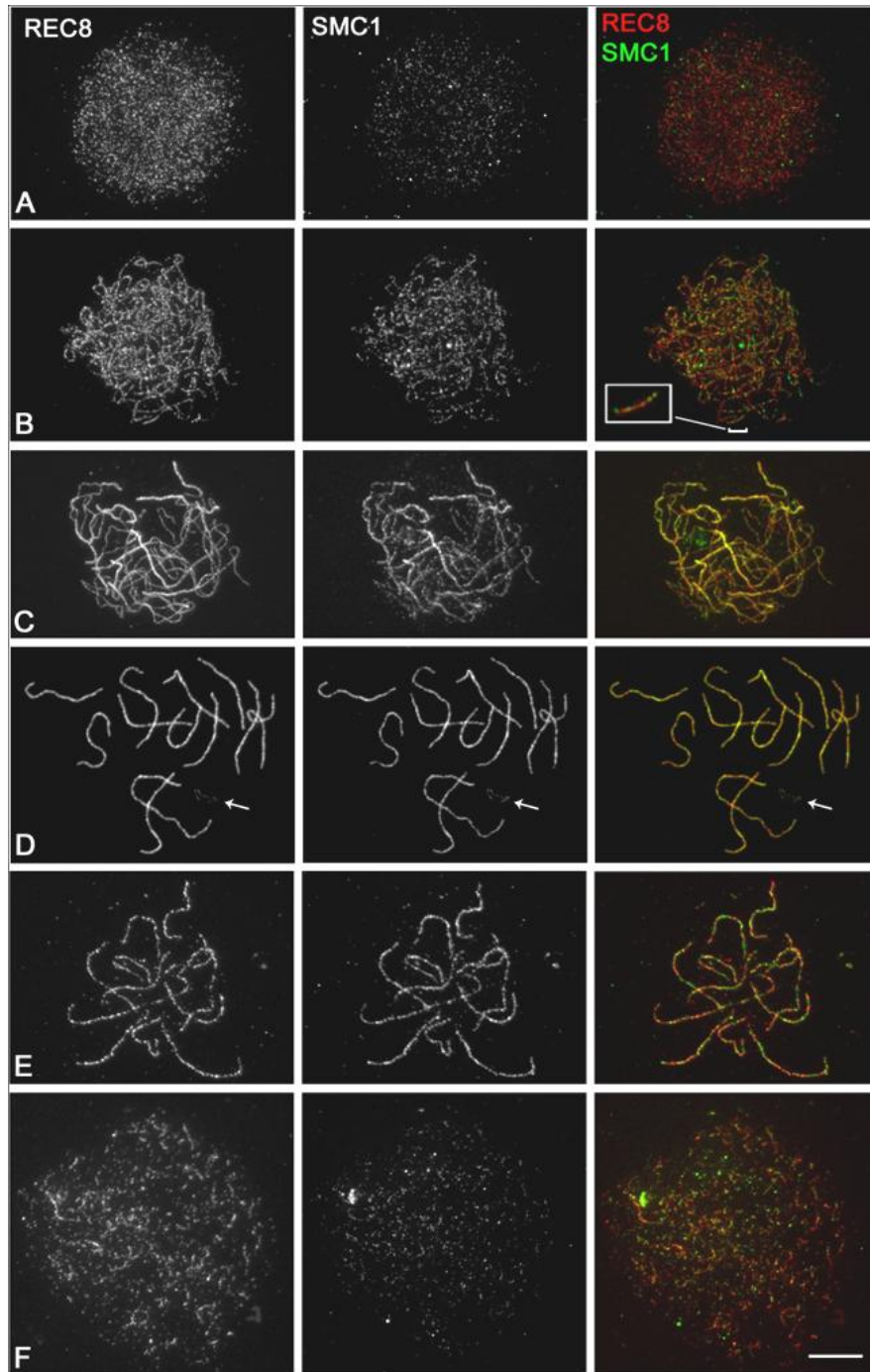


Figure 1. Colocalization of REC8 (left column) and SMC1 (middle column) with merged color image (right column with REC8 in red and SMC1 in green) in tomato SC spreads at different stages of prophase I. The same nucleus is shown in each row at (A) preleptotene, (B) leptotene, (C) zygotene, (D) early pachytene, (E) late pachytene, (F) diplotene. There are more REC8 than SMC1 foci at the earliest and latest stages examined here. Both cohesins vary in fluorescence intensity along AE/LEs. The two proteins colocalize (yellow signals) most in early pachytene (D). However, the two proteins more-or-less alternate along AE/LEs more often than they colocalize (see 2X enlarged inset shown in the right column of row B). The short arm of SC2 containing the NOR is often broken and/or asynapsed, as well as lightly stained (arrows) in row D. Bar = 10 μ m.

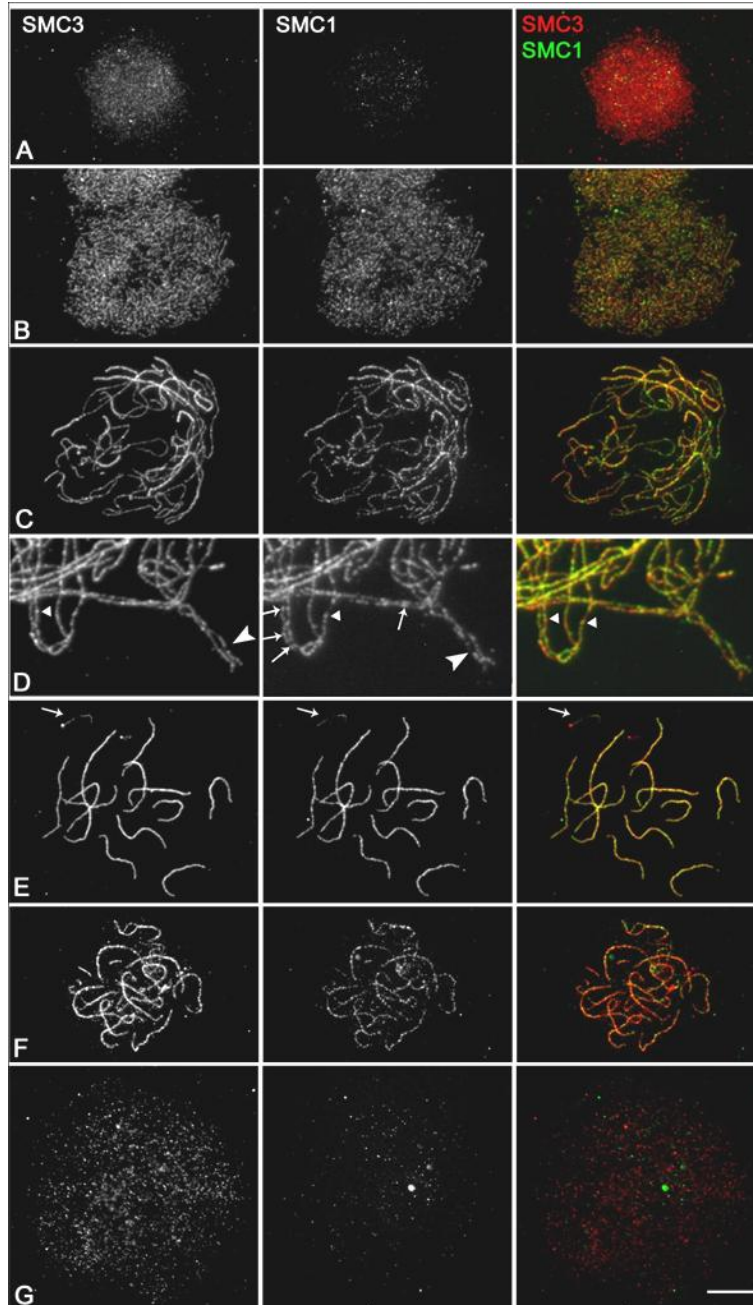


Figure 2. Colocalization of SMC3 (left column) and SMC1 (middle column) with merged color image (right column, SMC3 - red and SMC1 - green) in tomato SC spreads at different stages of prophase I. The same nucleus is shown in each row at (A) preleptotene, (B) leptotene, (C) zygotene, (D) zygotene, (E) early pachytene, (F) early diplotene, (G) diplotene. There are more SMC3 than SMC1 foci at the earliest and latest stages examined, and both cohesins vary in fluorescence intensity along AE/LEs. Note also that the intensity of the SMC3 signal is higher than that of SMC1 in early diplotene nuclei (F). In a portion of a zygotene nucleus (D), aligned AEs are shown. Bright SMC1 signals that are similar in intensity sometimes correspond at the same location on both AEs (arrows), in other cases the SMC1 signals do not correspond in intensity (small arrowheads). In addition, the SMC1 signal of one AE lacks any SMC1 signal at all on the other AE (large arrowheads, also observed for SMC3). SMC1 and SMC3 seem to alternate along AE/LEs more often than they colocalize. SMC1 and SMC3 localized together with similar fluorescence intensity (yellow signals) most in early pachytene (E). The short arm of SC2 containing the NOR is often broken and/or asynapsed, as well as lightly stained (arrows in E). Bar = 10 μ m for all but D, where the bar = 20 μ m.

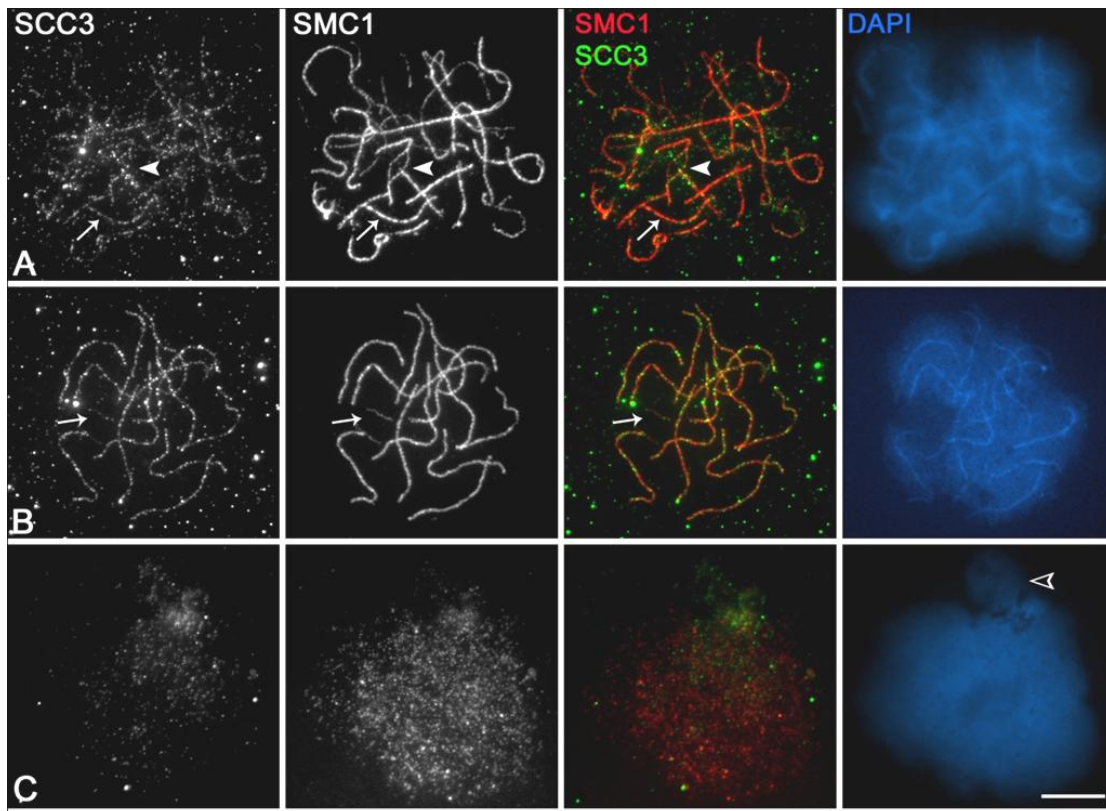


Figure 3. Colocalization of SCC3 (left column) and SMC1 (left center column) with merged color image for both cohesins (right center column, SMC1 - red and SCC3 - green) and corresponding DAPI images (right column). The DAPI images are shown here because SCC3 labeling is much reduced compared to the other cohesins. The same nucleus is shown in each row at (A) zygotene (B) pachytene, (C) diplotene. Although the background is higher than for the other cohesin antibodies, the punctate SCC3 signal is associated with both AEs (arrowheads) and LEs (arrows) in zygotene nuclei (A). At pachytene (B), the NOR (arrows) has reduced labeling for both SCC3 and SMC1. At diplotene (C), fewer SCC3 foci remain in the same nucleus compared to SMC1 foci. A tapetal cell nucleus that has only background levels of SCC3 and SMC1 signals can be seen just above the diplotene nucleus in the DAPI channel (open arrowhead in row C). The relatively high amount of signal for SCC3 and SMC1 that appears between the tapetal and PMC nuclei probably represents non-specific labeling. Bar = 10 μ m.

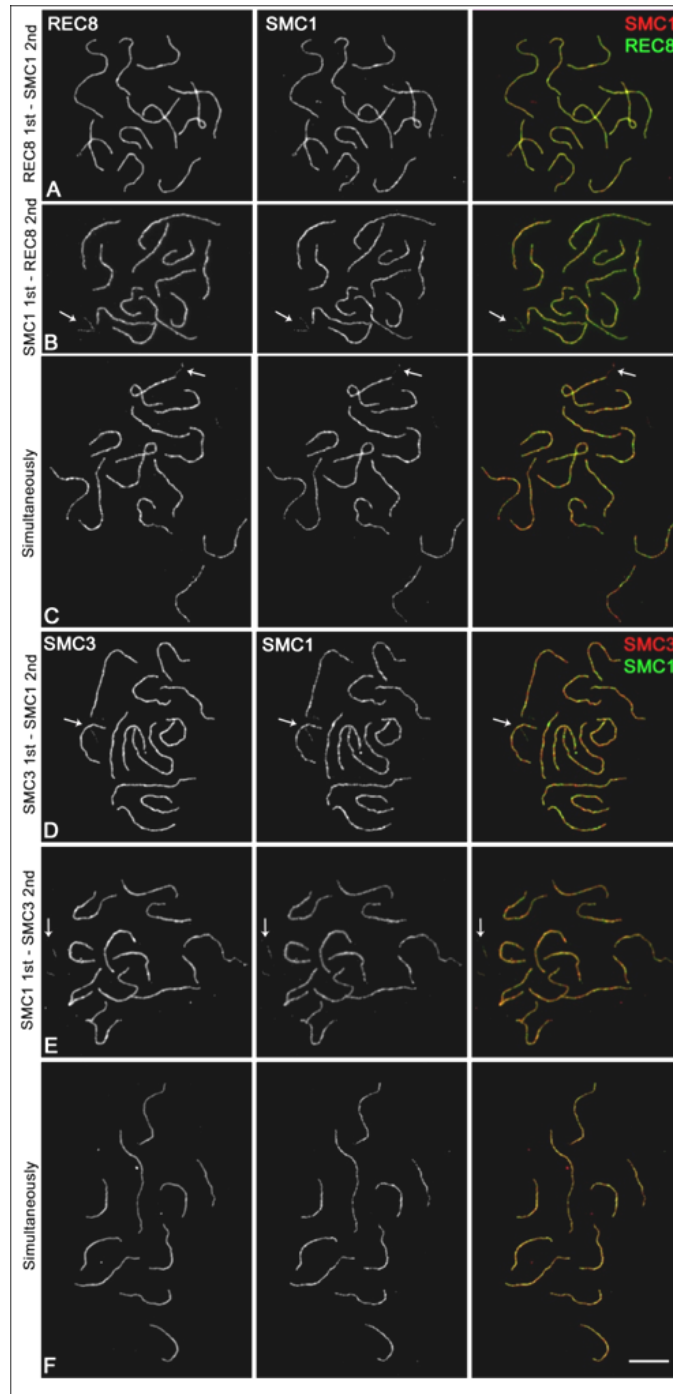


Figure 4. Colocalization of REC8 or SMC3 (left column) and SMC1 (middle column) with merged color image (right column, SMC1 - red and REC8 or SMC3 - green) on tomato pachytene SC spreads using sequential (Row A: REC8 first, image capture, SMC1 second. Row B: SMC1 first, image capture, REC8 second) (Row D: SMC3 first, image capture, SMC1 second. Row E: SMC1 first, image capture, SMC3 second) or simultaneous (Row C and Row F) antibody incubations. There are no obvious differences among the images indicating that the discontinuous AE/LE cohesin labeling is not due to antibody interference. The short arm of SC2 containing the NOR is often broken and/or asynapsed (arrows in B-E). Bar = 10 μ m.

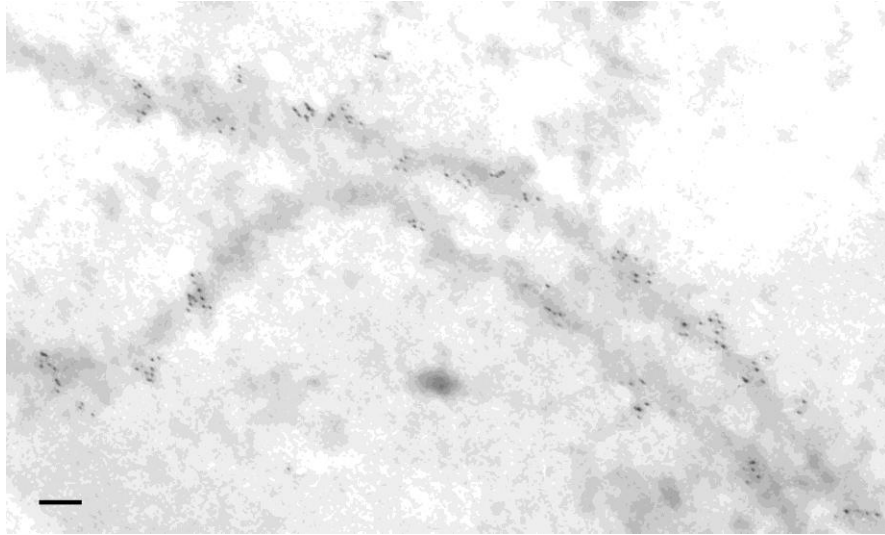


Figure 5. Electron microscopic immunolocalization of SMC3 protein on a segment of a tomato zygote SC that had been treated with DNase I prior to antibody incubations. SMC3 proteins are marked with 6-nm gold particles and are located specifically along axial and lateral elements in a discontinuous pattern similar to that observed by light microscopic immunofluorescence. Bar = 0.1 μm .

Patterns of cohesin proteins during early prophase I

REC8 and SMC1

The colocalization patterns of REC8 and SMC1 proteins were evaluated from preleptotene to diplotene in wild-type tomato nuclei (Figure 1). Before linear AEs were perceptible (preleptotene), numerous REC8 foci were observed compared to relatively few SMC1 foci in the same nuclei (Figure 1A). In leptotene nuclei, REC8 foci were still separate, but the foci were more clearly arranged in linear elements that correspond to AEs (Figure 1B). Similarly, the number of SMC1 foci increased in leptotene nuclei, and linear elements could be recognized. However, the SMC1 linear elements were often less distinct and shorter than those observed for REC8 in the same nucleus. Both REC8 and SMC1 foci were aligned along the same linear elements, but the two types of foci only rarely colocalized with similar intensity (as defined by the presence of yellow signals). Instead, most SMC1 and REC8 foci appeared in a more-or-less alternating pattern along the AEs, with minimal overlap of the two signals (Figure 1B, inset). At zygotene, REC8 and SMC1 signals along single AEs remained in an alternating pattern with relatively little colocalization (Figure 1C). However, in synapsed regions where the two LEs were closely aligned, the two signals often colocalized to yield yellow signals.

At pachytene, colocalization of REC8 and SMC1 proteins was extensive (Figure 1D). However, differences in relative staining intensity between the two proteins were still apparent with REC8 signals generally more intense than SMC1 signals. Later in pachytene (Figure 1E), both REC8 and SMC1 signals became more discontinuous and punctate, and the frequency of colocalized foci was reduced. This trend continued as SCs began to desynapse in diplotene. By middle diplotene (Figure 1F), a few linear elements were still discernable with anti-REC8, but most of the REC8 and SMC1 focal signals were dispersed within nuclei.

SMC3 and SMC1

The patterns of colocalization of SMC3 and SMC1 from pre-leptotene through diplotene were quite similar to REC8 and SMC1 through the same stages. Like REC8, SMC3 was present in greater amounts than SMC1 at preleptotene, and foci that were organized in distinct linear elements at leptotene appeared earlier with SMC3 than SMC1 (Figure 2A-B). The fluorescence intensity of SMC3 and SMC1 proteins varied so that the two proteins often appeared to be alternating in AEs from leptotene and zygotene nuclei (Figure 2B-D). In zygotene nuclei in which two homologous AEs were aligned but not yet synapsed, it was possible to compare focal patterns of the punctate SMC1 signal on the two AEs (Figure 2D, center column). SMC1 foci matched in some comparable locations on the two AEs (arrows), did not match in others (small arrowhead), and appeared to be absent altogether at some points of the aligned AEs (large arrowheads). However, we were unable to compare focal patterns along the entire lengths of homologous AEs in these spread preparations. The REC8 signal was more continuous than SMC1, but distinct regions with no REC8 signal were also observed (large arrowhead, Figure 2D, left column).

Colocalization of SMC1 and SMC3 at the same locations and with similar intensities was usually greater for SC segments than for AEs in zygotene nuclei (Figure 2C) and was greatest at pachytene (Figure 2E) although variation in staining intensities of the two proteins still evident. Most SMC1 and SMC3 foci did not colocalize in early diplotene nuclei (Figure 2F), and by middle-late diplotene (Figure 2G), numerous SMC3 foci and a few SMC1 foci were dispersed throughout nuclei with little discernable colocalization of the two proteins.

SCC3 and SMC1

As mentioned above, the SCC3 antibody labeled AEs and LEs but had a generally high background that made some meiotic stages more difficult to interpret (Figure 3). For example, we were not able to determine whether SCC3 appeared before, after or at the same time as SMC1 protein in preleptotene nuclei. SCC3 is present along both AEs and LEs in zygotene and pachytene, but in much reduced amounts and in a more punctate pattern than SMC1 (Figure 3A, 3B). However, it is not clear whether this pattern is real or a feature of this antibody. In mid-late diplotene nuclei, SMC1 is present in much larger amounts than SCC3, suggesting that SCC3 may be released from AE/LEs earlier than SMC1 (Figure 3C).

Cohesin proteins in heterochromatic regions of chromosomes

Using the length of chromatin loops as a marker, we evaluated whether there was any qualitative difference in cohesin localization in heterochromatin compared to euchromatin in pachytene SCs. All twelve tomato chromosomes have distinct blocks of pericentric heterochromatin (Peterson et al. 1996), and chromatin loops that are revealed by the SC spreading procedure are longer and extend farther from the SC in heterochromatic than in euchromatic regions from tomato (Lohmiller et al. 2008; Stack et al. 2009). This differentiation is most obvious during pachytene (Figure 6). In some pachytene SC spreads, we observed more intense and wider fluorescent signals for cohesin proteins in SC regions within pericentric heterochromatin compared to euchromatin (Figure 6A). However, this pattern was not consistently observed, even for all SCs within the same nucleus. Often there was little if any obvious difference in cohesin immunolabeling for most pachytene SC spreads from tomato (Figure 6B). When SC spreads were treated with DNase I to remove most of the overlying chromatin (Figure 6C), cohesin labeling was still variable along the SC length, but no obvious differentiation was

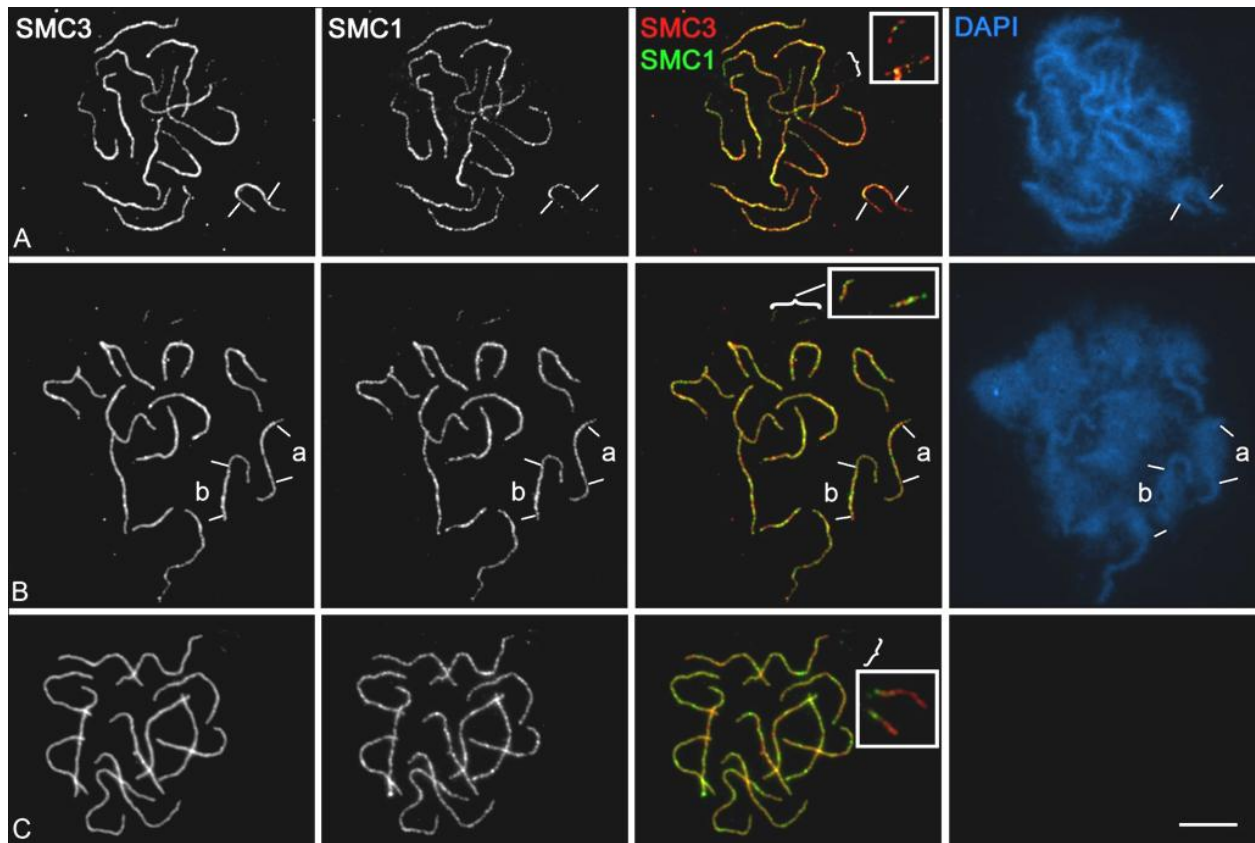


Figure 6. Cohesin labeling in heterochromatic regions of the genome. Colocalization of SMC3 (left column) and SMC1 (left center column) with merged color image (right center column, SMC3 – red, SMC1 - green) and corresponding DAPI images (right column). The loops of DNA in heterochromatin are longer than in euchromatin (borders between euchromatin and heterochromatin have been marked for some SCs with white lines in Rows A and B). (A) Some SC spreads have distinctly increased labeling of SMC3 in heterochromatic regions of SCs. Increased labeling of SMC1 in heterochromatin also occurs in this nucleus, although to a lesser extent than for SMC3. (B) Other SC spreads have little if any different cohesin labeling in heterochromatic regions of SCs. For example, the SC labeled (b) showed higher heterochromatic cohesin labeling but the SC labeled (a) did not. (C) After DNase I digestion (note the absence of DAPI signal for this nucleus), there is no obvious differential labeling of SMC3 or SMC1 in heterochromatic compared to euchromatic regions, but each cohesin still varied in intensity along the length of each SC. In contrast to the pericentric heterochromatin, cohesin labeling of the NOR was always reduced compared to the rest of the SCs. In addition, NORs are often asynapsed and/or broken off from the rest of SC2 (brackets). The cohesin signal of the NORs has been intensified and enlarged in the insets images. Bar = 10 μm (20 μm for inset images).

observed in heterochromatic compared to euchromatic sections. We also were unable to distinguish centromere positions based on the labeling patterns of the cohesin proteins. The nucleolus organizer region (NOR), located on the short arm of SC2, is also heterochromatic. In tomato SC spreads, the NOR is often asynapsed and/or broken off from the rest of the chromosome (Sherman and Stack 1992; Sherman and Stack 1995). In addition, the NOR does not stain well with DAPI (Figure 6). The signals for cohesins SMC1, SMC3, and REC8 in the NOR region were consistently less bright than for any other portion of any pachytene SC (Figure 6, also Figures 1, 2, and 5). Similar observations were made for SCC3, in spite of the higher background associated with this antibody (Figure 3B). The lower fluorescence intensity was not simply due to the fact that the NOR region was often asynapsed, as judged by comparison with AE labeling in leptotene and zygotene nuclei photographed with the same exposure settings (Figures 1, 2, 3). The less intense NOR fluorescence was also not caused by a lack of antibody accessibility because SC spreads that had been treated with DNase I to remove most overlying chromatin also showed the same pattern of reduced NOR cohesin labeling (compare Figure 6 A-B with Figure 6C). In contrast to pachytene nuclei, reduced cohesin labeling of the NOR was not obvious in leptotene or zygotene nuclei (Figures 1, 2).

DISCUSSION

The four cohesin proteins examined in this study displayed similar immunolocalization patterns during early prophase I in tomato. Each cohesin was associated with AEs and LEs of SCs from leptotene through early diplotene, and cohesin signals were discontinuous and variable in intensity along AE/LEs (Figures 1-3). Maximal colocalization of different cohesins was observed during early pachytene. However, the degree of colocalization was low during most

prophase I stages, and the temporal appearance patterns of some cohesins also differed. For example, SMC3 and REC8 foci were more numerous and appeared earlier in preleptotene, formed linear segments earlier in leptotene, and stayed longer into diplotene than SMC1 foci in tomato microsporocytes. SCC3 foci may have been released from AE/LEs earlier than SMC1 in diplotene nuclei, although the comparatively high background associated with the SCC3 antibody made these results less definite. Overall these results indicate that the associations of cohesin proteins with AE/LEs in tomato can be largely independent of one another during early prophase I.

The cytological patterns of cohesin proteins during early prophase I of meiosis have been examined in budding and fission yeasts, *C. elegans* and other invertebrates, a variety of mammals, and plants (*Arabidopsis* and maize, Klein et al. 1999; Eijpe et al. 2000a; Pasierbek et al. 2001; Prieto et al. 2001; Prieto et al. 2002; Kitajima et al. 2003; Pigozzi and Solari 2003; Eijpe et al. 2003; Cai et al. 2003; Pasierbek et al. 2003; Chan et al. 2003; Chelysheva et al. 2005; Lam et al. 2005b; Ding et al. 2006; Golubovskaya et al. 2006; Valdeolmillos et al. 2007; Severson et al. 2009; Suja and Barbero 2009). In these organisms, cohesins were integrally associated with AE/LEs, although the cohesin fluorescence signals along AE/LEs often appeared more-or less discontinuous. Some of the discontinuities could have been due to differences in preparation method (particularly the presence of detergents such as Triton X-100) and/or antibody interference in colocalizations both of which can affect cohesin labeling in mammals and *Arabidopsis* (Revenkova et al. 2001; Lam et al. 2005b). In tomato, antibody interference or limited accessibility is unlikely to be responsible for the discontinuous staining we observed because 1) discontinuous cohesin staining was detected with individual antibody labeling and with dual colocalizations, and 2) DNase-treated SC spreads in which most if not all of the

chromatin was removed also revealed discontinuous cohesin labeling by both LM and EM. However, all of our tomato SC preparations had been treated with the non-ionic detergent (NP-40) as part of the regular spreading procedure prior to fixation. Detergent, specifically Triton X-100, has been reported to extract cohesin proteins in chromosome preparations from Arabidopsis PMCs (Lam et al. 2005b). Discontinuous distribution of the cohesin AFD1 (=REC8) was also detected along AE/LEs in maize microsporocytes using a super-high-resolution light microscopic technique called three-dimensional structured illumination microscopy [3-D SIM, (Schemmelleh et al. 2008; Gustafsson et al. 2008; Wang et al. 2009)]. This method allows individual axes (AEs or LEs) to be followed at a resolution of ~100 nm in the XY axis and 250 nm in the Z-axis. The maize microsporocytes were fixed and embedded in polyacrylamide without any detergent exposure, but cells were later permeabilized with Triton X-100 before immunolabeling (Golubovskaya et al. 2006; Wang et al. 2009). Wang et al. (2009) observed that the discontinuous pattern of AFD1 localization was often mirrored on both LEs and suggested that underlying sequence or epigenetic information and/or AE assembly kinetics could be involved in the similar patterns. Even if detergent exposure is contributing to the discontinuous appearance of AFD1 in maize, the observation that both LEs are affected in the same way indicates an underlying structural/functional basis for the discontinuous pattern. Our resolution in tomato was not sufficient to compare LE localization patterns and aligned AEs showed only limited similarities in SMC3 and SMC1 focal patterns (Figure 2D). However, the alternating pattern of SMC1 with REC8 and SMC3 at all stages except early pachytene indicates that an underlying structural/functional cause is also likely to be responsible for the discontinuous cohesin patterns in tomato.

Differences in the intensity of each cohesin signal along individual AE/LEs were consistently observed in tomato SC spreads. Wang et al. (2009) observed that positions of SC twists using 3-D SIM corresponded to positions of more intense AFD1 fluorescence using conventional epifluorescence microscopy (see their Figure 1), and some of the variation we observed could be due to SC twists. However, differences in cohesin signals were still apparent in single AEs from tomato leptotene and zygotene nuclei and in LEs from maize nuclei using 3-D SIM. These results indicate that both SC twists and differences in cohesin levels along individual AE/LEs contribute to variations in cohesin signal intensity.

We did not detect consistent differences in cohesin labeling through such chromosomal landmarks as pericentric heterochromatin, kinetochores or euchromatin (Figure 1-3, 5-6), but tomato NORs were consistently less intensely fluorescent for all four cohesins compared to the rest of the LE length in pachytene nuclei. The reduced cohesin levels in the NOR may be related to the observation that the short arm of tomato SC#2 is often broken at the NOR (Sherman and Stack 1992; Sherman and Stack 1995). Such fragmentation near the NOR is not typically observed in squashes of tomato pachytene chromosomes fixed in acetic ethanol (Chang et al. 2008), so forces associated with dispersing chromatin to prepare SC spreads probably also contribute to the oft-observed NOR breakage. The differential labeling of the NOR in tomato is only noticeable at pachytene – early diplotene, and we were unable to distinguish the position of the NOR in leptotene or zygotene nuclei. Possibly the lower level of cohesins in tomato NORs at pachytene is due to loss of cohesins that had loaded earlier onto AEs in the NOR. Most other organisms showed no difference in cohesin staining in NOR, centromeres, pericentric heterochromatin, or heterochromatic knobs (in maize, Valdeolmillos et al. 2007; Wang et al. 2009; Suja and Barbero 2009) with two exceptions: reduced REC8 and SMC3 labeling through

pachytene SC in rDNA has also been observed in budding yeast (Klein et al. 1999), and reduced (or eliminated) levels of different cohesin proteins have been observed for sex chromosomes in animals (Pigozzi and Solari 2003; Page et al. 2006). The low cohesin levels in yeast NORs may be related to cohesin-independent SCC associated with tandem rDNA repeats (Nasmyth and Haering 2009). Possibly, SCC is also altered in animal sex chromosomes and tomato NORs.

The cytological behavior of different cohesins during meiosis has been reported for plants (Cai et al. 2003; Chelysheva et al. 2005; Lam et al. 2005b; Golubovskaya et al. 2006; Wang et al. 2009), but this study is the first to examine their colocalization patterns and loading/unloading order during different stages of early prophase I. However, similar colocalization and/or timing studies for cohesin proteins during meiosis have been reported for other organisms (Eijpe et al. 2003; Chan et al. 2003; Valdeolmillos et al. 2007). In rat spermatocytes, REC8 proteins appeared as spots shortly before premeiotic S phase, and two SMC proteins (SMC3 and the meiosis-specific SMC1 β) appeared later during leptotene along with two AE proteins, SYCP2 and SYCP3 (Eijpe et al. 2003). In *C. elegans*, SMC-1 and SMC-3 proteins loaded before and independently of REC-8 and SCC-3 (Chan et al. 2003). In grasshopper spermatocytes, SMC3 protein appeared before leptotene, and RAD21 (that is similar to SCC1) and stromal antigen protein 1 (SA1, that is similar to SCC3) appeared at zygotene, but only on synapsed axes (Valdeolmillos et al. 2007). In tomato, SMC3 and REC8 appeared first before leptotene followed by SMC1, and SMC3 and REC8 formed linear segments before SMC1 in early leptotene. Comparison of these results in different organisms is complicated by the fact that the same cohesins were not evaluated in the different studies. Nevertheless, it is clear that cohesin proteins do not have to be loaded onto meiotic chromosomes at the same time or as part of the same complex [(Eijpe et al. 2003; Chan et al. 2003; Valdeolmillos et al. 2007; Suja and Barbero

2009), this study]. Studies of amphibian oocyte nuclei have demonstrated that cohesins that are associated with lampbrush chromosomes are highly dynamic and quickly move on and off the axes during dictyotene (Austin et al. 2009). Such active interactions of cohesins with meiotic chromosomes may also occur earlier during prophase I and be partially responsible for the variety of cohesin immunolocalization patterns observed among different species.

The differential timing and localization of cohesins during meiosis in tomato and other organisms suggests that cohesins have other roles in addition to sister chromatid cohesion. Experiments in mitotic cells demonstrated that only those cohesins loaded during DNA replication are effective for sister chromatid cohesion and that cohesins loaded later are not “cohesive” (Guacci 2007; Austin et al. 2009; Nasmyth and Haering 2009). Similarly, in mammals, a large fraction of cohesin proteins are lost from chromosomes during mitotic prophase, and only about 10% of the total cohesins that were initially present on mitotic chromosomes remain into metaphase and are involved in sister chromatid cohesion (Sumara et al. 2000; Peters et al. 2008). This small subset of cohesins cannot be visualized by regular immunolabeling and can be seen only when individual cohesin subunits are directly labeled with a fluorescent tag. [The loss of easily-detectable cohesins from meiotic chromosomes in diplotene may be related to this mitotic prophase phenomenon (Suja and Barbero 2009)]. Based on this evidence, it is likely that cohesins loaded onto meiotic chromosomes during prophase I are incapable of providing sister chromatid cohesion.

If only a small subset of cohesins is required to provide SCC, what could be the function(s) of the rest of the cohesin proteins in meiosis? Cohesins are also involved in DNA repair and transcription control in somatic cells (Onn et al. 2008; Peters et al. 2008; Nasmyth and Haering 2009). Given the large number of DNA double-strand breaks induced by Spo11, a role

in DNA repair is particularly attractive for the non-cohesive cohesins during prophase I. Other possibilities include stabilization of meiotic chromosome structure, regulation of crossing over, or other functions related to the unique events that occur during prophase I of meiosis. Recent extensive work done by (Brar et al. 2009) has shown that Rec8 has multiple distinct and genetically separable meiotic functions in budding yeast including roles in chromosome pairing, recombination, chromosome morphogenesis, and SC assembly. So far, most work to evaluate the function of cohesin proteins in higher eukaryotes has examined null mutations that eliminate the essential role of cohesins in sister chromatid cohesion. Future experiments like those of (Brar et al. 2009) using targeted mutations in cohesin proteins will be useful in determining whether cohesins perform additional functions during meiotic prophase I in multicellular eukaryotes.

CHAPTER 3

In vivo BrdU LABELING METHOD TO STUDY THE MEIOTIC TIME-COURSE IN TOMATO POLLEN MOTHER CELLS

The duration of meiosis has been studied in many organisms (Bennett 1977). Even excluding female animals in which meiosis may be arrested for years, the time required for meiosis is highly variable, ranging from about six hours in budding yeast to three days in plants and twenty days in male animals (Bennett 1977). Meiotic duration in plants is affected by external factors, particularly temperature with faster meiotic progression at higher temperatures, and intrinsic factors including nuclear DNA content, ploidy level, and genotype (Bennett 1971; Bennett et al. 1973). In general, the larger the diploid genome, the longer the time required to complete meiosis. However, an increase in DNA content due to polyploidy does not cause a corresponding increase in meiotic duration in plants indicating that genotypic factors are also involved in the timing of meiosis. Although such genotypic effects have not been explored thoroughly, meiotic mutations usually do not cause arrest although they may cause a delay in progression and/or a reduction in fertility compared to wild-type plants (Bennett et al. 1973; Bennett 1977; Armstrong et al. 2002; Nonomura et al. 2006; Sanchez-Moran et al. 2007; Schubert 2009; Wang et al. 2010). Delays in meiotic progression can be useful in diagnosing the effects of a mutation as has been demonstrated in mice (Eijpe et al. 2003). Mutations that affect Prophase I are of particular interest since homologous chromosomes pair, synapse and recombine during that distinctive meiotic stage. Unfortunately, meiotic mutations affecting Prophase I are often difficult to evaluate since many of these mutations interfere with signature

events (such as synapsis) that are used for determining substages of prophase I. In these cases, alternative methods to evaluate meiotic duration are necessary to detect any delays caused by the mutation.

Several methods and techniques have been employed in plants to determine the overall duration of meiosis as well as the length of individual meiotic stages. One method takes advantage of the fact that pollen mother cells (PMCs) from different anthers of the same flower are often synchronized. The duration of different meiotic stages can be determined by periodically sampling individual anthers from the same flower and determining the stage of meiosis using cytological methods such as chromosome squashes or synaptonemal complex (SC) spreads (Bennett 1971; Stack and Anderson 1986b). Sampling anthers from a number of different flowers over a period of several days can establish the timing of individual stages from the beginning to the end of meiosis. This same principle can be applied to anthers or meiotic cells cultured *in vitro* (Ito and Stern 1967; Lim et al. 2001). However, this method is limited to plants with easily accessible flowers and is of limited usefulness when evaluating meiotic mutants. Another method involves the incorporation of thymidine analogs such as tritiated thymidine (H^3 -T) or 5-Bromo-2'-deoxy-uridine (BrdU) during premeiotic S-phase using pulse labeling, then evaluating the cytological stage of meiosis after different time periods have elapsed (Lima-De-Faria 1965; Bennett 1971; Armstrong and Jones 2001). This method can be applied to almost any plant species and provides a defined starting point for timing studies which is particularly important when evaluating meiosis in mutants. Of the two, BrdU labeling is preferred because it avoids the use of radioactive components, is comparatively easy to do, and has good resolution (Armstrong and Jones 2001; Armstrong et al. 2003). Several methods have been used to introduce BrdU (or H^3 -T) label into meiotic cells, but the easiest is to immerse the

cut end of a flower stem into labeling solution, (Bennett 1971) (Lima-De-Faria 1965; Armstrong and Jones 2001; Armstrong et al. 2003). Unfortunately, this procedure interferes with meiotic progression in some species such as tomato. Here, we describe a method that does not disturb meiotic development by introducing label through leaves just below the growing tip of an otherwise intact tomato plant. Using this procedure in combination with two types of chromosome preparation techniques, we have evaluated meiotic progression during early prophase I in pollen mother cells (PMCs) from wild-type and two asynaptic mutants (*as1* and *asb*) of tomato.

METHODS AND MATERIALS

Plant material

Flowering tomato plants [wild-type *Solanum lycopersicum* var. cherry, accession LA4444 and asynaptic mutants, *as1* and *asb* (Soost 1951)] were moved from a greenhouse into a controlled environment growth chamber with a 16-hour light cycle at constant 21°C temperature and allowed to equilibrate for seven days before BrdU labeling was initiated. BrdU labeling and subsequent growth (up to 6 days after labeling) occurred in the growth chamber. All plants were used before they were three months old.

BrdU Labeling

The following procedure was developed initially using aqueous 1% eosin (Lima-De-Faria 1965)) as a surrogate to evaluate the movement of BrdU through the plant. Eosin, a red dye, is easily observed by eye. Preliminary experiments showed that PMCs from flower buds about 3.0 mm long were likely to be in premeiotic S-phase. When flower buds at the growing tip were the appropriate size, petioles of two leaves immediately below the shoot apex and on opposite sides

of the stem were cut at a 45 degree angle leaving about 3cm of the petiole attached to the stem. A Tygon tube filled with aqueous 2.5×10^{-3} M BrdU (Sigma-Aldrich) was immediately linked to each cut petiole (Figure 1). If necessary, parafilm was wrapped around a petiole to increase its diameter so the tube fit better (Figure 1, arrowheads). Grease (high vacuum - Dow Corning) was applied to seal the petiole-tube joint. A small funnel was attached to the opposite end of each tube, and additional BrdU solution was added to bring the final volume to ~ 5 ml (Figure 1 arrows). Each funnel was held 5 cm higher than the two cut branches to impose a pressure and to facilitate introduction of BrdU solution. After 2.5 hrs, a total of about 6ml BrdU solution had been taken up by the plant. A clip was used to close each tube then the two tubes were removed from the petioles. After BrdU labeling, the plants were allowed to continue growing for 6 – 129 hours before buds were removed for chromosome preparation.

Preparation of chromosomes from tomato PMCs

Synaptonemal complex (SC) spreads were made using a hypotonic bursting technique described in detail by (Stack and Anderson 2009). Chromosome squashes were made as described by (Armstrong and Jones 2001) with the following modifications. Anthers from buds labeled with BrdU were fixed using 1:3 glacial acetic acid: absolute ethanol. After being fixed for at least three hours at -20°C , the anthers were rinsed three times with distilled water. Both ends of each anther were cut off using a sharp scalpel blade, and the anthers were digested for three hours at 37°C in a moist chamber using a mixture of 0.3% (w/v) of each enzyme Cellulase RS (Onozuka R10), Pectolyase Y23 (Sigma) and cytohelicase (Sigma) in 10 mM sodium citrate, pH 4.5 (Ross et al. 1996; Chang 2004; Stack et al. 2009). After digestion, anthers were washed twice with distilled water and used immediately. One anther was transferred with a small amount of water to a slide and broken up into very small clumps using a dissecting needle.



Figure 1. Method to label tomato PMC cells with BrdU. Tubes connect two cut petioles to the BrdU solution that is held in the tubes and in open funnels (arrows) above the sites of the cuts. The tube-petiole sites are sealed with high-vacuum grease and parafilm (arrowheads).

A drop of 45% acetic acid was added beside the cell mixture, and a needle was used to mix the acetic acid with the dissociated cells from the anther. The slide was heated over an alcohol lamp for about 2 seconds, a siliconized cover glass was placed on the drop, and the cells were squashed. The cover glass was removed using the dry ice method, and slides were allowed to air dry. Slides were used immediately or stored at -80°C for several months.

Antibodies, immunolabeling, microscopy, and image analysis

Axial elements and lateral elements of SCs were detected using chicken antibodies to tomato SMC1 and rabbit antibodies to tomato SMC3, diluted 1:20 and 1:200, respectively (Lhuissier et al. 2007; Lohmiller et al. 2008). Goat anti-chicken tetramethyl rhodamine isothiocyanate (TRITC; Jackson) and goat anti-rabbit TRITC (Jackson) were used at working dilutions of 1:100 and 1:50, respectively. BrdU was detected using antibodies and solution from a kit (Roche) according to the manufacturer's directions, with the following modifications. Chromosome squashes and SC spreads were first treated for 10 minutes with 0.1M ammonium chloride then blocked for 15 min. with 500 μl 10% antibody dilution buffer (ADB: 10% normal goat serum, 3% bovine serum albumin (BSA), 0.05% Triton X-100, 0.05% sodium azide in 10 mM Tris-buffered saline, pH 8) to reduce background (Lohmiller et al. 2008). The rest of the steps were done as per kit directions. The slides were washed three times, and Vectashield antifade mounting medium (Vector laboratories) containing 10 $\mu\text{g}/\text{ml}$ 4', 6-diamidino-2-phenylindole (DAPI) was mounted on the slides before photographing using a Leica DRM 5000 fluorescence microscope (Lohmiller et al. 2008).

RESULTS

BrdU labeling

We found that removing and placing the top flowering portion of a tomato plant into BrdU solution caused almost immediate cessation of meiotic development in tomato anthers, even though the cuttings appeared to remain healthy for up to two days. To avoid this problem, we developed an alternative BrdU labeling method that does not disturb the development of tomato PMCs by introducing BrdU into the transpiration stream through the vascular systems of two cut leaves located immediately below the shoot apex. Using this method, the rest of the plant remains intact and healthy, as do the PMCs in developing flowers.

We used the red dye eosin to mimic the movement of BrdU through the plant because it can be traced easily by eye. We found that if the eosin solution was introduced through the petiole of only one lower leaf, one half of each leaf and two or three anthers out of five in each bud around the shoot apical meristem were labeled with eosin. However, if the eosin solution was introduced through two petioles on opposite sides of the stem below the apical meristem, entire leaves and all the anthers in every bud in the upper plant were stained red with eosin. The speed of the eosin dye traveling through the transpiration system was ~ 0.18 cm/min, and we calculated that about 100 minutes would be enough time for eosin to travel from the cut petioles to PMC cells in most plants. When plants were labeled with BrdU for 100 minutes, PMCs were indeed labeled, but only lightly. When we increased the BrdU pulse to 2.5 hr (150 min), BrdU labeling was heavy, indicating that more time was necessary to allow BrdU to be taken up by PMCs and incorporated into replicating DNA.

We introduced BrdU to plants with young buds at different developmental stages that corresponded to different bud lengths and found that a bud length of 3.0 mm (and corresponding

anther length of ~1.4 mm) was most likely to have PMCs in premeiotic S-phase. However, bud length is only a rough indicator of anther development, and many plants exposed to the BrdU pulse label did not have labeled PMCs. Because tapetal nuclei were labeled in many of these buds (Figure 2), BrdU was available, but the PMCs were not undergoing S-phase when exposed to BrdU. This complication reduced the number of time points available to estimate meiotic progression. In addition, once buds were exposed to BrdU, anthers became more sensitive to handling and even minor perturbations affected PMC development. Therefore, we were unable to take advantage of the synchronous development of PMCs within anthers to chart meiotic development at different time points within a single bud. Instead, PMCs from entire buds were used at each time point to make chromosome squashes or SC spreads. Despite these problems, we were able to document an extended prophase I delay in two meiotic mutants compared to wild-type tomato.

Patterns of BrdU labeling through early prophase I in wild-type tomato

Defining the zero time point as immediately after the 150 minute BrdU pulse label, we obtained labeled wild-type tomato PMCs at 6, 7, 20, 24, and 28 hours after BrdU pulse labeling. These rather short time periods were chosen in order to concentrate on the timing of Prophase I substages.

Two different chromosome preparation methods were used for two buds at 6 and 7 hours post-labeling, and both gave similar results (Figure 3). PMCs from one bud that was fixed with 1:3 acetic ethanol and squashed revealed that chromosomes were just beginning to condense in the leptotene stage of meiosis (Figure 3A). BrdU label was found throughout the nuclear volume indicating that BrdU label was probably incorporated rather early in S-phase when euchromatin is being replicated. PMCs from another bud on a different plant were used to prepare SC spreads

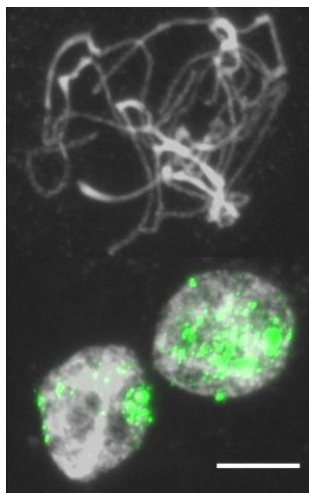


Figure 2. Immunofluorescent localization of BrdU (green) in two tapetal cell nuclei (bottom) but not in a meiotic pachytene nucleus (top). These nuclei are from the same bud and have been counterstained with DAPI (white). Scale bar = 10 μ m

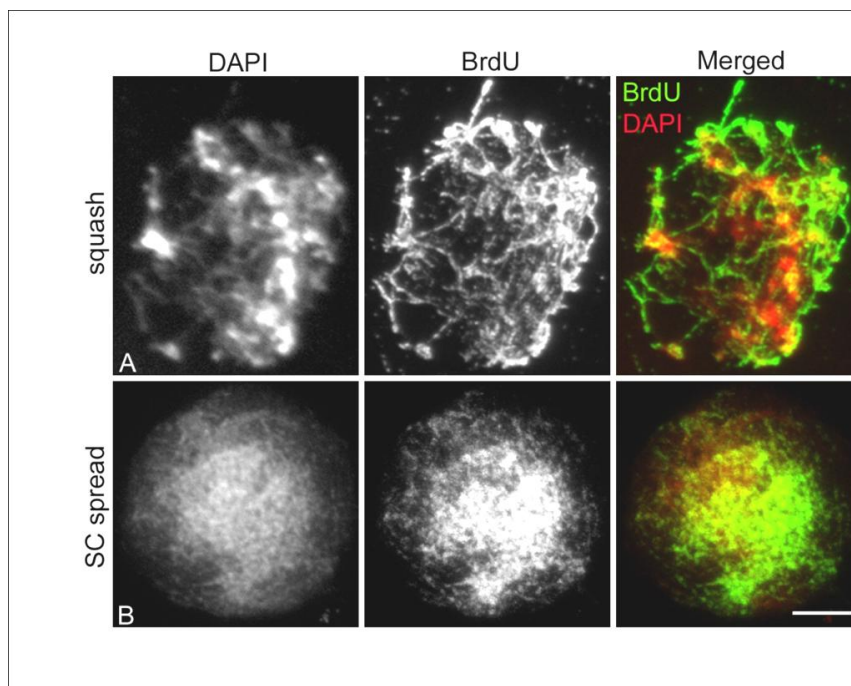


Figure 3. Immunolocalization of BrdU in leptotene PMCs. The same nucleus is shown in each row with DAPI (left), BrdU (middle), and the merged image (DAPI - red, BrdU - green). The nucleus in the top row (A) was fixed in 1:3 acetic ethanol and squashed, and the nucleus in the bottom row (B) was prepared using the SC spreading procedure. Scale bar = 10 μ m

(Figure 3B). This method of preparation disperses the loops of chromatin that are attached along the axial and lateral elements (AEs, LEs) of the two homologous chromosomes and reveals SC spreads made from a third plant 20 hrs post-BrdU labeling were also in leptotene (Figure 4) based on the presence of short linear stretches of SMC1 and SMC3 (cohesin components of axial and lateral elements) observed at this time point. Two distinct types of BrdU labeling patterns were detected from two different buds from the same plant. BrdU was evenly distributed over the entire nucleus in some spreads while BrdU was more limited in other spreads (Figure 4). The more limited BrdU labeling pattern also seemed to be associated with more condensed chromatin by DAPI staining. The latter pattern would indicate that PMCs incorporating BrdU were later in S-phase and BrdU was mostly incorporated into late-replicating heterochromatin. The other pattern suggests that the PMCs were exposed to BrdU earlier in S-phase so that BrdU was incorporated into both euchromatin and heterochromatin.

SC spreads prepared from PMCs that were 20-28 hours post-BrdU labeling were in the zygotene stage of prophase I (Figure 5). SMC1 immunolabeling showed a synaptic pattern typical of mid-late zygotene in tomato (Stack and Anderson 1986b) in which the distal euchromatic portions of the bivalents were synapsed while pericentric heterochromatic segments were unsynapsed. In these preparations, the BrdU signal was mostly excluded from the distal euchromatic portions of the chromosomes, presumably because these portions of the chromosomes had already replicated before BrdU was available to the cells. However, DNA in the pericentric, asynapsed heterochromatic regions was heavily labeled with BrdU. Within these heterochromatic regions, the BrdU signal was interrupted by unlabeled segments that probably correspond to previously-replicated DNA segments. In several areas, the patterns of unlabeled and labeled chromatin extending from AE/LEs in both unsynapsed and synapsed segments were

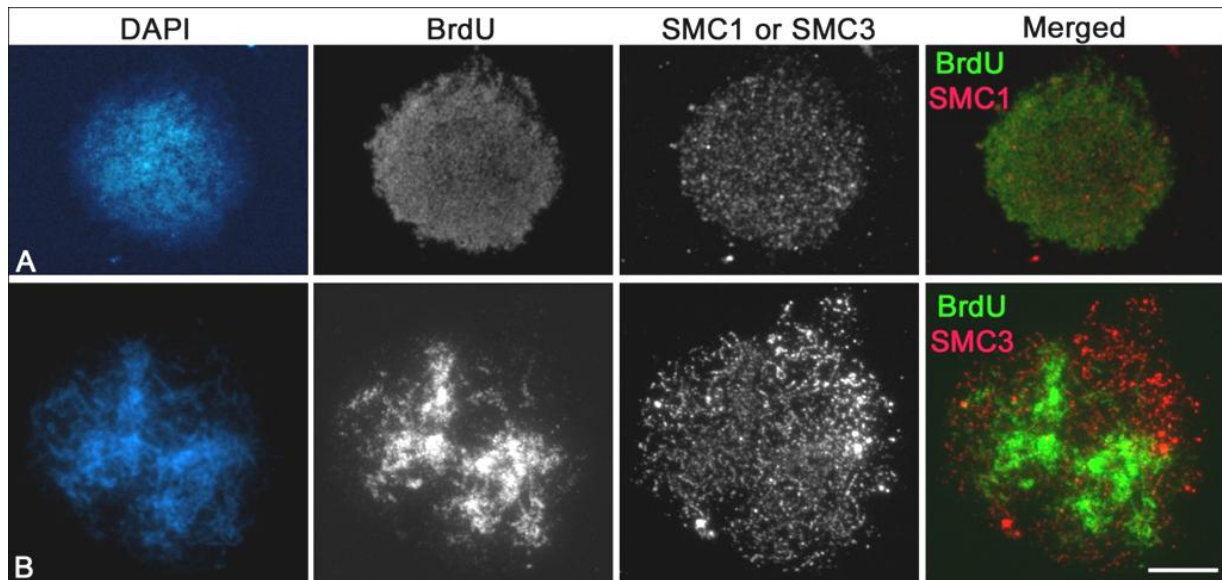


Figure 4. Coimmunolocalization of BrdU and SMC1/SMC3 in leptotene PMCs from two different buds. The same nucleus is shown in each row with DAPI (left), BrdU (left center), SMC1 or SMC3 (right center), and the merged image (right, SMC1/SMC3 - red and BrdU - green). (A) This PMc nucleus is uniformly stained by BrdU. (B) BrdU may have been incorporated at a later stage of S-phase since most of the label is present in more condensed parts of the nucleus, that usually correspond to heterochromatin. Scale bar = 10 μ m

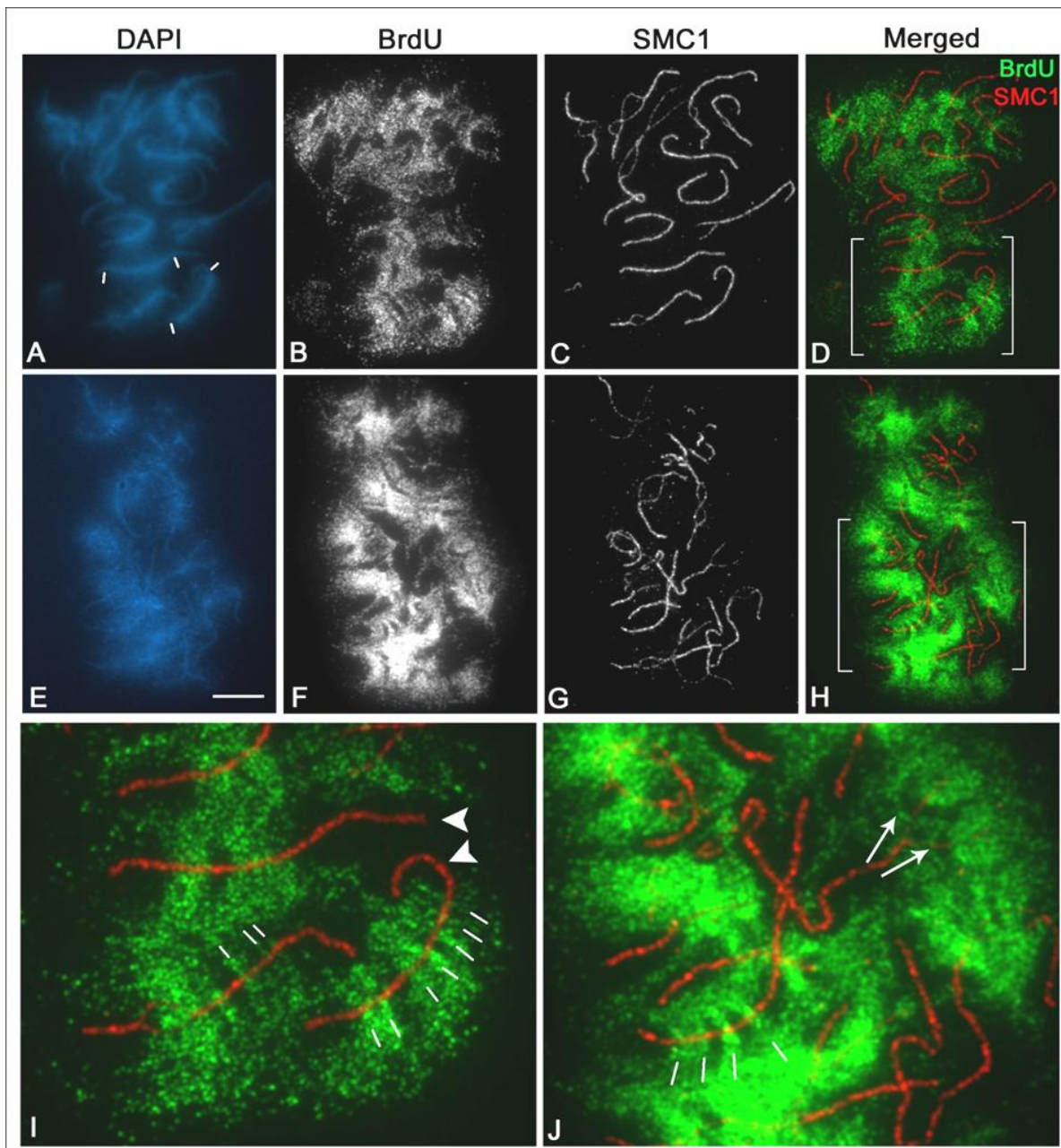


Figure 5. Coimmunolocalization of BrdU and SMC1 on tomato SC spreads at late zygotene. The overlay of merged signals shows SMC1 in red and BrdU in green. The same nucleus is shown in each row (A-D, E-H), and the position of euchromatin/heterochromatin borders for some SCs have been shown in (A). Both nuclei have BrdU labeling that is mostly incorporated in the heterochromatic portions of each bivalent, which are also usually the last parts to synapse. Bracketed parts of (D) and (H) have been enlarged in (I) and (J), respectively. (I) Distinct loops of BrdU-labeled chromatin extend from the SC (some indicated by white lines) and are separated from each other by sections of unlabeled chromatin. Arrowheads indicate unlabeled distal euchromatic region of two SCs (see borders marked in A). (J) Another example of distinct sections of BrdU-labeled and -unlabeled chromatin along zygotene SCs (some marked by white lines). Arrows indicate an unlabeled section of chromatin that is located at the same corresponded location on the two unsynapsed AEs of this SC. Scale bar = 10 μ m for (A-H) and 30 μ m for (I and J).

the same for both homologous chromosomes (Figure 5 D,H,I,J). Such patterns indicate that premeiotic DNA replication patterns were essentially identical for both homologous chromosomes.

Patterns of BrdU labeling in tomato meiotic mutants

Both asynaptic mutants, *as1* and *asb*, had substantial delays in the progression of meiosis. In *as1*, zygotene-like SC spreads were observed 40 hours after BrdU labeling. We were not able to obtain labeled PMCs from *as1* at later time points, so the delay may have been even longer. The delay in *asb* was even more pronounced with zygotene-like SC spreads still present 129 hours after BrdU labeling. Meiotic progress in wild-type tomato, in comparison, would have proceeded past pachytene by 40 hours post-labeling and into microspore or pollen formation at 129 hours post-labeling [Figure 6, (Bennett 1973; Stack and Anderson 1986b).

DISCUSSION

A popular and effective method for labeling replicating DNA in pollen mother cells is to place the cut end of a stem with flowers in a solution containing $^3\text{H-T}$ or BrdU. This method has been successfully used in a number of species including cereals (wheat, rye, barley), liliaceous species (*Lilium*, *Allium*), and *Arabidopsis* (Bennett 1971; Bennett 1973; Armstrong and Jones 2001; Armstrong et al. 2003). We found that this method was not useful for tomato, however, because cutting the stem off from the plant, even at a site far from the flowers, stopped the development of meiotic cells almost immediately. To avoid this arrest, we developed a method to introduce BrdU through cut petioles in an otherwise intact plant. Tomato PMCs continued to develop through the early stages of meiosis using this method of labeling.

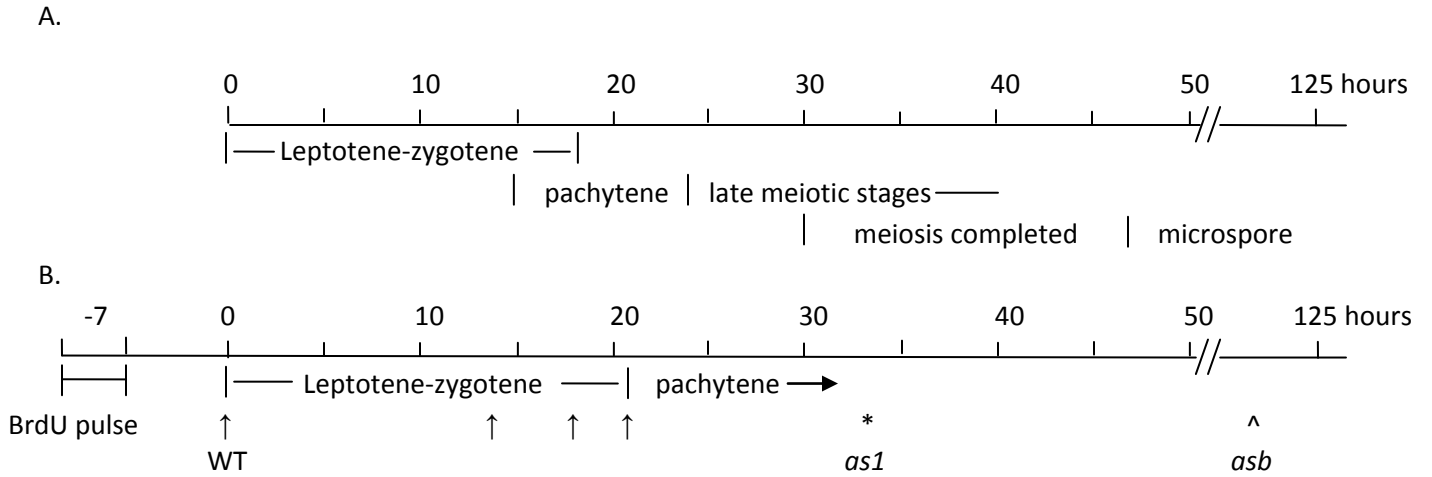


Figure 6. (A) Time course of meiosis in tomato using data from (Bennett et al. 1973; Stack and Anderson 1986b). Time zero was set as the onset of leptotene. (B) Tomato meiotic time course estimated by BrdU labeling of nuclear DNA (this work). The BrdU pulse was 2.5 hours. Bud samples were collected at the times indicated below the line (WT - ↑, *as1* - *, *asb* - ^). The onset of leptotene occurs about seven hours after BrdU labeling. Sampling times in the text include the seven hours before leptotene onset, but have been adjusted here to facilitate comparison with line A. Samples at 33 hours (*as1*) and at 122 hours (*asb*) after the onset of leptotene still have PMCs in a zygotene-like stage.

Previous studies on the duration of meiosis in tomato have used sequential sampling of anthers that are synchronized within a bud. Bennett (1973) estimated a total meiotic duration of 24-30 hours at 20 °C with the majority of that time (18 hours) required to complete prophase I. Stack and Anderson (1986b) estimated a total meiotic duration of 47 hours at 21-24 °C with prophase I lasting about 24 hours. It is not clear whether the differences in meiotic timing are due to different investigators, different plant cultivars, or some other factor(s). Although we did not carefully determine the length of time required for completion of pre-meiotic S-phase to the initiation of meiosis (leptotene) in tomato, (Armstrong et al. 2003) estimated that S-phase and G2 are of similar durations equal to about 5-9 hours in Arabidopsis. If tomato required slightly longer times for these events [as one would expect based on the close relationship between genome size and meiotic stage length (Bennett 1971)], then leptotene should start no later than 10-18 hours after BrdU incorporation. We observed leptotene cells only 6 hours after BrdU incorporation, a time well within expectation. In addition, we observed zygotene cells 24-28 hours after BrdU incorporation (or ~ 17-21 hours after the beginning of leptotene), a time consistent with previous estimates [Figure 2; (Bennett 1973; Stack and Anderson 1986b)]. Therefore, the method of incorporating BrdU through petioles of an otherwise intact plant did not appear to substantially alter meiotic progression in wild-type tomato.

We applied the same BrdU labeling technique to examine the length of early prophase I substages in two meiotic mutants, *asl* and *asb*. Traditional estimates of the lengths of prophase I substages using synaptic extent are not possible because each mutation causes extensive and persistent asynapsis during prophase I. Because of the asynapsis, the pachytene substage of meiosis is never observed, and cells appear to be in the zygotene substage well beyond the time normally required for zygotene (Figure 7). For example, zygotene-like cells were observed for

asl and *asb* at 33 and 122 hours after meiosis began (or 40 and 129 hours after the BrdU pulse label). In comparison, PMCs from wild-type tomato would have progressed at least to diplotene at 33 hours and would have completed meiosis and formed microspores or pollen by 122 hours (Figure 6). Thus, both asynaptic mutations cause substantial delays in the progression of meiosis although PMCs from plants homozygous for each mutation eventually complete meiosis and produce pollen, most of which is non-functional.

The BrdU labeling patterns observed in PMCs differed to some extent depending on whether cells were exposed to BrdU early or later during pre-meiotic S-phase. When BrdU label was incorporated in both euchromatin and heterochromatin, cells were presumably exposed to BrdU early in S-phase (Figure 3-4) while nuclei with BrdU label incorporated primarily, if not exclusively, in heterochromatic segments were probably exposed to BrdU later in S-phase (Figure 5). SC spreads of nuclei with BrdU incorporated into heterochromatin revealed small, distinct segments of labeled DNA interspersed with unlabeled segments of DNA (Figure 5). These segments were the same on both homologous chromosomes, indicating that virtually identical patterns of replication occurred in both chromosomes prior to synapsis. Similar observations have been made for meiotic cells in other organisms (Allen 1979; Latos-Bielenska and Vogel 1992; Guttenbach et al. 1999), but with less defined patterns and lower resolution than we demonstrate here. The identical pattern of BrdU labeling on both homologous chromosomes during meiosis in tomato is probably related to temporal patterns of replication in somatic cells that are related to gene density, transcriptional activity, histone modifications, nuclear positioning, and AT/GC-content of particular chromosomal domains (Zink 2006).

CHAPTER 4:

ALTERED INTERFERENCE AMONG MLH1 FOCI IS ASSOCIATED WITH CHANGES IN COHESIN PROTEINS IN TOMATO MEIOTIC MUTANT *asl*

INTRODUCTION

Synapsis between homologous chromosomes during prophase I of meiosis is dependent on the formation of programmed DNA double-strand breaks (DSBs) in a number of organisms including budding yeast, mammals, and higher plants (Keeney 2001). The pattern of synaptic initiation (synapsis = formation of the synaptonemal complex) between homologs is related to the distribution of crossovers in many organisms. In general, chromosomal regions that synapse earlier are more likely to have crossovers than regions that synapse later (Zickler and Kleckner 1999). In many plants and animals, distal euchromatic chromosome segments initiate synapsis before more proximal chromosome segments, and a large fraction of crossovers occur in these distal segments (Zickler and Kleckner 1999). Similarly, a close correspondence between synapsis and crossing over has been observed in maize inversion heterozygotes in which the frequency of inversion loops is equal to the frequency of anaphase I bridges (Maguire 1966; Maguire and Riess 1994). The best evidence for a close association between synaptic initiation sites and crossovers comes from budding yeast where mutational analysis of ZMM proteins (Zip1-4, Mer3, Msh4, Msh5) has shown a direct link between the two events (Lynn et al. 2007). However, this close association is absent in at least two plant species, *Allium fistulosum* and *A. porrum*, in which synapsis begins in distal chromosome regions while crossing over occurs close to the centromere (Albini and Jones 1984; Albini and Jones 1988; Stack and Roelofs 1996).

Nevertheless, the preponderance of evidence indicates that crossing over (or a commitment to crossing over) occurs prior to or concurrent with synaptic initiation (Schwacha and Kleckner 1997; Zickler and Kleckner 1999). Interference between crossovers (in which one crossover reduces the likelihood of another crossover nearby) may be imposed at the time of synaptic initiation, at least in budding yeast, but it is not yet clear when crossover interference might be imposed in multicellular eukaryotes (Fung et al. 2004; Berchowitz and Copenhaver 2010).

In higher plants, the relationship between synapsis and crossing over has been examined in greatest detail in mutants that do not complete synapsis (Rhoades 1947; Miller 1963; Nel 1979; Kitada and Omura 1984; Kaul and Murthy 1985; Sosnikhina et al. 1992; Havekes et al. 1994; Havekes et al. 1997; Sosnikhina et al. 1999; Pawlowski et al. 2003; Pawlowski et al. 2004). Many of the asynaptic mutants previously studied arose spontaneously and were initially identified by their reduced fertility. The reduction in fertility in these mutants is usually caused by the presence of univalents at metaphase I. Univalents form when no crossover occurs between homologous chromosomes. Without the formation of at least one crossover (often called the obligate chiasma) between homologs, the univalents segregate randomly at anaphase I, and genetically unbalanced gametes are formed. The frequency of univalents is related to the extent of asynapsis as shown by the close correspondence between the number of bivalents observed at pachytene and the number of chiasmate bivalents observed at metaphase I among three different asynaptic mutants in tomato (Havekes et al. 1994). Similar observations have been made for maize asynaptic mutants (Rhoades 1947; Miller 1963; Nel 1979). The specific defect of most asynaptic mutants in plants is unknown, as indicated by the general *as* designation of the mutations, but disruption of synapsis is often associated with a loss of crossover control. These results highlight the close relationship between synapsis and crossing over in plants.

The limited synapsis and increased frequency of univalents in asynaptic mutants leads to the prediction that offspring recovered from these plants would have reduced levels of crossing over. This expectation was observed for certain genetic intervals in the *as* mutant of maize (Nel 1979). However, studies on different intervals in the same *as* mutant demonstrated increased levels of crossing over compared to wild-type frequencies (Rhoades and Dempsey 1949). Similarly, both normal and increased levels of crossing over were observed for different genetic intervals in several asynaptic mutants of tomato (Soost 1951; Moens 1969). More recent work on maize plants in which both RAD51 genes were disrupted demonstrated reduced homologous synapsis but near-normal levels of crossing over in offspring recovered from female gametes (Li et al. 2007). In both maize and tomato, higher frequencies of double crossovers were reported for asynaptic mutants as compared to wild-type plants (Rhoades and Dempsey 1949; Miller 1963; Moens 1969; Nel 1973). One explanation for these unexpected results is that only gametes with higher levels of crossing over (and possibly higher amounts of homologous synapsis) contribute to viable progeny (Rhoades and Dempsey 1949; Soost 1951; Moens 1969). However, Dempsey (1958) found no evidence to support this hypothesis using haploid and diploid gametes from maize asynaptic mutants. The data on crossover frequencies in *as* mutants come primarily from offspring recovered from female gametes that are less affected by the mutations than male gametes. Plants carrying the homozygous *as* mutation are often essentially male-sterile (Rhoades and Dempsey 1949; Soost 1951; Dempsey 1958; Moens 1969).

To evaluate the unexpectedly high levels of crossing over associated with reduced levels of homologous synapsis in certain asynaptic mutants, we decided to use a cytogenetic approach that allows crossover patterns to be analyzed in a large sample of cells, regardless of whether the gametes formed from these cells are competent to make viable offspring. We chose to examine

the *asI* mutant of tomato because it disrupts synapsis but has little or no effect on crossover frequency according to linkage studies (Soost 1951; Moens 1969). In both studies, the reported frequency of double crossovers was higher than wild-type, also suggesting a defect in normal crossover interference. Additional work on the relationship between synapsis and crossing over was performed in the *asI* mutant using both light and electron microscopy (Havekes et al. 1994; Havekes et al. 1997). Here we extend this work using immunolocalization of proteins involved in crossing over (MLH1) and SC structure (cohesin proteins). MLH1 is a cytological marker for crossovers that are formed through the interference pathway (Anderson et al. 1999; Moens et al. 2002; Hollingsworth and Brill 2004; Guillon et al. 2005; Lhuissier et al. 2007; Falque et al. 2007; Berchowitz and Copenhaver 2010). MLH1 foci associated with pachytene chromosomes (usually on SC spreads) have been used to examine crossover patterns and interference in both animals and plants (Baker et al. 1996; Anderson et al. 1999; Lhuissier et al. 2007). MLH1 is found in a large subset (about 70%) of RNs in tomato (Lhuissier et al. 2007). The remaining RNs are thought to mark crossovers generated through the non-interference (MUS81) pathway (Hollingsworth and Brill 2004; Lhuissier et al. 2007).

In the *asI* mutant, we report increased frequencies of MLH1 foci on SC segments and decreased interference between MLH1 foci as compared to wild-type. These changes in crossing over are associated with reduced levels of cohesin proteins in SCs from *asI*, suggesting that cohesin proteins are closely involved in proper SC formation and crossover control in tomato.

MATERIALS AND METHODS

Plants: Tomato (*Solanum lycopersicum*) plants [wild-type = var. cherry, accession LA4444 and *as1* mutants (Soost 1951)] were grown from seed in a temperature-controlled greenhouse. A line of *as1* plants was maintained by cuttings from a single, homozygous plant and used for all of the experiments here. Only young plants/cuttings (≤ 3 months) were used to prepare chromosome spreads.

Antibodies: Antibodies to tomato SMC3, SMC1, and MLH1 proteins were raised in rabbits and used in previous studies (Lhuissier et al. 2007; Lohmiller et al. 2008). To facilitate colocalization studies of different cohesins, we also used antibodies to tomato SMC1 that had been raised in chicken (Lohmiller et al. 2008). Rabbit antibodies to Arabidopsis MRE11, SYN1/REC8, and SCC3 were used as in previous studies (Cai et al. 2003; Chelysheva et al. 2005; Lohmiller et al. 2008). We used the pQE31 vector (Qiagen) to add a 6X HIS tag and to express part of the C-terminus (amino acids 831-1110) of tomato RAD50 protein in *E. coli*. Expressed proteins were purified using Ni²⁺-NTA agarose beads and used to immunize rabbits to raise polyclonal antibodies. MRE11, RAD50, MLH1, and SMC1 antibodies were affinity-purified using Immuno-Pure Gentle Purification Ag/Ab procedure (Pierce) in a column containing the appropriate expressed, purified, recombinant proteins that were covalently attached to amino-link beads (Pierce).

SC spreads, immunocytochemistry, BAC-FISH, image and data analysis: SC spreads were made from pollen mother cells (PMCs) using a hypotonic bursting technique for LM (Lohmiller et al. 2008; Stack and Anderson 2009) and a sucrose-spreading technique for EM (Anderson et al. 1997). SC spreads were labeled with anti-AtSCC3 serum (1:1000), anti-SISMC3 serum (1:200 for LM and 1:1200 for EM), anti-AtREC8/AtSYN1 serum (1:5000) and/or affinity-purified

antibodies to S1SMC1 protein (1:25), S1MLH1 protein (1:200), AtMRE11 (1:500), S1RAD50 (1:400), or S1RAD51 (1:100). Secondary antibodies were goat anti-chicken tetramethyl rhodamine iso-thiocyanate (TRITC; Jackson Labs; diluted 1:100) and goat anti-rabbit 488 (Molecular Probes; diluted 1:500). DAPI (4', 6-diamidino-2-phenylindole; 10µg/ml in water) was used to counterstain SC spreads, and Vectashield (Vector Laboratories) was used to mount coverslips. Labeled chromosome spreads were imaged using a Leica 5000 fluorescence microscope equipped with a grayscale CCD camera and IP Lab (ver. 4) software (Lohmiller et al. 2008). Each fluorochrome was imaged using the same settings and exposure times for every SC spread. Grayscale images were assigned artificial colors in IP Lab. The signal intensity of each image was uniformly adjusted to increase contrast and reduce background using the levels command of Adobe Photoshop CS2. Color images for each SC set were merged using Photoshop CS2. Silver-staining was performed after immunolabeling by washing off the cover glass in Tris-buffered saline, air-drying, fixing in 4% paraformaldehyde (pH 8.5) for 5 minutes, washing in water, air-drying, and staining with 33% (w/w) silver nitrate in distilled water at 40° C for 15 minutes using a nylon screen (Sherman et al. 1992). Fluorescence in situ hybridization (FISH) using bacterial artificial chromosomes (BACs) containing tomato DNA was performed on SC spreads as described by (Stack et al. 2009). The immunogold labeling procedure for electron microscopy was similar to that used for immunofluorescence except that SCs were prepared using the sucrose-spreading procedure, secondary antibodies were conjugated to 6 nm gold particles (Electron Microscopy Sciences), and SCs were stained with aqueous 2% uranyl acetate (Lohmiller et al. 2008; Stack and Anderson 2009). Chromosome spreads were examined and photographed in an AEI801 electron microscope. Statistics were performed using Minitab ver. 15 software.

RESULTS

Incomplete synapsis and delayed meiotic progression in the *as1* mutant:

Substages of prophase I are usually defined based on the extent of synapsis, but this method is not useful in *as1* meiocytes in which synapsis is never completed. However, we were able to distinguish “early” and “late” stages of Prophase I in SC spreads from *as1* meiocytes using two other parameters: anther length and cell wall thickness. In wild-type tomato, anthers 1.5 - 1.8 mm in length contain primary microsporocytes with thin cell walls, which correspond to leptotene and zygotene stages in SC spreads. Anthers 1.9 - 2.2 mm in length contain primary microsporocytes with uneven callose cell wall thickenings, which correspond to pachytene in SC spreads (Stack and Anderson 1986b). SC spreads from *as1* primary microsporocytes were defined as “early” (corresponding to leptotene-zygotene) if they had thin cell walls and were prepared from anthers ≤ 1.8 mm long and as “late” (corresponding to pachytene) if they had uneven cell wall thickenings and were ≥ 1.9 mm long (Figure 1).

The amount of synapsis (SC formation) we observed in SC spreads from *as1* PMCs was consistent with our divisions of early and late stages. In early stage (leptotene-zygotene) SC spreads, most chromosomes were represented by AEs, and very few, if any, SC segments were observed (see examples in Figures 11 and 12). Among late (= pachytene) stage SC spreads, SC segments were often observed, but the amount of synapsis varied greatly among SC sets. A sample of fourteen silver-stained SC spreads from a single bud ranged from 1% to 73% synapsis with an overall average of 29% synapsis (Table 1; Figure 2). These numbers are similar to those reported by (Havekes et al. 1994) who observed an average of 25% synapsis for the *as1* mutant (range = 4% - 70%) in 19 SC spreads. The synaptic extent observed for individual bivalents also varied greatly. Within the same nucleus, some chromosomes were completely asynapsed, others

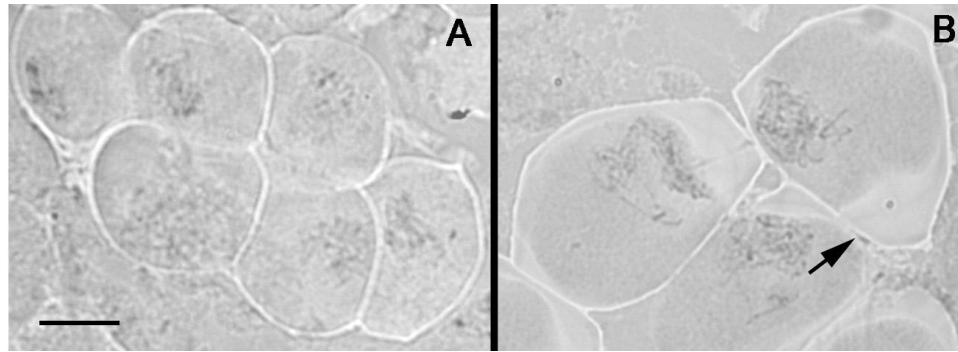


Figure 1. Phase contrast images of *asI* primary microsporocytes stained with 2% aceto-orcein at (A) early (1.8 mm anther length) and (B) late (2.3 mm anther length) prophase I stages. Note the thin, even cell walls (bright outlines) around early stage PMCs compared to the uneven cell wall thickenings (arrow) of late stage PMCs. Bar = 10 μ m.

Table 1. Total length of axial components (AEs and LEs) in SC spreads from tomatoes of different genotypes.

Genotype	No. sets	Mean % synapsis (SD)	Mean total AE/LE length* (μ m) per set (SD)	Comparison with WT (Holm-Sidak pairwise comparison after ANOVA)
<i>asI</i>	14	29.0 (19.1)	811.9 (87.0)	P < 0.001
<i>asb</i>	6	3.8 (2.9)	556.4 (45.5)	P > 0.17
WT	10	100 (0)	505.3 (53.4)	

* = total AE length + (total SC length * 2)

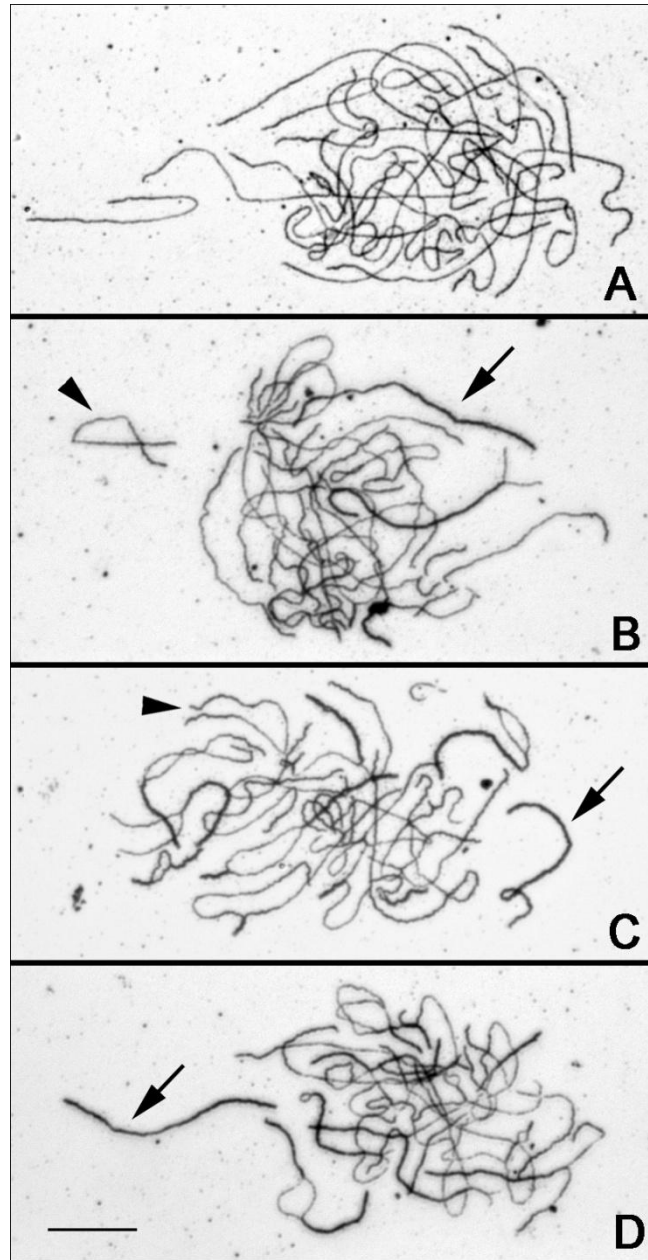


Figure 2. Examples of silver-stained SC spreads from a single, late-stage (pachytene) bud from *as1*. The amount of synapsis for (A) is 1%, (B) 20%, (C) 32% and (D) 46%. Each set except (A) has one SC that is completely synapsed along its length (arrows), but most are partially synapsed. In (B) and (C), chromosomes that are completely asynapsed are also present (some indicated with arrowheads). Bar = 10 μ m.

were partially synapsed, and sometimes a bivalent was fully synapsed (Figure 2B-D). We were not able to count the number of bivalents per cell because we could not follow individual AEs and SC segments with confidence using LM analysis. However, our results are consistent with the results of Havekes et al. (1994) who used EM analysis and found an average of six bivalents (defined as at least one SC segment linking two homologs) per nucleus.

In many plant meiotic mutants, meiosis is delayed compared to wild-type (Franklin et al. 2006). We observed a similar delay in meiotic progression in the *as1* mutant. Wild-type anthers that were 2.3 mm long contained PMCs at diakinesis-metaphase I while anthers of the same length from *as1* plants still contained PMCs at the zygotene-like stage. A similar delay for *as1* was observed using *in vivo* BrdU labeling during pre-meiotic S-phase (Chapter 3).

Synapsis is homologous in the *as1* mutant

In silver-stained SC spreads from *as1*, synapsis occurs between AEs of similar lengths and the ends of the chromosomes are well-matched [Figure 2, (Havekes et al. 1994)]. This observation suggests that synapsis is homologous in the *as1* mutant. To test this, we performed single-copy BAC-FISH on SC spreads from *as1* using four different single-copy probes, one each for chromosomes 1, 2, 4, and 10 (Table 2, Figure 3). We often observed only one signal for each probe, and we were frequently able to verify the presence of an SC at the signal location using phase images that were captured prior to the FISH procedure (Figure 3A). We also observed a number of examples of two signals for one probe, and we could often verify that the two signals were present on non-synapsed AEs (Figure 2B). These results demonstrate that synapsis is homologous in the *as1* mutant and that the presence of two signals is due to asynapsis, not non-homologous synapsis.

Table 2. Frequency of single and double signals of single copy BAC-FISH probes on SC spreads from *asl* PMCs.

Experiment	BAC	SC	Arm location*	Total # obs. nuclei	# obs. with one signal (%)	# obs. with two signals (%)
1	106H06	2	0.73L	7	6 (86)	1 (14)
	234C10	10	0.63L	11	5 (45)	6 (55)
2	130I12	1	0.86S	8	3 (38)	5 (63)
	053M02	4	0.75L	18	15 (83)	3 (17)
	234C10	10	0.63L	27	13 (48)	14 (52)

*as a fraction of arm length from the kinetochore; L – long arm; S - short arm; data from tomato FISH map at http://solgenomics.net/cview/map.pl?map_id=13.

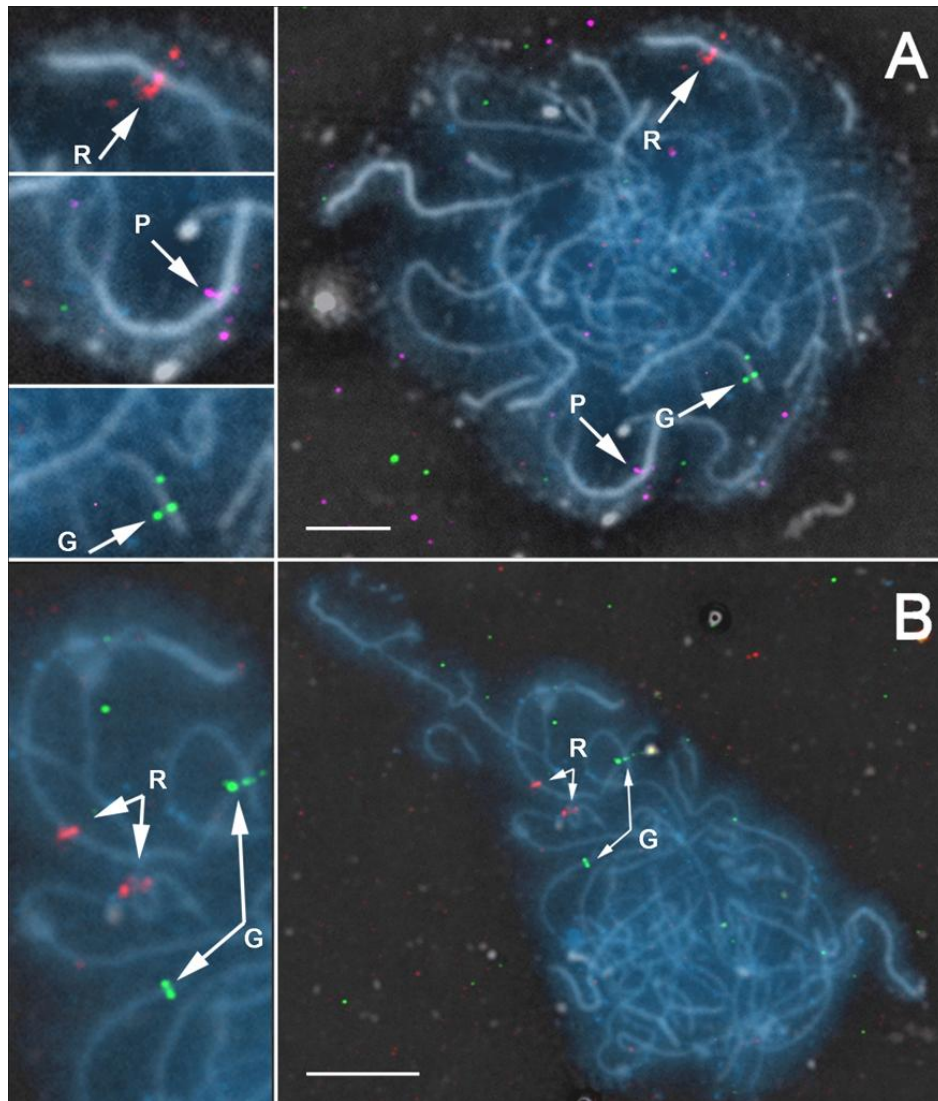


Figure 3. BAC-FISH on SC spreads from *as1* PMCs. Each set of SCs (depicted in white using inverted phase image) is overlaid with the corresponding DNA image (DAPI, blue). The positions of the single-copy BAC-FISH probes are shown in red (R; BAC234C10 on chromosome 10 long arm), green (G; BAC130I12 on chromosome 1 short arm), and purple (P; BAC053M02 on chromosome 4 long arm). In SC spreads, FISH signals often extend to one or both sides of the AE/SC axis because the chromatin is dispersed around the axes during the spreading procedure (Chang et al. 2007; Stack et al. 2009). (A) Each of the three BAC probes is present as a single signal (arrows), and each signal is associated with an SC segment (shown at high magnification in inset images at left). (B) The red and green probes each are present at two locations (linked arrows), and both signals are associated with AEs (shown at higher magnification in inset image at left). The purple probe was present as a single signal in this nucleus, but was not closely associated with either an SC or AE (not shown). Bar = 5 μ m for A (10 μ m for inset images) and 10 μ m for B (20 μ m for inset image).

The relative frequency of one compared to two signals varied among the different FISH probes (Table 1). Single FISH signals were observed for chromosomes 2 and 4 in > 80% nuclei compared to single signals in < 50% of nuclei for chromosomes 1 and 10. Although the sample sizes are not large (and not all probes worked in each nucleus), there was a general tendency for the long arms of longer chromosomes (such as chromosomes 2 and 4) to have a single signal more often than the long arm of a shorter chromosome (chromosome 10) or the short arm of a long chromosome (chromosome 1).

Focal patterns of MLH1 in the *as1* mutant were different from wild type

Although the *as1* mutation interrupts normal synapsis, it appears to have little or no effect on crossover frequency (Soost 1951; Moens 1969). To evaluate this rather unexpected finding at the cytogenetic level, we examined the frequency and distribution of MLH1 foci (Figures 4-6). The number of MLH1 foci per nucleus was more variable for the *as1* mutant (range = 2 - 32 MLH1 foci per nucleus) than for wild-type tomato (range = 10 – 21 MLH1 foci per nucleus), and the variation was not normally distributed (Figure 5). Using the Mann-Whitney Rank Sum Test, we found that the median number of MLH1 foci per nucleus was not significantly different for *as1* and wild-type (15.0 and 14.5, respectively, $P > 0.6$; Table 3). Almost all MLH1 foci were associated with SCs in *as1*, but we also observed MLH1 foci that appeared to be associated with AE (Figure 4C). These AE-associated foci were not common (15/86 total MLH1 foci = 15%), and seven of the AE-associated MLH1 foci were found in only one nucleus of the seven nuclei examined. AE-associated MLH1 foci were not considered, except in the calculations of the number of MLH1 foci per nucleus.

The differences between MLH1 foci in wild-type and *as1* were more striking when considering the number of foci per SC or SC segment (Figures 4 and 6). In wild-type tomato,

each SC usually had one MLH1 focus, and some SCs had two MLH1 foci. We also occasionally observed SCs with zero or three foci. In comparison, SC segments from *as1* were relatively short and variable in length, but many short SC segments had one or two MLH1 foci and longer SC segments had as many as six MLH1 foci, something we never observed in wild-type tomato. Accordingly, *as1* averaged significantly more MLH1 foci per μm SC compared to wild-type (Table 3). We also determined distances between adjacent MLH1 foci on the same SC segment (interfocus distance) using absolute distances (μm SC) between MLH1 foci. The average interfocus distance was significantly higher for wild-type tomato than for *as1* (11.5 and 3.3 μm SC, respectively; Table 3). Using inter-focus distances, we estimated interference between MLH1 foci on pachytene SCs in wild-type and late stage *as1* nuclei with the gamma model (de Boer et al. 2006; Lhuissier et al. 2007). The interference parameter (v) of the gamma model estimates the strength of interference. In this model, MLH1 foci have no interference if $v = 1$ while higher values of v indicate more interference and more even spacing of foci along SCs. We found that $v = 4.5$ for wild-type and $v = 1.7$ for *as1*. We did not make an adjustment to account for chromosome-end effects as described by (de Boer et al. 2006), because we could rarely follow individual partially-synapsed SCs from *as1*. Such adjustments would tend to decrease the v values observed (Lhuissier et al. 2007). Nevertheless, the lower value of v for the *as1* mutant indicates reduced interference (and less even distribution) of MLH1 foci compared to wild-type, at least on synapsed SC segments.

Table 3. MLH1 foci characteristics in SC spreads from pachytene stage wild-type and late stage *asl* primary microsporocytes.

Genotype	Median no. MLH1 foci per nucleus (no. nuclei)	Median no. MLH1 foci per μm SC (no. SC sgmts; no. nuclei)	Median inter-focus distance in μm SC (no. obs.; no. nuclei)
wild-type	14.5 (54)	0.06 (60; 5)	11.5 (26; 10)
<i>asl</i>	15.0 (81)	0.15 (57; 7)	3.3 (49; 10)
	Mann-Whitney Rank Sum Test P > 0.6	Mann-Whitney Rank Sum Test P < 0.001	Mann-Whitney Rank Sum Test P < 0.001

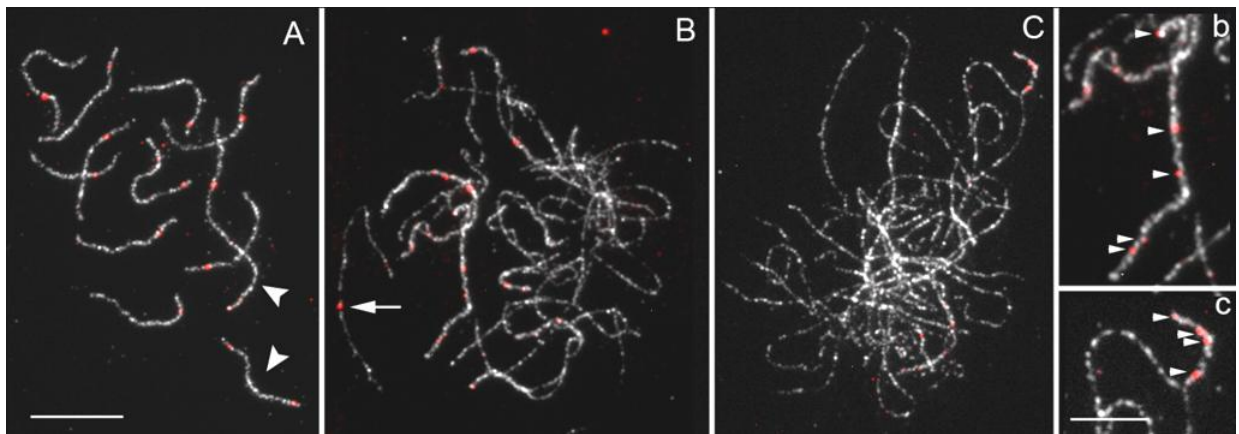


Figure 4. Immunofluorescent localization of MLH1 (red) and SMC1 (white) in SC spreads (A) from wild-type at pachytene and (B, C) from *asl* at late stage (equivalent to pachytene). In wild-type, two SCs have two MLH1 foci (large arrowheads), and each of the other SCs has one MLH1 focus for a total of 14 MLH1 foci. In the *asl* mutant, MLH1 foci are mostly associated with SC, but sometimes MLH1 foci are associated with AE (arrow). The total number of MLH1 foci is 21 in (B) and 10 in (C). Portions of B and C are shown at higher magnification at right (b and c, respectively). (b) Five MLH1 foci (small arrowheads) are present on this fully synapsed SC. (c) The short SC segment of this partially synapsed bivalent has four MLH1 foci (small arrowheads). Bar = 10 μm for (A-C) and 20 μm for (b-c).

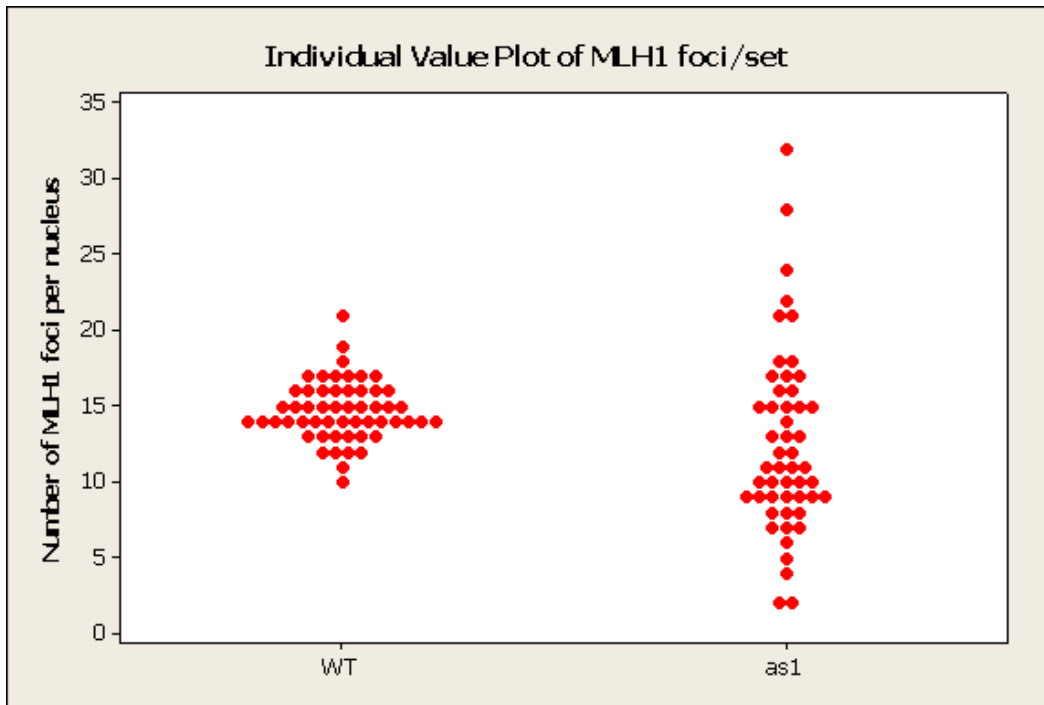


Figure 5. Plot comparing number of MLH1 foci per nucleus for wild-type (pachytene) and *as1* (late stage). Neither population is normally distributed, and the two medians (wild-type = 14.5; *as1* = 15.0) are not significantly different (Mann-Whitney Rank Sum test, $P > 0.6$).

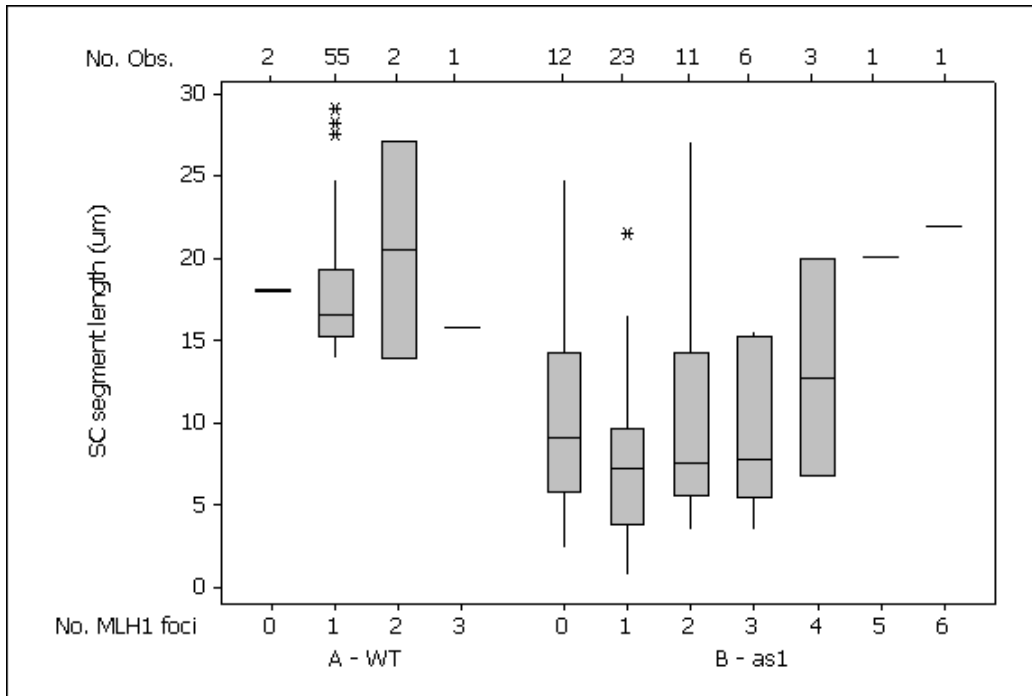


Figure 6. Boxplot showing SC segment length for wild-type (pachytene) and *as1* (late stage) as grouped by the number of MLH1 foci (0 – 6) per SC segment. The number of observations in each class is shown at the top of the plot. For each box, the lower boundary indicates the 25th percentile, the middle line indicates the median, and the upper boundary indicates the 75th percentile. Vertical whisker bars indicate 10th and 90th percentile boundaries, and outliers are shown with asterisks. For wild-type, most SCs had one MLH1 focus. For *as1*, most SC segments had 0 – 2 MLH1 foci, but up to 6 foci were observed for longer SC segments. In general, SC segments (median values) for *as1* were shorter than those for wild-type.

MLH1 is present in a subset of RNs in the *asl* mutant

We evaluated the presence of MLH1 in RNs from *asl* using EM immunogold labeling of SCs prepared by a sucrose-spreading procedure. The immunogold labeling is more specific with less background at the EM level using the sucrose-spreading procedure, although it yields fewer complete sets of SCs than the hypotonic spreading procedure we typically use for LM immunolabeling. At the LM level, sucrose-spread SCs labeled with MLH1 in a frequency and pattern similar to our usual procedure (Figure 7). By EM, we verified that MLH1 foci in the *asl* mutant and in wild-type corresponded to RNs (Figures 8, 9). However, not all RNs observed by EM in the mutant or wild-type were labeled. About 82% of the SC-associated RNs in wild-type and about 72% of the SC-associated RNs in *asl* were MLH1-positive (Table 4A; Figures 8, 9). These frequencies are similar to those reported for wild-type tomato by (Lhuissier et al. 2007). We also observed MLH1-labeled RNs that were associated with AEs, as observed by LM (Figures 9E and 4). Other unlabeled RNs were associated with AEs, but definitively identifying them as RNs is more problematic, and we did not attempt to quantify MLH1-positive and MLH-negative AE-associated RNs in *asl*.

RNs in the *asl* mutant were larger than RNs in wild type

We measured the length (parallel to LE axes) and width (perpendicular to LE axes) of MLH1-positive RNs from *asl* and wild-type SC spreads (Table 4B; Figure 10). While *asl* and wild-type RNs did not differ in length (132 nm and 133 nm, respectively, $p > 0.9$), RNs from *asl* were significantly wider than RNs from wild-type (92 nm compared to 69 nm, $p < 0.001$). Both RN sizes are larger than the average 100 x 50 nm size previously reported for RNs (Anderson and Stack 2005), and the difference is likely caused by the immunolabeling procedures that

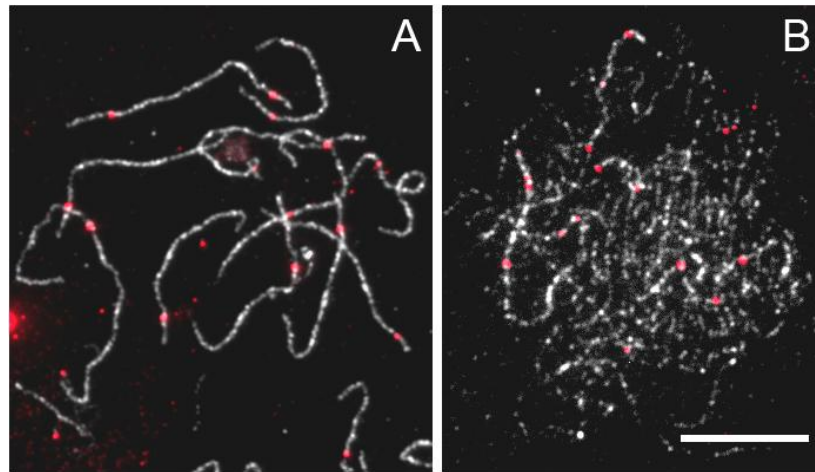


Figure 7. Immunofluorescent localization of MLH1 (red) and SMC1 (white) on sucrose-spread SCs from wild-type (A) and *as1* (B). The labeling pattern is similar to SC spreads made using the hypotonic spreading procedure (as in Figure 4). Scale bar = 10 μ m.

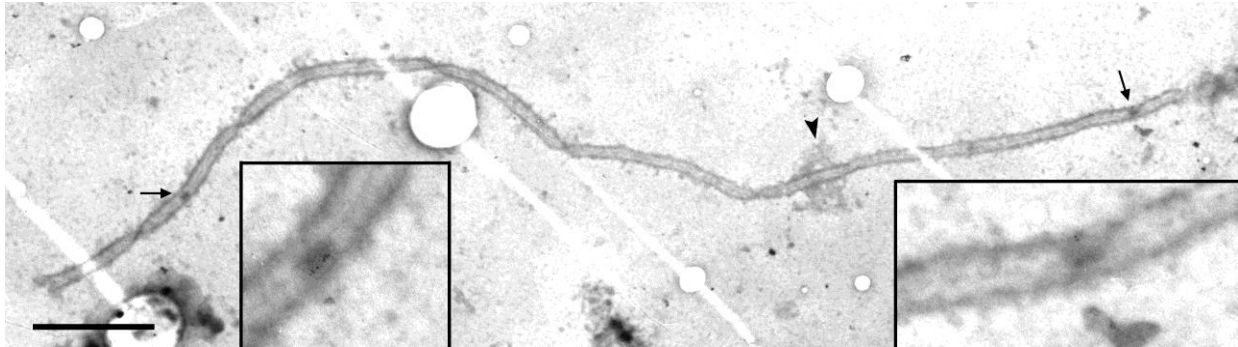


Figure 8. Electron micrograph of DNase I-treated sucrose-spread pachytene SC from wild-type that was labeled with anti-MLH1 and 6 nm gold-conjugated secondary antibodies. This SC has a kinetochore (arrowhead) and two RNs (arrows) that are shown at higher magnification (4x) in insets. The RN to the left in the long arm is labeled while the RN to the right in the short arm is not labeled. Scale bar = 1 μm for main figure and 0.25 μm for insets.

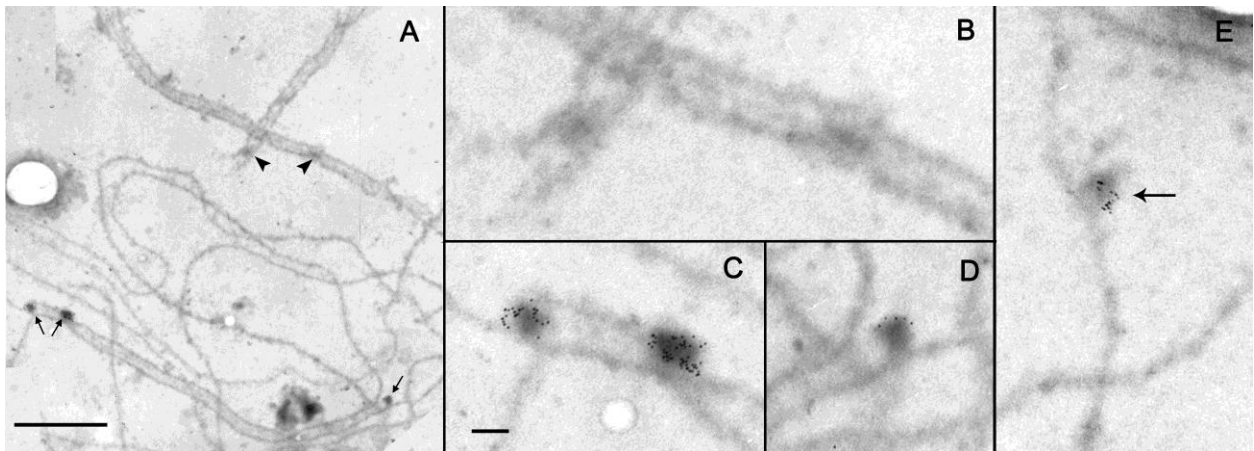


Figure 9. Electron micrograph of DNase I-treated sucrose-spread late-stage SCs from *as1* that have been labeled with anti-MLH1 and 6 nm gold-conjugated secondary antibodies. (A) Three labeled RNs (arrows) and two non-labeled RNs (arrowheads) are associated with SC segments. The non-labeled (B) and labeled (C, D) RNs are presented at higher magnification (4x) to the right. (E) Some labeled RNs were associated with AEs (arrows). Scale bars = 1 μm for (A) and 100 nm for (B-E).

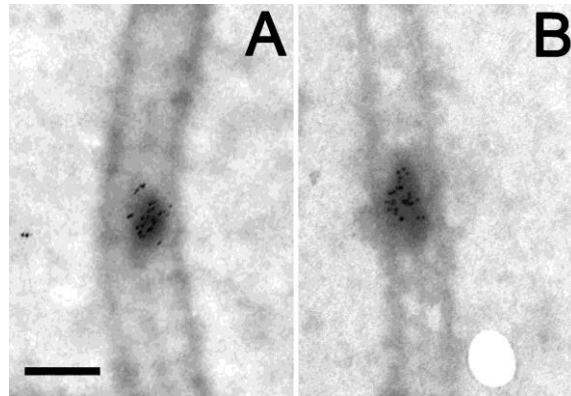


Figure 10. Electron micrographs of MLH1-labeled RNs from (A) wild-type and (B) *as1* showing the larger size of RNs from *as1*. Scale bar = 100 nm.

Table 4. Immunolabeling and size characteristics of RNs from wild-type and *as1* SC spreads.

A. Frequency of MLH1-labeled RNs				
Genotype	# SCs or SC segments obs.	No. RNs obs.	No. MLH1-pos. RNs (%)	No. MLH1-neg. RNs (%)
wild-type	26	33	27 (82)	6 (18)
<i>as1</i>	33	79	57 (72)	22 (28)
B. Average size of pachytene (or “late”) stage MLH1-labeled RNs				
Genotype		No. RNs obs.	RN length (nm) Mean (SD)	RN width (nm) Mean (SD)
wild-type		19	133 (24)	69 (11)
<i>as1</i>		44	132 (30)	92 (23)
t- test			P > 0.9	P < 0.001

expose the RNs to aqueous solutions for several hours before fixation for EM. We also noted a general tendency for MLH1 foci from *as1* to be larger than those from pachytene SC spreads in wild-type, which could be related to the difference in size observed at the EM level.

Focal patterns of MRE11 and RAD50 in *as1* were similar to those in wild type

To evaluate whether the higher frequency of MLH1 foci in *as1* is a result of a defect in an earlier stage of meiotic recombination, we examined immunolocalization patterns of MRE11 and RAD50 proteins. Both proteins are involved in meiotic recombination shortly after DSB formation, and defects in either protein cause asynapsis in Arabidopsis (Bleuyard et al. 2004; Puizina et al. 2004). In wild-type tomato, numerous MRE11 and RAD50 foci were associated with AEs and SCs in leptotene and zygotene nuclei, and RAD50 foci were brighter and more distinct though less numerous than MRE11 foci at these early stages [Figure 11, (Lohmiller et al. 2008)]. In comparison, we also observed numerous MRE11 and RAD50 foci associated with AEs and SCs in early *as1* nuclei, and the foci were similar in size and intensity to MRE11 and RAD50 foci in wild-type (Figure 11). The average number of MRE11 and RAD50 foci per nucleus in *as1* was not statistically different from that of wild-type tomato (Table 5). Thus, the cytological patterns of MRE11 and RAD50 foci are similar in both the *as1* mutant and wild-type tomato.

RAD51 patterns in *as1* and wild type were similar

Increased numbers of DSBs (as measured by RAD51 foci) are correlated with increased numbers of crossovers, at least in *C. elegans* (Tsai et al. 2008). To evaluate whether a similar situation is occurring in the *as1* mutant, we examined the immunolabeling pattern of RAD51 in wild-type tomato at zygotene compared to early stage *as1* mutant (Figure 12). Our observations

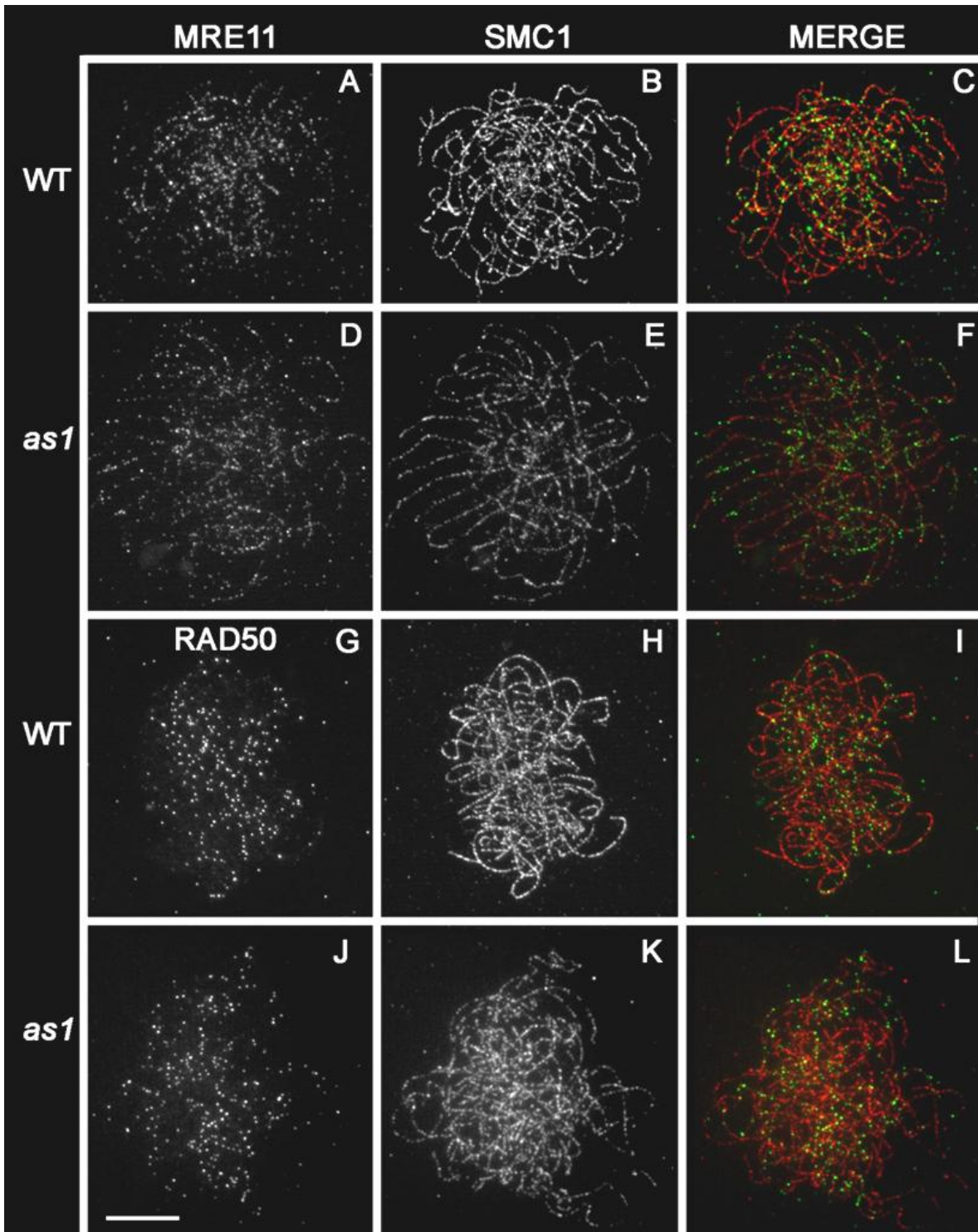


Figure 11. Immunofluorescent co-localization of (A, D) MRE11 and (B,E) SMC1 or (G, J) RAD50 and (H, K) SMC1 on SC spreads from wild-type at leptotene (A-C; G-I) and *as1* at early stage (D-F, J-L). In the merged images (C, F, I, L), MRE11 and RAD50 are in green and SMC1 is in red. Numerous MRE11 and RAD50 foci are present in early stages of both wild-type and *as1*. Scale bar = 10 μ m.

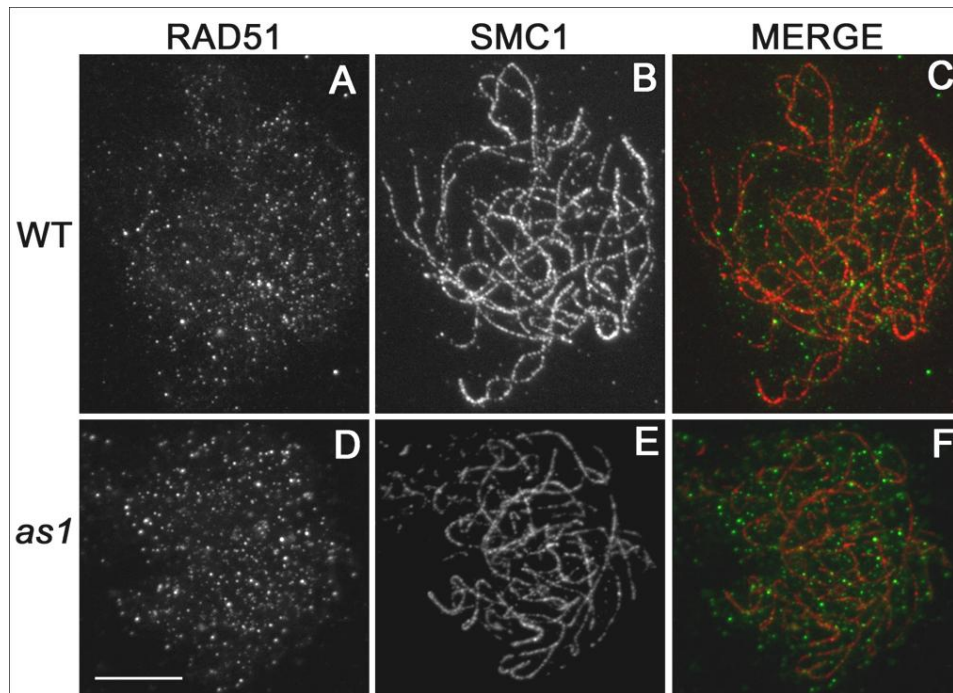


Figure 12. Immunofluorescent co-localization of (A, C) RAD51, (B,D) SMC1, and the merged images (C,E) with RAD51 in green and SMC1 in red in a zygote SC spreads from wild-type (A-C) and an early SC spread from *as1* (C-E). Numerous RAD51 foci that vary in size are present in early stages of both wild-type and *as1* nuclei. Scale bar = 10 μ m.

Table 5. Frequencies of MRE11, RAD50 and RAD51 foci in leptotene-zygotene wild-type and early stage *as1* SC spreads.

Foci type	Genotype	No. Nuclei Obs.	Mean number of foci per nucleus (Std. Dev.)	P Value (t-test)
MRE11	WT	8	584 (164)	0.182 (NS)
	<i>as1</i>	8	459 (190)	
RAD50	WT	10	239 (183)	0.645 (NS)
	<i>as1</i>	10	269 (76)	
RAD51	WT	14	281 (113)	0.548 (NS)
	<i>as1</i>	9	310 (112)	

of RAD51 foci were similar for both genotypes. RAD51 foci were variable in intensity and were present on AEs and SCs and in the surrounding chromatin in both wild-type and *asl*. In addition, the frequencies of RAD51 foci were similar in both wild-type and *asl* nuclei (Table 5).

Therefore, we found no obvious difference in RAD51 labeling in wild-type compared to *asl*.

Cohesin immunolabeling was altered for three of the four cohesin proteins in *asl*

Four cohesin proteins (SMC1, SMC3, REC8, and SCC3) are components of AE/LEs in wild-type tomato primary microsporocytes [(Lhuissier et al. 2007; Lohmiller et al. 2008), Chapter 3). Cohesin immunolabeling reveals synaptic patterns from leptotene through early diplotene stages even though the immunofluorescence signals are variable in intensity and sometimes discontinuous, especially along the length of AEs in wild-type tomato. This appears to be a property of the AE/LEs instead of a problem with antibody accessibility since removing overlying chromatin with DNase does not change the discontinuity of the fluorescent signals. However, the more discontinuous signal for SCC3 may be related also to the higher background observed with this antibody compared to the other cohesin antibodies (Chapter 3).

Cohesin immunolabeling in SC spreads from *asl* revealed similarities as well as differences compared to wild-type tomato (Figure 13). The SMC3 signal in the *asl* mutant was indistinguishable from that of wild-type for both AEs and LEs of SCs (Figures 13A, 13E1). However, immunofluorescence signals for SMC1, SCC3 and REC8 were much reduced in the *asl* mutant, and AE/LEs were barely, if at all, visible using standard immunolabeling procedures and imaging (Figure 13 F1-H1). When the images from Figure 13 F1-H1 were equally enhanced using software, the SMC3 signal became overexposed, but still no clear signal was observed for SCC3 in the *asl* mutant (Figure 13 F2 and H2). Additional enhancement of SMC1 and REC8 images showed that both cohesins were present along AE/LEs (albeit at reduced levels), but the

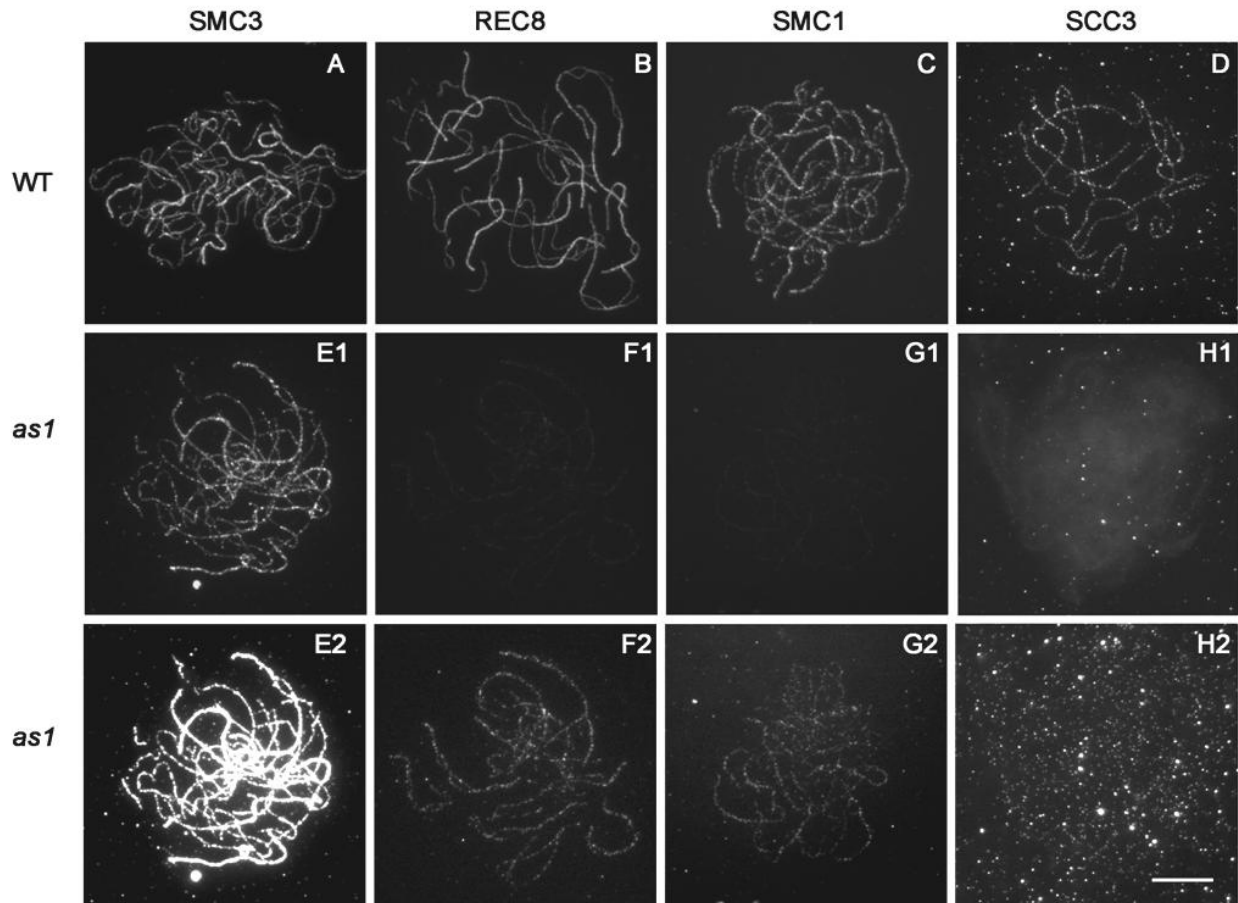


Figure 13. Immunofluorescent localization of SMC3 (A, E1, E2), REC8 (B, F1, F2), SMC1 (C, G1, G2), and SCC3 (D, H1, H2) on tomato SC spreads from wild-type (A-D) and *as1* (E1 – H2). The corresponding DAPI image has been superimposed over the SCC3 signal to show the outline of the SC spread (H1). The images in A-D and E1-H1 were all captured with the same settings and time exposure and enhanced the same way. Under these conditions, SMC3 immunofluorescence is similar for wild-type (A) and *as1* (E1), but the signals for REC8, SMC1, and SCC3 are barely visible in *as1* compared to wild-type. After additional enhancement was applied equally to E2-H2, the SMC3 signal was over-enhanced (E2), REC8 (F2) and SMC1 (G2) signals became visible along both SC and AE segments (although the signals remained rather spotty and discontinuous), and no definite SCC3 (H2) signal could be detected. Scale bar = 10 μ m.

SMC1 and REC8 signals were still more discontinuous in the *as1* mutant than in wild-type tomato (Figure 13F2, 13G2). To test whether the absent/reduced fluorescence of SCC3, SMC1 and REC8 in the *as1* mutant was caused by AE/LE breakdown during the spreading procedure, we labeled SC spreads from *as1* with both SMC1 and SMC3 (Figure 14) or silver-stained the SC spreads after SMC1 labeling (Figure 15). In both cases, we observed continuous AEs and SCs with SMC3 labeling and with silver-staining in spite of the discontinuous SMC1 label. In addition, AE/LEs of *as1* SC spreads visualized by EM showed no clear difference in AE/LE structure compared to wild-type (Figures 8-10). However, the central element was less continuous and the width of the central region between the LEs was sometimes more narrow in the mutant (Figures 8-10). Lack of antibody accessibility also does not account for the reduced and discontinuous SMC1 labeling in *as1* because treating *as1* SC spreads with DNase increased the cohesin fluorescence signals only slightly, similar to results previously observed for wild-type tomato SC spreads (Chapter 3). Together, these results show that the pattern of SMC1, REC8 and SCC3 immunolabeling observed in the *as1* mutant is most likely due to reduced presence of these proteins in AE/LEs.

AE/LEs are longer in the *as1* mutant

The alteration in cohesin proteins in *as1* suggested that chromosome compaction may also be effected in this mutant, based on similar changes in other cohesin mutants (Novak et al. 2008). To test this, we measured the total AE/LE length [= AE length + (SC length X 2)] in “late” stage SC spreads from *as1* and compared them to wild-type pachytene total AE/LE length. We also measured total AE/LE length in the *asb* mutant to assess whether asynapsis, *per se*, contributes to any differences in AE length at later stages. We found that the average length of AE/LE was significantly longer in *as1* than in either wild-type or *asb* (Table 1; Figure 16; one-

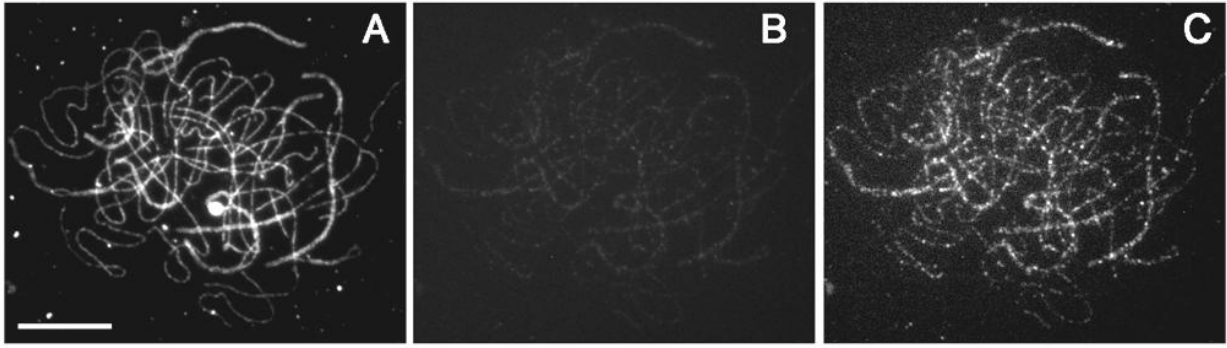


Figure 14. Colocalization of (A) SMC3 and (B, C) SMC1 on a late stage SC spread from *asl*. The image in (B) was captured with the same settings and exposure time as (A). The image in (C) has been enhanced additionally in Photoshop to show the discontinuous SMC1 signal. Scale bar = 10 μ m.

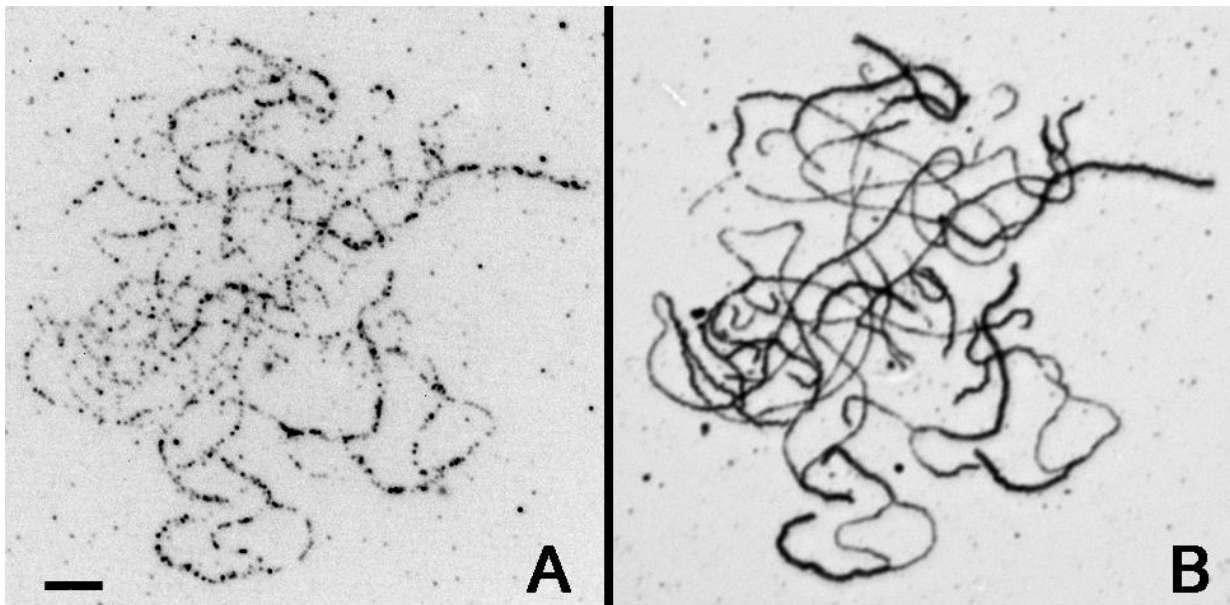


Figure 15. Late stage SC spread from *asl* immunolabeled with SMC1 (A, inverted fluorescent image) then stained with silver and photographed using light field microscopy (B). The discontinuities of the SMC1 signal along both AE and SC segments are not caused by AE/LE breakdown as demonstrated by the continuous silver staining of AEs and SCs. Scale bar = 5 μ m.

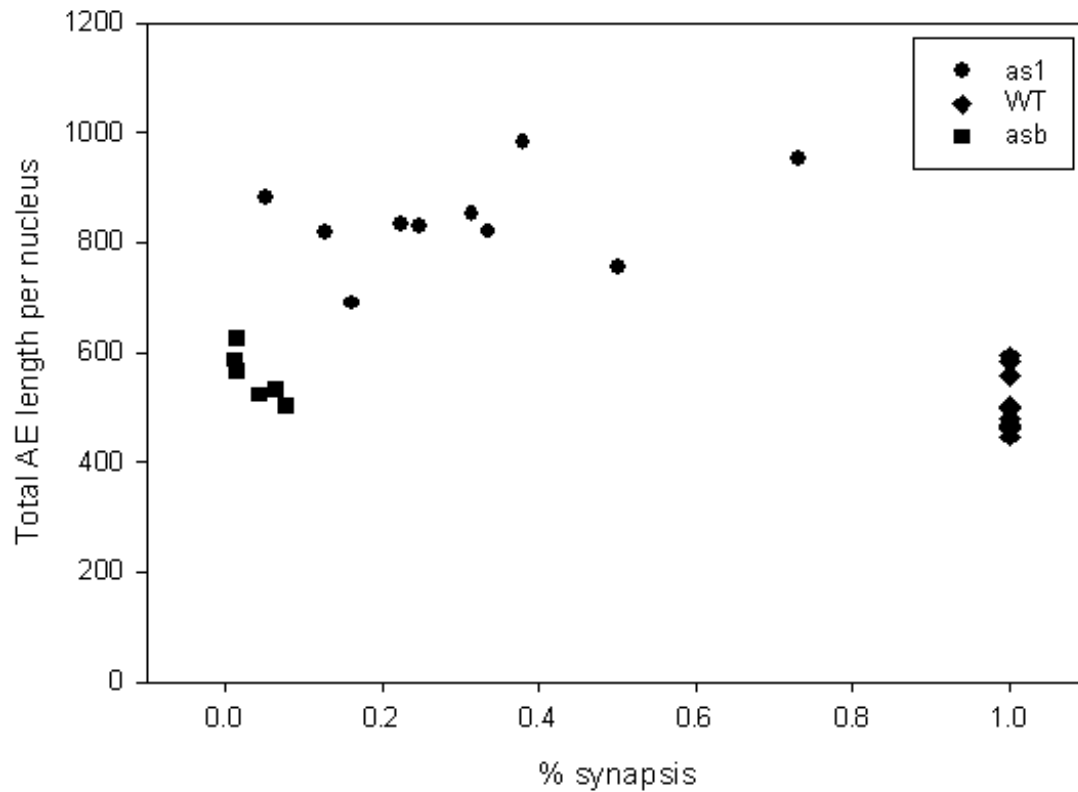


Figure 16. Distribution of AE lengths (total μm per nucleus) as a function of the amount (%) of synopsis for wild-type pachytene, *as1* and *asb* late stage SC spreads. Both wild-type and *asb* are similar in total AE length, and each group is tightly clustered although wild-type is completely synapsed while *asb* SC spreads have < 10% synopsis. In comparison, total AE lengths for *as1* are more variable and significantly longer (see Table 1) than wild-type or *asb*. In addition, there is no relationship between the amount of synopsis and AE length in *as1* nuclei.

way ANOVA, $P < 0.001$). Subsequent, pairwise multiple comparisons (Holm-Sidak method) showed that total AE/LE length in wild-type and *asb* were not significantly different ($P > 0.15$), but *asI* was significantly different from both wild-type and *asb* ($P < 0.001$). Thus, the greater length of AE/LEs in the *asI* mutant is not simply explained by the asynaptic phenotype since the *asb* mutant averages only 4% synapsis. We observed a high level of variability in the fraction of synapsis for SC spreads from *asI*, but there was no clear relationship between % synapsis and total AE/LE lengths (linear regression, $R^2=0.14$; $P > 0.25$).

DISCUSSION

In tomato, *asI* is a spontaneous, recessive, meiosis-specific mutation that causes incomplete synapsis and frequent univalent formation (Soost 1951). Plants carrying the *asI* mutation are almost completely male sterile, but seed set is reduced by only half when *asI* is used as the female parent with pollen from wild-type plants (Soost 1951). Rather surprisingly, offspring from *asI* mutants exhibit normal levels of crossing over, which may reflect selection for high levels of crossing over to produce viable eggs (Soost 1951; Moens 1969). However, offspring from *asI* mutants also had higher frequencies of double crossovers than expected (Soost 1951; Moens 1969), suggesting that crossover interference was altered compared to wild-type. Such results are not unique - the maize *as* mutant also has an asynaptic phenotype that is associated with reduced crossover interference (Rhoades and Dempsey 1949; Dempsey 1958), although various levels of crossing over (reduced, normal, and higher) have been reported for different genetic intervals (Rhoades and Dempsey 1949; Dempsey 1958; Miller 1963; Nel 1979). Because most spontaneous mutations affecting synapsis in plants have not been characterized at the molecular level, the exact genetic defects responsible for the mutations have not been

identified. Nevertheless, these uncharacterized mutations can be informative. For example, (Pawlowski et al. 2003) found that several different maize synaptic mutants were aberrant for RAD51 focal localization and the severity of the synaptic defects was correlated with the extent of the RAD51 focal defects. Therefore, new immunolabeling techniques can be useful in evaluating the relationship between recombination and synapsis, even in mutants in which the specific molecular defect is not known. We applied this approach to more closely examine synapsis and recombination in the tomato *as1* mutant.

Because synapsis is never complete in the tomato *as1* mutant, determining substages of prophase I using synaptic progress is not possible. However, we were able to use anther length and cell wall thickness to distinguish two stages in *as1* PMCs, early and late, which were comparable to leptotene-zygotene and pachytene, respectively, in wild-type PMCs (Figure 1). We found very little, if any, synapsis in early stage *as1* PMCs, and substantial amounts of synapsis were observed only during late stage *as1* PMCs (Figure 2). Thus, synaptic initiation was greatly delayed in *as1*, which suggests that the meiotic defect occurs very early, possibly upon entry into meiosis. We also documented a substantial delay in meiotic progression in *as1* compared to wild-type PMCs using BrdU labeling (Qiao and Anderson chapter 2). Such delays of meiotic progression are commonly observed in plant meiotic mutants (Sanchez-Moran et al. 2007).

Among late stage *as1* nuclei, we verified that synapsis was homologous by using single-copy BAC-FISH on four different chromosomes (chromosomes 1, 2, 4, 10, Figure 3, Table 2). For each BAC probe, we observed nuclei with either one or two signals per BAC, and, in the majority of cases, we were able to determine that single BAC-FISH signals corresponded to synapsed (SC) segments and two BAC-FISH signals corresponded to asynapsed AE segments.

Thus, the presence of two signals is not due to non-homologous synapsis, but to lack of synapsis between the two homologs at the site of interest. We also observed that the amount of synapsis was highly variable both between nuclei and between different bivalents within the same nucleus (Tables 1 - 2, Figures 2 - 3). Based on our BAC-FISH data, longer chromosomes were more likely to be synapsed than shorter chromosomes, and the long arm of each chromosome was more likely to be synapsed than the short arm. For example, the long arms of two long chromosomes (chromosomes 2 and 4) were synapsed in more than 80% of the nuclei, the long arm of the shorter chromosome 10 was synapsed in less than 50% of the nuclei, and the short arm of chromosome 1 was synapsed in less than 40% of the nuclei (Table 2). This data is in accord with previous observations of synaptic patterns in *as1* (Havekes et al. 1994). Havekes et al. (1994) also noted that the synaptic pattern in *as1* is similar to the pattern of distribution of single RNs on SCs from wild-type tomato (Sherman and Stack 1995). Sherman and Stack (1995) found that if an SC had only one RN, it was invariably found in the long arm of the chromosome, and they suggested that this distribution may reflect the location of synaptic initiation sites. If so, then the pattern of synaptic initiation in *as1*, even though delayed, is similar to that in wild-type tomato.

The presence of univalents at meiosis I indicated that crossover control was also disturbed in the *as1* mutant (Soost 1951; Moens 1969; Havekes et al. 1994; Havekes et al. 1997). We evaluated crossing over in the *as1* mutant using MLH1 foci as a marker of crossovers generated through the interference pathway and found significant differences in the frequency and distribution of MLH1 foci in *as1*. The average total number of MLH1 foci per late stage nucleus was significantly lower and more variable for *as1* compared to wild-type pachytene nuclei (Figures 4 - 5, Table 3). We also observed considerable variability in the number of

MLH1 foci on SC segments from *asl*. SC segments from *asl* were generally shorter than SCs from wild-type tomato, and about 20% of these segments had no MLH1 foci. However, many other short SC segments often had up to three MLH1 foci, and longer SC segments had as many as six MLH1 foci, something we never observed for wild-type (Figure 6). In comparison, most wild-type SCs had only one MLH1 focus with two and three MLH1 foci per SC occurring much less frequently [this work, (Lhuissier et al. 2007)]. Thus, in spite of the reduction in the average number of MLH1 foci per nucleus, the average frequency of MLH1 foci per μm SC was over two-fold higher for *asl* compared to wild-type.

We examined the distribution of MLH1 foci by applying the gamma model to interfocus distances to evaluate spacing between adjacent MLH1 foci. If foci are randomly spaced (no interference), $\nu = 1$. MLH1 foci that are less randomly (more evenly) spaced (demonstrating interference) have $\nu > 1$. We estimated ν using absolute (μm) not relative (%) distances between MLH1 foci because we were unable to reliably follow the entire length of partially synapsed chromosomes in *asl*. Also due to the limited synapsis of *asl*, we did not adjust values of ν in *asl* or wild-type for the limited range of interfocus distances that are experimentally observable (de Boer et al. 2006; Lhuissier et al. 2007). We observed a significant difference in the distribution of MLH1 foci with $\nu = 1.7$ for *asl* and $\nu = 4.5$ for wild-type. In comparison, (Lhuissier et al. 2007) observed $\nu = 6.9 - 7.9$ (unadjusted values, see their Table 2) for MLH1 foci for the two longest chromosomes of tomato. Part of the difference in wild-type ν values from our work and that of Lhuissier may be their use of relative (% of long arm) distance between adjacent MLH1 foci on only the two longest chromosomes while we used μm measurements (again because of the difficult of following *asl* chromosomes) for SCs and SC segments of any length. In any case, we found that interference between MLH1 foci is

considerably reduced for *as1* compared to wild-type. The ν values for the *as1* mutant are similar to those for early recombination nodules (that were also calculated using absolute interfocus distances; (Anderson et al. 2001; Lhuissier et al. 2007)). Thus, based on MLH1 foci, the *as1* mutation has a profound effect on the frequency and distribution of crossing over.

Our results on MLH1 frequency and interference are consistent with previous reports of an elevated frequency of double crossovers in *as1* (Soost 1951; Moens 1969). The data are also consistent with their observed “normal” level of crossing over in *as1* when we combine the higher frequency of MLH1 foci on SC segments with the reduced chance (compared to wild-type) that the segment will be synapsed (Table 2). We suggest that this combination of factors may apply to other asynaptic mutants in which the frequency of double crossovers is elevated [such as *as* in maize, (Rhoades and Dempsey 1949; Dempsey 1958; Dempsey 1959)].

Furthermore, differing observations of reduced, normal or enhanced levels of crossing over in different genetic intervals from asynaptic mutants may be a consequence of the specific interval examined and how frequently it synapses combined with elevated MLH1 (crossover) frequency and reduced interference.

Associated with changes in MLH1 foci, the *as1* mutant also showed differences in cohesin components of AE/LEs. Fluorescence signals for SMC1, REC8 and SCC3 were much reduced in *as1*, but SMC3 signals were similar in both *as1* and wild-type (Figure 13). Additional enhancement of the fluorescent signals revealed that both SMC1 and REC8 were present along AEs and LEs of *as1*, but we did not observe any detectable labeling for SCC3 even with additional enhancement of the images. The reduced signals for these cohesins could be due to initially reduced amounts of the proteins in AE/LEs or to enhanced extraction of the proteins during the chromosome spreading process such as that reported by (Lam et al. 2005b) for

cohesin protein SMC3 in Arabidopsis chromosome preparations in the presence of Tween detergent. Chromosomes in our SC spreads are routinely prepared using the detergent NP-40 (not Tween 20), but even if cohesins are extracted with NP-40 detergent, three of the cohesins are more susceptible than SMC3 in *asI* or than all four cohesins in wild-type. In either case, it is clear that three of the four cohesins are altered in AE/LEs of *asI* compared to wild-type. Such differences could lead to changes in AE length similar to those reported for deletions of SMC1 β (and SYCP3) in mammals (Yuan et al. 2000; Yuan et al. 2002; Novak et al. 2008) and for the Rec8 mutant in fission yeast (Ding et al. 2006).

Although the immunolabeling characteristics of three of the cohesins are altered in the *asI* mutant, functional chiasmata form, and sister chromatid cohesion (SCC) remains intact through meiosis (Soost 1951) (Moens 1969) (Havekes et al. 1994) (our observations). The wild-type labeling of SMC3 in AE/LEs of *asI* combined with the presence (albeit at reduced levels) of REC8 and SMC1 is apparently sufficient to assure meiotic SCC. This observation is consistent with evidence that only a fraction of the cohesin complex is sufficient to assure mitotic SCC in mammalian cells and meiotic SCC in budding yeast (Peters et al. 2008; Brar et al. 2009). Thus, cohesins seem to have both mitotic and meiotic roles in addition to their highly conserved function in sister chromatid cohesion.

What is the defect in *asI*?

Asynapsis is a common phenotype that can be caused by a variety of defects including mutations in genes involved in early recombination events (*e.g.* *SPO11*, *MRE11*, *RAD50*) or AE/SC structure [such as *REC8/SYNI/AFD1*, *ZIP1*, *ASY1*, *ZEP1* (Sym and Roeder 1996; Armstrong et al. 2002; Cai et al. 2003; Golubovskaya et al. 2006; Zhang et al. 2006; Wang et al. 2010)]. Although the *asI* mutation has not been mapped (because tomato is an inbred species

with few polymorphisms) and the specific defect is not known at the molecular level, Havekes et al. (1994) had earlier noted similarities between the asynaptic phenotypes of the *as1* mutant of tomato and *rad50s* and *dmc1* mutants in budding yeast, and they suggested that *as1* could represent a mutation in one of these proteins. If so, then one might expect to see changes in immunolocalization patterns of early recombination-related proteins similar to those reported by Pawlowski et al. (2003) who observed reductions in RAD51 foci that correlated with the severity of asynaptic phenotypes in maize mutants. To test the proposal of Havekes et al. (1994), we examined MRE11, RAD50 and RAD51 foci in early stage nuclei from *as1* compared to leptotene-zygotene stage nuclei from wild-type. We observed no detectable differences in the frequencies or other immunolabeling characteristics of these proteins (Figure 11-12). Based on this evidence, it seems unlikely that a mutation in *MRE11*, *RAD50*, *RAD51* or *SPO11* (that would also be expected to alter RAD51 focal properties) is responsible for the *as1* phenotype. However, we cannot exclude the possibility that a small mutation has occurred in one of the genes, which interferes with the activity but not the nuclear localization pattern of the protein. If so, then the mutation would also have to affect cohesin core deposition in *as1*, and so far, no mutant of any of the three genes has been reported to have an effect on the formation of a cohesin core or on the deposition of other SC-associated proteins (Gallego et al. 2001; Chin and Villeneuve 2001; Bleuyard et al. 2004; Puizina et al. 2004; Cherry et al. 2007; Borde 2007; Acharya et al. 2008). On the other hand, an *mre11* mutant in *Coprinus* caused defects in chromosome condensation (Gerecke and Zolan 2000), so perhaps this aspect has not been sufficiently examined in this group of mutants.

A few other mutations (*ndj1/tam1*, *tid1/rdh4*, *msh4*, *sgs1*) that reduce crossover interference have been reported, particularly in budding yeast (Ross-Macdonald and Roeder

1994; Conrad et al. 1997; Chua and Roeder 1997; Novak et al. 2001; Shinohara et al. 2003; Wu and Burgess 2006; Oh et al. 2007; Getz et al. 2008). The yeast *ndj1/tam1* mutation was particularly regarded as a mutation similar to that of tomato *as1* (Chua and Roeder 1997). Ndj1 is a telomere-associated protein that affects bouquet formation and chromosome synapsis (Conrad et al. 1997; Chua and Roeder 1997). The *ndj1/tam1* defect may be related to the maize *pam1* mutant that has similar bouquet, synapsis and crossover deficiencies (Golubovskaya et al. 2002). Ndj1 has recently been shown to have a more direct effect on recombination than previously thought, and Ndj1 has been proposed to stabilize strand invasion intermediates that lead to recombination events [both crossovers and non-crossovers, (Wu and Burgess 2006)]. In our spreading experiments, three-dimensional organization is lost, so we were not able to determine whether the *as1* mutant affects bouquet formation. However, none of these mutations have been reported to have any effect on cohesin proteins such as that seen in *as1*.

Another possibility for the *as1* defect is mutation of a cohesin or a cohesin-interacting protein (such as cohesin loading factors or kinesins responsible for phosphorylating cohesins during meiosis). Particularly attractive is a mutation specifically affecting REC8 as it is the only meiosis-specific cohesin in plants (Schubert 2009), and the *as1* mutation affects only meiosis. In wild-type tomato, REC8 is loaded onto the meiotic chromosome axis at approximately the same time as SMC3 and before SMC1 or SCC3 (Figure 11, Chapter 2). Therefore, a mutation that affects REC8 loading could potentially affect the stable integration of SMC1 and SCC3 into AE structure without affecting SMC3.

In plants, deletion (or RNAi suppression) of *REC8* leads to complete asynapsis, no homologous chromosome alignment, chromosome fragmentation at meiosis I, and aborted pollen grains (Cai et al. 2003; Golubovskaya et al. 2006; Zhang et al. 2006). Even the least severe

allele (*afd1-4*) of a mutant allele series of maize AFD1 caused disruption in AE formation, homologous pairing (and RAD51 foci), bouquet formation, and sister chromatid cohesion (Golubovskaya et al. 2006). If the *as1* mutation involves REC8, it obviously has a less severe phenotype than any of these null or near-null REC8 mutations in other plants.

The *as1* mutation affects the formation of the cohesin core, which in turn affects meiotic chromosome structure and the ability to form full-length SC, and the change in cohesin axis structure is associated with a reduction of interference between MLH1 foci on SC segments of *as1*. An increasing number of studies have documented a close association between meiotic axis (AE/LE and/or SC) structure and crossover control (Zickler and Kleckner 1999; Kleckner 2006; Wood et al. 2010). Two *C. elegans* mutants (*him-3* and *dpy-28*) that affect axis structure also have reduced crossover interference (Nabeshima et al. 2004; Tsai et al. 2008). *HIM-3* codes for a LE component that is reduced in the *him-3* mutant. *DPY-28* codes for a condensin component (that also has a role in dosage compensation in *C. elegans*), and *dpy-28* mutants are defective in chromosome compaction (Tsai et al. 2008). In *C. elegans*, interference is usually complete so that only a single crossover occurs on each bivalent. In *him-3* and *dpy-28* mutants, bivalents with two and even three crossovers have been observed. Similarly, PCH2/TRIP13 in budding yeast and mice coordinately influence chromosome axis structure and crossing over (Li and Schimenti 2007; Börner et al. 2008; Zanders and Alani 2009; Joshi et al. 2009; Roig et al. 2010). Mutants of *pch2/trip13* in both yeast and mice alter the distribution of HOP1/RED1 (HORMAD1/HORMAD2) on AE/LEs, reduce meiotic chromosome length, and reduce crossover (or MLH1 foci) interference. In addition, synapsis is incomplete in mouse *trip13* mutants (Li and Schimenti 2007; Roig et al. 2010). These studies illustrate the close correspondence between meiotic chromosome axis behavior and crossover control.

The role of the meiosis-specific cohesin REC8 in regulating crossing over has been recently addressed in an elegant study in budding yeast by Brar et al. (2009). Brar et al. (2006) had earlier established the importance of REC8 phosphorylation in combination with recombination for establishing the step-wise loss of cohesion during anaphase I and anaphase II. Brar et al. (2009) found that REC8 has functions in chromosome pairing, cohesion, synapsis, and recombination that are at least partially genetically separable based on different levels of REC8 phosphorylation. The *rec8-29A* mutant (in which 29 phosphorylation sites of REC8 were mutated to alanine) is particularly interesting with regard to the tomato *as1* mutant. The *rec8-29A* mutant has a severe prophase I delay, but the protein is produced at a wild-type level and loads on to chromosome axes during meiosis (Brar et al. 2006). Sister chromatid cohesion and AE formation are normal, normal levels of DSBs occur with normal timing, and synapsis is homologous in *rec8-29A* (Brar et al. 2009). However, synapsis is never completed in the *rec8-29A* mutant, recombination is delayed, and only half the normal level of crossovers occurs (Brar et al. 2009). Interference between crossovers was not examined in this mutant. With the exception of the reduction in crossover frequency (that was based on recombination at only one site – the artificial *HIS4/LEU2* hotspot) and the normal loading of *rec8-29A* onto chromosome axes, these phenotypes are remarkably similar to those of tomato *as1*.

Our data on *as1* together with observations from other organisms (particularly the *rec8-29A* mutant of budding yeast) support the hypothesis that REC8 is a key player in the defects observed in tomato *as1*. Whether this is a direct effect through mutation of REC8 itself or an indirect effect through mutation of other proteins that promote cohesin loading [such as SCC2, SCC4, or HTP-3, (Onn et al. 2008; Severson et al. 2009)], other proteins that influence the meiotic chromosome axis [such as PCH2/TRIP13, HOP1/ASY1, (Zanders and Alani 2009; Joshi

et al. 2009; Roig et al. 2010)] or kinases that phosphorylate REC8 (Brar et al. 2006; Brar et al. 2009) will require detailed molecular characterization of the *as1* mutation. More importantly, our results show that meiotic chromosome axis structure, synapsis and crossover control are all intimately linked in plants.

CHAPTER 5:

GENERAL DISCUSSION

Findings and significance of this study

In this study, we used an immunocytological approach to study recombination and synapsis in primary microsporocytes from tomato plants. We found that cohesin proteins load onto chromosome cores during prophase I in wild-type tomato meiocytes (Chapter 2). All four cohesin proteins showed discontinuity and variation in intensities along SCs, and two of the cohesins, REC8 and SMC3, loaded earlier in leptotene and persisted longer at diplotene compared to another cohesin, SMC1. This study was the first to examine the dynamics of cohesin proteins during meiotic prophase in plants. The different loading times and variable labeling intensities of cohesin proteins along AE/LEs are broadly similar to results obtained in other organisms. Because the four cohesins would be expected to act together at the same time in an equal stoichiometry to provide sister chromatid cohesion, the results also suggest that cohesin proteins have additional functions during meiosis in plants.

We also examined the relationship between synapsis and crossing-over in an asynaptic mutant (*as1*) of tomato (Chapters 3 and 4). We developed a new *in vivo* method to label developing microsporocytes with BrdU during premeiotic S-phase and found that the asynaptic defect was associated with a severe delay in the progression of meiotic prophase I. Our *in vivo* labeling method avoids the developmental arrest of tomato flowers that occurs with a different but commonly used method. We found that synapsis, though incomplete, was homologous in *as1*. Compared to wild-type, three cohesins (REC8, SCC3 and SMC1) were reduced in the SCs of zygotene-pachytene microsporocytes from *as1*, and the cohesin defects may be related to

another defect in chromosome condensation. The *asl* mutant also showed distinct differences in the MLH1 crossover pathway. The frequency of MLH1 foci was not different from wild-type on a per cell basis, but the frequency of MLH1 foci per μm SC length was higher than wild-type. The higher frequency of MLH1 foci on SC segments was associated with a reduction of interference among MLH1 foci in *asl* plants. Although the mutation causing the phenotypes of *asl* is still unknown, our results are the first in any organism to demonstrate that cohesin proteins are associated with crossover interference.

In summary, our results provide a better understanding of the roles of cohesin and recombination proteins in relation to genetic recombination, synapsis, and crossover interference in a higher plant. All of the proteins we studied are evolutionarily conserved, so our experimental results provide insights into the control of meiotic crossing over in other organisms. Our results also have implications in more practical arenas. For example, understanding the molecular mechanisms of genetic recombination could lead to the development of plants with altered (particularly increased) recombination frequencies to speed up breeding of new plant varieties. A model for crossing over and genetic interference in tomato

Based on evidence from this work and previous work on synapsis and recombination in tomato and other plants (Stack and Anderson 1986a, 1986b; Stack et al. 1993; Anderson et al. 2001; Anderson and Stack 2005), I propose the following model [that is modified based on one previously proposed by Stack and Anderson (1986b)]. In this model, genetic interference is determined by two important factors, development of recombination sites (*i.e.*, the time required for formation of D-loop intermediates at each DSB site and then their subsequent fates) and communication among recombination sites (= DSB sites) on the same chromosome. The fate of an individual DSB would be related to both of these temporal and spatial considerations.

Temporally, some recombination sites (such as those at synaptic initiation sites and/or recombination hotspots) would develop into crossover intermediates earlier than other recombination sites. Spatially, recombination sites would “talk” to each other via interference signals. Once an early-developing recombination site was committed to be a designated CO, an interference signal would be produced from the designated CO site and spread out to cause adjacent later-developing recombination sites to go through NCO pathways. Interference signals would fade with distance from the designated CO site, so later-developed sites that are far away from the generator of the interference signal would still have an opportunity to develop into a designated CO. Axial elements, especially REC8 proteins, would have a key role in the transmission signal for interference. The interference signal in this model may be through modifications of cohesin proteins that would begin at the site of a designator CO. Such modifications could include one or more of the following: phosphorylation, methylation, acetylation, ubiquitination, or SUMOylation reactions. Possibly, similar modifications of non-cohesin AE components could also be involved.

Our model can account well for the phenotypes observed in the *as1* mutant. Recombination proteins that are involved in the development of each DSB site presumably play important roles in both initiating and receiving interference signals. Early recombination proteins in *as1* seem to function well, since the immunolocalization patterns of MRE11, RAD50, and RAD51 in *as1* do not differ from the patterns in wild type. Also, MLH1 foci that represent the last event of the DSBR pathway to a crossover occur in *as1* nuclei. Therefore, the weakened interference in *as1* is probably not due to defects in generators and acceptors of the interference signal, but to disruption of the medium of interference. In *as1*, alterations in axial element structure (*i.e.*, represented by observed reductions in SMC1, SCC3, and REC8 cohesin proteins)

disrupt transmission of the interference signal. Without the interference signal, later-developing recombination sites, even those that are close to CO-designated sites, are able to go through the CO pathway instead of being forced into the NCO pathway (as would occur in the presence of interference). The reduction of interference in the *asI* mutant leads to the observed reduced inter-focus distances among CO/MLH1 foci and increased density of CO/MLH1 foci on SC segments.

Directions for further research

Based on our analysis of *asI*, REC8 plays a key role in regulating meiotic recombination in tomato. While we do not yet know the exact molecular defect of *asI*, the mutation seems most likely to be in REC8 itself or in a REC8-regulating protein. In either case, REC8 protein is produced, but it is not incorporated into AE/LEs in the normal manner. Thus, the *asI* mutation is more likely to be similar to a hypomorphic type of mutation than to a null mutation. Most evaluations of *REC8* have involved null mutants (Klein et al. 1999; Cai et al. 2003; Puizina et al. 2004; Bannister et al. 2004; Xu et al. 2005; Zhang et al. 2008). Only two studies, one in maize (Golubovskaya et al. 2006) and one in budding yeast (Brar et al. 2009) have analyzed different non-null mutants of *REC8*. Although neither study examined genetic interference, both showed varying effects of the different *REC8* mutations on synapsis and recombination. Further studies of *REC8* using approaches such as RNAi or targeted mutation of phosphorylation sites of *REC8* (like that of Brar et al. 2009) would be useful in making *rec8* hypomorphic mutants in plants and animals, and we predict that some *rec8* hypomorphic mutants will mimic the phenotypes shown in the *asI* mutants. Such experiments will play an important role in better defining the role(s) of *REC8* in controlling meiotic recombination rates and genetic interference.

References

- Acharya SN, Many AM, Schroeder AP, Kennedy FM, Savytsky OP, Grubb JT, Vincent JA, Friedle EA, Celerin M, Maillet DS, Palmerini HJ, Greischar MA, Moncalian G, Williams RS, Tainer JA, Zolan ME. (2008) *Coprinus cinereus rad50* mutants reveal an essential structural role for Rad50 in axial element and synaptonemal complex formation, homolog pairing and meiotic recombination. *Genetics* 180:1889-1907.
- Adelfalk C, Janschek J, Revenkova E, Blei C, Leibe B, Göb E, Alsheimer M, Benavente R, de Boer E, Novak I, Höög C, Scherthan H, Jessberger R. (2009) Cohesin SMC1 β protects telomeres in meiocytes. *J Cell Biol* 187:185-199.
- Agarwal S, Roeder GS. (2000) Zip3 provides a link between recombination enzymes and synaptonemal complex proteins. *Cell* 102:245-255.
- Alani E, Padmore R, Kleckner N. (1990) Analysis of wild-type and *rad50* mutants of yeast suggests an intimate relationship between meiotic chromosome synapsis and recombination. *Cell* 61:419-436.
- Albini SM. (1994) A karyotype of the *Arabidopsis thaliana* genome derived from synaptonemal complex analysis at prophase I of meiosis. *Plant J* 5:665-672.
- Albini SM, Jones GH. (1984) Synaptonemal complex-associated centromeres and recombination nodules in plant meiocytes prepared by an improved surface-spreading technique. *Exp Cell Res* 155:589-592.
- Albini SM, Jones GH. (1988) Synaptonemal complex spreading in *Allium cepa* and *Allium fistulosum*. II. Pachytene observations: the SC karyotype and the correspondence of late recombination nodules and chiasmata. *Genome* 30:399-410.
- Allen JW. (1979) BrdU-dye characterization of late replication and meiotic recombination in Armenian hamster germ cells. *Chromosoma* 74:189-207.
- Anderson LK, Doyle GG, Brigham B, Carter J, Hooker KD, Lai A, Rice M, Stack SM. (2003) High resolution crossover maps for each bivalent of *Zea mays* using recombination nodules. *Genetics* 165:849-865.
- Anderson LK, Hooker KD, Stack SM. (2001) The distribution of early recombination nodules on zygotene bivalents from plants. *Genetics* 159:1259-1269.
- Anderson LK, Offenbergh HH, Verkuijlen WMHC, Heyting C. (1997) RecA-like proteins are components of early meiotic nodules in lily. *Proc Natl Acad Sci USA* 94:6868-6873.
- Anderson LK, Reeves A, Webb LM, Ashley T. (1999) Distribution of crossing over on mouse synaptonemal complexes using immunofluorescent localization of MLH1 protein. *Genetics* 151:1569-1579.

- Anderson LK, Royer SM, Page SL, McKim KS, Lai A, Lilly MA, Hawley RS. (2005) Juxtaposition of C(2)M and the transverse filament protein C(3)G within the central region of *Drosophila* synaptonemal complex. *Proc Natl Acad Sci USA* 102:4482-4487.
- Anderson LK, Stack SM. (2002) Meiotic recombination in plants. *Curr Genom* 3:507-525.
- Anderson LK, Stack SM. (2005) Recombination nodules in plants. *Cytogenet Genome Res* 109:198-204.
- Aravind L, Koonin EV. (1998) Phosphoesterase domains associated with DNA polymerases of diverse origins. *Nucleic Acids Res* 26:3746-3752.
- Armstrong SJ, Caryl AP, Jones GH, Franklin FCH. (2002) Asy1, a protein required for meiotic chromosome synapsis, localizes to axis-associated chromatin in *Arabidopsis* and *Brassica*. *J Cell Sci* 115:3645-3655.
- Armstrong SJ, Franklin FCH, Jones GH. (2003) A meiotic time-course for *Arabidopsis thaliana*. *Sex Plant Reprod* 16:141-149.
- Armstrong SJ, Jones GH. (2001) Female meiosis in wild-type *Arabidopsis thaliana* and in two meiotic mutants. *Sex Plant Reprod* 13:177-183.
- Armstrong SJ, Jones GH. (2003) Meiotic cytology and chromosome behaviour in wild-type *Arabidopsis thaliana*. *J Exp Bot* 54:1-10.
- Assenmacher N, Hopfner K-P. (2004) MRE11/RAD50/NBS1: complex activities. *Chromosoma* 113:157-166.
- Austin C, Novikova N, Guacci V, Bellini M. (2009) Lampbrush chromosomes enable study of cohesin dynamics. *Chrom Res* 17:165-184.
- Bailis JM, Roeder GS. (2000) Pachytene exit controlled by reversal of Mek1-dependent phosphorylation. *Cell* 101:211-221.
- Baker SM, Plug AW, Prolla TA, Bronner CE, Harris AC, Yao X, Christie D-M, Monell C, Arnheim N, Bradley A, Ashley T, Liskay RM. (1996) Involvement of mouse *Mlh1* in DNA mismatch repair and meiotic crossing over. *Nature Genet* 13:336-342.
- Bannister LA, Reinholdt LG, Munroe RJ, Schimenti JC. (2004) Positional cloning and characterization of mouse *mei8*, a disrupted allele of the meiotic cohesin *Rec8*. *Genesis* 40:184-194.
- Bannister LA, Schimenti JC. (2004) Homologous recombinational repair proteins in mouse meiosis. *Cytogenet Genome Res* 107:191-200.
- Baudat F, Manova K, Yuen JP, Jasin M, Keeney S. (2000) Chromosome synapsis defects and sexually dimorphic meiotic progression in mice lacking *Spo11*. *Mol Cell* 6:989-998.

- Bennett MD. (1971) The duration of meiosis. *Proc Roy Soc Lond B* 178:277-299.
- Bennett MD. (1973) The duration of meiosis, Balls M, Billett F. (eds): *The cell cycle in development and differentiation*, pp 111-131 (Cambridge University Press,).
- Bennett MD. (1977) The time and duration of meiosis. *Phil Trans Roy Soc Lond B* 277:201-226.
- Bennett MD, Finch RA, Smith JB, Rao MK. (1973) The time and duration of female meiosis in wheat, rye and barley. *Proc R Soc Lond B* 183:301-319.
- Berchowitz LE, Copenhaver GP. (2010) Genetic interference: Don't stand so close to me. *Curr Genom* 11:91-102.
- Bergerat A, de Massy B, Gadelle D, Varoutas PC, Nicolas A, Forterre P. (1997) An atypical topoisomerase II from Archaea with implications for meiotic recombination. *Nature* 386:414-417.
- Bhalla N, Dernburg AF. (2005) A conserved checkpoint monitors meiotic chromosome synapsis in *Caenorhabditis elegans*. *Science* 310:1683-1686.
- Bhalla N, Dernburg AF. (2008) Prelude to a Division. *Annu Rev Cell Devel Biol* 24:397-424.
- Bhalla N, Wynne DJ, Jantsch V, Dernburg AF. (2008) ZHP-3 acts at crossovers to couple meiotic recombination with synaptonemal complex disassembly and bivalent formation in *C. elegans*. *PLoS Genetics* 4:e1000235. doi:10.1371/journal.pgen.1000235.
- Bishop DK. (1994) RecA homologs Dmc1 and Rad51 interact to form multiple nuclear complexes prior to meiotic chromosome synapsis. *Cell* 79:1081-1092.
- Bishop DK, Park D, Xu L, Kleckner N. (1992) DMC1: A meiosis-specific yeast homolog of E. coli recA required for recombination, synaptonemal complex formation, and cell cycle progression. *Cell* 69:439-456.
- Bishop DK, Zickler D. (2004) Early decision: meiotic crossover interference prior to stable strand exchange and synapsis. *Cell* 117:9-15.
- Bleuyard J-Y, Gallego ME, White CI. (2004) Meiotic defects in the *Arabidopsis rad50* mutant point to conservation of the MRX complex function in early stages of meiotic recombination. *Chromosoma* 113:197-203.
- Bolcun-Filas E, Costa Y, Speed R, Taggart M, Benavente R, de Rooij DG, Cooke HJ. (2007) SYCE2 is required for synaptonemal complex assembly, double strand break repair, and homologous recombination. *J Cell Biol* 176:741-747.
- Borde V. (2007) The multiple roles of the Mre11 complex for meiotic recombination. *Chrom Res* 15:551-563.

- Borde V, Lin W, Novikov E, Petrini JH, Lichten M, Nicolas A. (2004) Association of Mre11p with double-strand break sites during yeast meiosis. *Mol Cell* 13:389-401.
- Börner GV, Barot A, Kleckner N. (2008) Yeast Pch2 promotes domainal axis organization, timely recombination progression, and arrest of defective recombinosomes during meiosis. *Proc Natl Acad Sci USA* 105:3327-3332.
- Börner GV, Kleckner N, Hunter N. (2004) Crossover/noncrossover differentiation, synaptonemal complex formation, and regulatory surveillance at the leptotene/zygotene transition of meiosis. *Cell* 117:29-45.
- Brar GA, Hochwagen A, Ee LS, Amon A. (2009) The multiple roles of cohesin in meiotic chromosome morphogenesis and pairing. *Mol Biol Cell* 20:1030-1047.
- Brar GA, Kiburz BM, Zhang Y, Kim JE, White F, Amon A. (2006) Rec8 phosphorylation and recombination promote the step-wise loss of cohesins in meiosis. *Nature* 441:532-536.
- Buermeyer AB, Deschênes SM, Baker SM, Liskay RM. (1999) Mammalian DNA mismatch repair. *Ann Rev Genet* 33:533-564.
- Cai X, Dong F, Edelmann RE, Makaroff CA. (2003) The Arabidopsis SYN1 cohesin protein is required for sister chromatid arm cohesion and homologous chromosome pairing. *J Cell Sci* 116:2999-3007.
- Carballo JsA, Johnson AL, Sedgwick SG, Cha RS. (2008) Phosphorylation of the Axial Element Protein Hop1 by Mec1/Tel1 Ensures Meiotic Interhomolog Recombination. *Cell* 132:758-770.
- Carpenter ATC. (1975) Electron microscopy of meiosis in *Drosophila melanogaster* females: II: the recombination nodule - a recombination-associated structure at pachytene? *Proc Natl Acad Sci USA* 72:3186-3189.
- Celerin M, Merino ST, Stone JE, Menzie AM, Zolan ME. (2000) Multiple roles of Spo11 in meiotic chromosome behavior. *EMBO J* 19:2739-2750.
- Chan RC, Chan A, Jeon M, Wu TF, Pasqualone D, Rougvie AE, Meyer BJ. (2003) Chromosome cohesion is regulated by a clock gene paralogue TIM-1. *Nature* 423:1002-1009.
- Chang, S-B. (2004) Cytogenetic and molecular studies on tomato chromosomes using diploid tomato and tomato monosomic additions in tetraploid potato. 1-125. Wageningen University. Wageningen, The Netherlands.
- Chang S-B, Anderson LK, Sherman JD, Royer SM, Stack SM. (2007) Predicting and testing physical locations of genetically mapped loci on tomato pachytene chromosome 1. *Genetics* 176:2131-2138.

- Chang S-B, Yang T-J, Datema E, Vugt Jv, Vosman B, Kuipers A, Meznikova M, Szinay D, Lankhorst RK, Jacobsen E, de Jong H. (2008) FISH mapping and molecular organization of the major repetitive sequences of tomato. *Chrom Res* 16:919-933.
- Chelysheva L, Diallo S, Vezon D, Gendrot G, Vrielynck N, Belcram K, Rocques N, Marquez-Lema A, Bhatt AM, Horlow C, Mercier R, Mezard C, Grelon M. (2005) AtREC8 and AtSCC3 are essential to the monopolar orientation of the kinetochores during meiosis. *J Cell Sci* 118:4621-4632.
- Chelysheva L, Grandont L, Vrielynck N, le Guin S, Mercier R, Grelon M. (2010) An easy protocol for studying chromatin and recombination protein dynamics during *Arabidopsis thaliana* meiosis: Immunodetection of cohesins, histones and MLH1. *Cytogenet Genome Res* 129:143-153.
- Cherry SM, Adelman CA, Theunissen JW, Hassold TJ, Hunt PA, Petrini JHJ. (2007) The Mre11 complex influences DNA repair, synapsis, and crossing over in murine meiosis. *Curr Biol* 17:373-378.
- Chin GM, Villeneuve AM. (2001) *C. elegans* mre-11 is required for meiotic recombination and DNA repair but is dispensable for the meiotic G2 DNA damage checkpoint. *Genes Devel* 15:522-534.
- Chua PR, Roeder GS. (1997) Tam1, a telomere-associated meiotic protein, functions in chromosome synapsis and crossover interference. *Genes Devel* 11:1786-1800.
- Cohen PE, Pollack SE, Pollard JW. (2006) Genetic analysis of chromosome pairing, recombination, and cell cycle control during first meiotic prophase in mammals. *Environ Mol Mutagenesis* 27:398-426.
- Colaiácovo MP. (2006) The many facets of SC function during *C. elegans* meiosis. *Chromosoma* 115:195-211.
- Colaiácovo MP, MacQueen AJ, Martínez-Pérez E, McDonald K, Adamo A, La Volpe A, Villeneuve AM. (2003) Synaptonemal complex assembly in *C. elegans* is dispensable for loading strand-exchange proteins but critical for proper completion of recombination. *Devel Cell* 5:463-474.
- Cole F, Keeney S, Jasin M. (2010) Evolutionary conservation of meiotic DSB proteins: more than just Spo11. *Genes & Development* 24:1201-1207.
- Conrad MN, Dominguez AM, Dresser ME. (1997) Ndj1p a meiotic telomere protein required for normal chromosome synapsis and segregation in yeast. *Science* 276:1252-1255.
- Copenhaver GP, Housworth EA, Stahl FW. (2002) Crossover interference in arabidopsis. *Genetics* 160:1631-1639.

- Costa Y, Speed R, Öllinger R, Alsheimer M, Semple CA, Gautier P, Maratou K, Novak I, Höög C, Benavente R, Cooke HJ. (2005) Two novel proteins recruited by synaptonemal complex protein 1 (SYCP1) are at the centre of meiosis. *J Cell Sci* 118:2755-2762.
- Cowan CR, Cande WZ. (2002) Meiotic telomere clustering is inhibited by colchicine but does not require cytoplasmic microtubules. *J Cell Sci* 115:3747-3756.
- Cowan CR, Carlton PM, Cande WZ. (2002) Reorganization and polarization of the meiotic bouquet-stage cell can be uncoupled from telomere clustering. *J Cell Sci* 115:3757-3766.
- D'Amours D, Jackson SP. (2002) The Mre11 complex: at the crossroads of DNA repair and checkpoint signalling. *Nat Rev Mole Cell Biol* 3:317-327.
- de Boer E, Dietrich AJJ, Höög C, Stam P, Heyting C. (2007) Meiotic interference among MLH1 foci requires neither an intact axial element structure nor full synapsis. *J Cell Sci* 120:731-736.
- de Boer E, Heyting C. (2006) The diverse roles of transverse filaments of synaptonemal complexes in meiosis. *Chromosoma* 115:220-234.
- de Boer E, Stam P, Dietrich AJJ, Pastink A, Heyting C. (2006) Two levels of interference in mouse meiotic recombination. *PNAS USA* 103:9607-9612.
- de Jager M, van Noort J, van Gent DC, Dekker C, Kanaar R, Wyman C. (2001) Human Rad50/Mre11 is a flexible complex that can tether DNA ends. *Mol Cell* 8:1129-1135.
- De Muyt A, Mercier R, Mezard C, Grelon M. (2009) Meiotic recombination and crossovers in plants, Benavente R, Volff J-N (eds), vol. 5 ed: Meiosis, pp 14-25 (Karger, Basel).
- Dempsey E. (1958) Occurrence of crossover strands in the diploid gametes of *as* plants. *MNL* 32:73-79.
- Dempsey E. (1959) Analysis of crossing over in haploid gametes of asynaptic plants. *MNL* 33:54-55.
- Dernburg AF, McDonald K, Moulder G, Barstead R, Dresser M, Villeneuve AM. (1998) Meiotic recombination in *C. elegans* initiates by a conserved mechanism and is dispensable for homologous chromosome synapsis. *Cell* 94:387-398.
- Ding D-Q, Sakurai N, Katou Y, Itoh T, Shirahige K, Haraguchi T, Hiraoka Y. (2006) Meiotic cohesins modulate chromosome compaction during meiotic prophase in fission yeast. *J Cell Biol* 174:499-508.
- Dion E, Li L, Jean M, Belzile F. (2007) An *Arabidopsis MLH1* mutant exhibits reproductive defects and reveals a dual role for this gene in mitotic recombination. *Plant J* 51:431-440.

- Dobson MJ, Pearlman RE, Karaiskakis A, Spyropoulos B, Moens PB. (1994) Synaptonemal complex proteins: occurrence, epitope mapping and chromosome disjunction. *J Cell Sci* 107:2760.
- Dong F, Cai X, Makaroff CA. (2001) Cloning and characterization of two arabidopsis genes that belong to the RAD21/REC8 family of chromosome cohesin proteins. *Gene* 271:99-108.
- Dong F, Song J, Naess SK, Helgeson JP, Gebhardt C, Jiang J. (2000) Development and applications of a set of chromosome-specific cytogenetic DNA markers in potato. *Theor Appl Genet* 101:1001-1007.
- Dong H, Roeder GS. (2000) Organization of the yeast Zip1 protein within the central region of the synaptonemal complex. *J Cell Biol* 148:417-426.
- Doutriaux MP, Couteau F, Bergounioux C. (1998) Isolation and characterisation of the RAD51 and DMC1 homologs from *Arabidopsis thaliana*. *Molec Gen Genet* 257:283-291.
- Dresser ME, Giroux CN. (1988) Meiotic chromosome behavior in spread preparations of yeast. *J Cell Biol* 106:567-573.
- Edelmann W, Cohen PE, Kane M, Lau K, Morrow B, Bennett S, Umar A, Kunkel T, Cattoretti G, Chaganti R, Pollard JW, Kolodner RD, Kucherlapati R. (1996) Meiotic pachytene arrest in MLH1-deficient mice. *Cell* 85:1125-1134.
- Egelman EH. (2001) Does a Stretched DNA Structure Dictate the Helical Geometry of RecA-like Filaments? *J Mol Biol* 309:539-542.
- Eijpe M, Heyting C, Gross B, Jessberger R. (2000a) Association of mammalian SMC1 and SMC3 proteins with meiotic chromosomes and synaptonemal complexes. *J Cell Sci* 113:673-682.
- Eijpe M, Offenbergh HH, Goedecke W, Heyting C. (2000b) Localisation of RAD50 and MRE11 in spermatocyte nuclei of mouse and rat. *Chromosoma* 109:123-132.
- Eijpe M, Offenbergh HH, Jessberger R, Revenkova E, Heyting C. (2003) Meiotic cohesin REC8 marks the axial elements of rat synaptonemal complexes before cohesins SMC1 β and SMC3. *J Cell Biol* 160:657-670.
- Emmanuel El, Levy AA. (2002) Tomato mutants as tools for functional genomics. *Curr Opin Plant Biol* 5:112-117.
- Falque M, Anderson LK, Stack SM, Gauthier F, Martin O. (2009) Two types of meiotic crossovers coexist in maize. *Plant Cell* 21:3915-3925.
- Falque M, Mercier R, Mezard C, de Vienne D, Martin OC. (2007) Patterns of recombination and MLH1 foci density along mouse chromosomes: Modeling effects of interference and obligate chiasma. *Genetics* 176:1453-1467.

- Fawcett DW. (1956) The fine structure of chromosomes in the meiotic prophase of vertebrate spermatocytes. *J Biophys Biochem Cytol* 2(4):402-406.
- Foss E, Lande R, Stahl FW, Steinberg CM. (1993) Chiasma interference as a function of genetic distance. *Genetics* 133:681-691.
- Franklin AE, McElver J, Sunjevaric I, Rothstein R, Bowen B, Cande WZ. (1999) Three-dimensional microscopy of the Rad51 recombination protein during meiotic prophase. *Plant Cell* 11:809-824.
- Franklin FCH, Higgins JD, Sanchez-Moran E, Armstrong SJ, Osman KE, Jackson N, Jones GH. (2006) Control of meiotic recombination in *Arabidopsis*: role of the MutL and MutS homologues. *Biochem Soc Trans* 34:542-544.
- Froenicke L, Anderson LK, Weinberg J, Ashley T. (2002) Male mouse recombination maps for each autosome identified by chromosome painting. *Am J Hum Genet* 71:1353-1368.
- Fukuda T, Daniel K, Wojtasz L, Toth A, Höög C. (2010) A novel mammalian HORMA domain-containing protein, HORMAD1, preferentially associated with unsynapsed meiotic chromosomes. *Exp Cell Res* 316:158-171.
- Fung JC, Rockmill B, Odell M, Roeder GS. (2004) Imposition of crossover interference through the nonrandom distribution of synapsis initiation complexes. *Cell* 116:795-802.
- Furuse M, Nagase Y, Tsubouchi H, Murakami-Murofushi K, Shibata T, Ohta K. (1998) Distinct roles of two separable *in vitro* activities of yeast Mre11 in mitotic and meiotic recombination. *EMBO J* 14:6412-6425.
- Gallego ME, Jeanneau M, Granier F, Bouchez D, Bechtold N, White CI. (2001) Disruption of the *Arabidopsis* *RAD50* gene leads to plant sterility and MMS sensitivity. *Plant J* 25:31-41.
- Gerecke EE, Zolan ME. (2000) An *mre11* mutant of *Coprinus cinereus* has defects in meiotic chromosome pairing, condensation and synapsis. *Genetics* 154:1125-1129.
- Getz TJ, Banse SA, Young LS, Banse AV, Swanson J, Wang GM, Browne BL, Foss HM, Stahl FW. (2008) Reduced mismatch repair of heteroduplexes reveals "non"-interfering crossing over in wild-type *Saccharomyces cerevisiae*. *Genetics* 178:1269.
- Giroux CN, Dresser ME, Tiano HF. (1989) Genetic control of chromosome synapsis in yeast meiosis. *Genome* 31:88-94.
- Golubovskaya IN, Hamant O, Timofejeva L, Wang C-JR, Braun D, Meeley R, Cande WZ. (2006) Alleles of *afd1* dissect Rec8 functions during meiotic prophase I. *J Cell Sci* 119:3315.

- Golubovskaya IN, Harper LC, Pawlowski WP, Schichnes D, Cande WZ. (2002) The *pam1* gene is required for meiotic bouquet formation and efficient homologous synapsis in maize (*Zea mays* L.). *Genetics* 162:1979-1993.
- Goodyer W, Kaitna S, Couteau F, Ward JD, Boulton SJ, Zetka M. (2008) HTP-3 links DSB formation with homolog pairing and crossing over during *C.elegans* meiosis. *Devel Cell* 14:263-274.
- Grelon M, Vezon D, Gendrot G, Pelletier G. (2001) *AtSPO11-1* is necessary for efficient meiotic recombination in plants. *EMBO J* 20:589-600.
- Guacci V. (2007) Sister chromatid cohesion: the cohesin cleavage model does not ring true. *Genes to Cells* 12:693-708.
- Guillon H, Baudat F, Grey C, Liskay RM, de Massy B. (2005) Crossover and noncrossover pathways in mouse meiosis. *Mol Cell* 20:563-573.
- Gustafsson MGL, Shao L, Carlton PM, Wang C-J, Golubovskaya IN, Cande WZ, Agard DA, Sedat JW. (2008) Three-dimensional resolution doubling in wide-field fluorescence microscopy by structured illumination. *Biophysical Journal* 94:4957-4970.
- Guttenbach M, Haaf T, Steinlein C, Caesar J, Schinzel A, Schmid M. (1999) Ectopic NORs on human chromosomes 4qter and 8q11: rare chromosomal variants detected in two families. *Journal of Medical Genetics* 36:339-342.
- Hamant O, Golubovskaya I, Meeley R, Fiume E, Timofejeva L, Schleiffer A, Nasmyth K, Cande WZ. (2005) A REC8-dependent plant shugoshin is required for maintenance of centromeric cohesion during meiosis and has no mitotic functions. *Curr Biol* 15:948-954.
- Hamant O, Ma H, Cande WZ. (2006) Genetics of meiotic prophase I in plants. *Annu Rev Plant Biol* 57:267-302.
- Hamer G, Gell K, Kouznetsova A, Novak I, Benavente R, Höög C. (2006) Characterization of a novel meiosis-specific protein within the central element of the synaptonemal complex. *J Cell Sci* 119:4025-4032.
- Hamer G, Wang H, Bolcun-Filas E, Cooke HJ, Benavente R, Höög C. (2008) Progression of meiotic recombination requires structural maturation of the central element of the synaptonemal complex. *J Cell Sci* 121:2445-2451.
- Harper L, Golubovskaya I, et al. (2004) A bouquet of chromosomes. *J Cell Sci* 117:4025-4032.
- Hassold TJ. (1996) Mismatch repair goes meiotic. *Nature Genet* 13:261-262.
- Havekes FW, de Jong JH, Heyting C. (1997) Comparative analysis of female and male meiosis in three meiotic mutants of tomato. *Genome* 40:879-886.

- Havekes, FWJ. (1999) Homologous chromosome pairing and recombination during meiosis in wild type and synaptic mutants of tomato. p. 1-115. Ph.D. dissertation, Landbouwwuniversiteit Wageningen, The Netherlands.
- Havekes FWJ, de Jong JH, Heyting C, Ramanna MS. (1994) Synapsis and chiasma formation in four meiotic mutants of tomato (*Lycopersicon esculentum*). *Chromosome Res* 2:315-325.
- Hayashi M, Chin GM, Villeneuve AM. (2007) *C. elegans* germ cells switch between distinct modes of double-strand break repair during meiotic prophase progression. *PLoS Genetics* 3:2068-2084.
- Heyer W-D. (1994) The search for the right partner: homologous pairing and DNA strand exchange proteins in eukaryotes. *Experientia* 50:223-233.
- Heyting C. (1996) Synaptonemal complexes: structure and function. *Curr Opin Cell Biol* 8:389-396.
- Heyting C, Dietrich AJJ, Moens PB, Dettmers RJ, Offenbergh HH, Redeker EJW, Vink ACG. (1989) Synaptonemal complex proteins. *Genome* 31:81-87.
- Heyting C, Dietrich AJJ, Redeker EJW, Vink ACG. (1985) Structure and composition of synaptonemal complexes, isolated from rat spermatocytes. *Eur J Cell Biol* 36:307-314.
- Heyting C, Moens PB, van Raamsdonk W, Dietrich AJJ, Vink ACG, Redeker EJW. (1987) Identification of two major components of the lateral elements of synaptonemal complexes of the rat. *Eur J Cell Biol* 43:148-154.
- Hillers KJ. (2005) Crossover interference. *Curr Biol* 14:R1036-R1037.
- Hirano T. (2002) The ABCs of SMC proteins: two-armed ATPases for chromosome condensation, cohesion, and repair. *Genes Devel* 16:399-414.
- Hodges CA, Revenkova E, Jessberger R, Hassold TJ, Hunt PA. (2005) SMC1 β -deficient female mice provide evidence that cohesins are a missing link in age-related nondisjunction. *Nat Genet* 37:1351-1355.
- Hoffmann ER, Borts RH. (2004) Meiotic recombination intermediates and mismatch repair proteins. *Cytogenet Genome Res* 107:232-248.
- Hollingsworth NM, Brill SJ. (2004) The Mus81 solution to resolution: generating meiotic crossovers without Holliday junctions. *Genes Devel* 18:117-125.
- Hollingsworth NM, Goetsch L, Byers B. (1990) The *HOP1* gene encodes a meiosis-specific component of yeast chromosomes. *Cell* 61:73-84.

- Hollingsworth NM, Ponte L. (1997) Genetic interactions between *Hop1*, *RED1*, and *MEK1* suggest that *MEK1* regulates assembly of axial element components during meiosis in the yeast *Saccharomyces cerevisiae*. *Genetics* 147:33-42.
- Hunter N, Borts RH. (1997) Mlh1 is unique among mismatch repair proteins in its ability to promote crossing-over during meiosis. *Genes Devel* 11:1573-1582.
- Hunter N, Kleckner N. (2001) The single-end invasion: An asymmetric intermediate at the double-strand break to double-Holliday junction transition of meiotic recombination. *Cell* 106:59-70.
- Ito M, Stern H. (1967) Studies of meiosis in vitro: I. In vitro culture of meiotic cells. *Developmental Biology* 16:36-53.
- Jackson N, Sanchez-Moran E, Buckling E, Armstrong S, Jones GH, Franklin FCH. (2006) Reduced meiotic crossover and delayed prophase I progression in AtMLH3-deficient *Arabidopsis*. *EMBO J* 25:1315-1323.
- Jeffress JK, Page SL, Royer SM, Belden ED, Blumenstiel JP, Anderson LK, Hawley RS. (2007) The formation of the central element of the synaptonemal complex may occur by multiple mechanisms: The roles of the N- and C-terminal domains of the Drosophila C(3)G protein in mediating synapsis and recombination. *Genetics* 177:2445-2456.
- Jessberger R. (2002) The many functions of SMC proteins in chromosome dynamics. *Nat Rev Mole Cell Biol* 3:767-778.
- Jessberger R, Frei C, Gasser SM. (1998) Chromosome dynamics: the SMC protein family. *Curr Opin Genet Dev* 8:254-259.
- John B. (1990) *Meiosis.*, Cambridge University Press, Cambridge.
- Joshi N, Barot A, Jamison C, Börner GV. (2009) Pch2 links chromosome axis remodeling at future crossover sites and crossover distribution during yeast meiosis. *PLoS Genetics* 5:e1000557-doi:10.1371/journal.pgen.1000557.
- Kaul MLH, Murthy TKG. (1985) Mutant genes affecting higher plant meiosis. *Theor Appl Genet* 70:449-466.
- Keeney S. (2001) Mechanism and control of meiotic recombination initiation. *Curr Top Dev Biol* 52:1-53.
- Keeney S, Giroux CN, Kleckner N. (1997) Meiosis-specific DNA double-strand breaks are catalyzed by Spo11, a member of a widely conserved protein family. *Cell* 88:375-384.
- Keeney S, Neale MJ. (2006) Initiation of meiotic recombination by formation of DNA double-strand breaks: mechanism and regulation. *Biochem Soc Trans* 34:523-525.

- King JS, Mortimer RK. (1990) A polymerization model of chiasma interference and corresponding computer simulation. *Genetics* 126:1127-1138.
- Kitada K, Omura T. (1984) Genetic control of meiosis in rice, *Oryza sativa* L. IV. Cytogenetical analyses of asynaptic mutants. *Can J Genet Cytol* 26:264-271.
- Kitajima TS, Kawashima SA, Watanabe Y. (2004) The conserved kinetochore protein shugoshin protects centromeric cohesion during meiosis. *Nature* 427:510-517.
- Kitajima TS, Yokobayashi S, Yamamoto M, Watanabe Y. (2003) Distinct cohesin complexes organize meiotic chromosome domains. *Science* 300:1152-1155.
- Kleckner N. (2006) Chiasma formation: chromatin/axis interplay and the role(s) of the synaptonemal complex. *Chromosoma* 115:175-194.
- Kleckner N, Zickler D, Jones GH, Dekker J, Padmore R, Henle. (2004) A mechanical basis for chromosome function. *PNAS USA* 101:12592-12597.
- Klein F, Mahr P, Galova M, Buonomo SBC, Michaelis C, Nairz K, Nasmyth K. (1999) A central role for cohesins in sister chromatid cohesion, formation of axial elements, and recombination during yeast meiosis. *Cell* 98:91-103.
- Kolas NK, Cohen PE. (2004) Novel and diverse functions of the DNA mismatch repair family in mammalian meiosis and recombination. *Cytogenet Genome Res* 107:216-231.
- Kolodner RD, Marsischky GT. (1999) Eukaryotic DNA mismatch repair. *Curr Opin Genet Devel* 9:89-98.
- Kouznetsova A, Novak I, Jessberger R, Höög C. (2005) SYCP2 and SYCP3 are required for cohesin core integrity at diplotene but not for centromere cohesion at the first meiotic division. *J Cell Sci* 118:2271-2278.
- Ku H-M, Vision TJ, Liu J, Tanksley SD. (2000) Comparing sequenced segments of the tomato and *Arabidopsis* genomes: Large-scale duplication followed by selective gene loss creates a network of synteny. *Proc Natl Acad Sci USA* 97:9121-9126.
- Kudo NR, Anger M, Peters AHFM, Stemmann O, Theussl HC, Helmhart W, Kudo H, Heyting C, Nasmyth K. (2009) Role of cleavage by separase of the Rec8 kleisin subunit of cohesin during mammalian meiosis I. *J Cell Sci* 122:2686-2698.
- Kudo NR, Wassmann K, Anger M, Schuh M, Wirth KG, Xu H, Helmhart W, Kudo H, McKay M, Maro B, Ellenberg J, de Boer P, Nasmyth K. (2006) Resolution of chiasmata in oocytes requires separase-mediated proteolysis. *Cell* 126:135-146.
- Lam SY, Horn SH, Radford SJ, Housworth EA, Stahl FW, Copenhaver GP. (2005a) Crossover interference on nucleolus organizing region-bearing chromosomes in *Arabidopsis*. *Genetics* 170:807-812.

- Lam WS, Yang X, Makaroff CA. (2005b) Characterization of *Arabidopsis thaliana* SMC1 and SMC3: evidence that AtSMC3 may function beyond chromosome cohesion. *J Cell Sci* 118:3037-3048.
- Lammers JH, Offenbergh HH, van Aalderen M, Vink AC, Dietrich AJJ, Heyting C. (1994) The gene encoding a major component of the lateral elements of synaptonemal complexes of the rat is related to X-linked lymphocyte-regulated genes. *Mol Cell Biol* 14:1137-1146.
- Lammers JH, van Aalderen M, Peters AH, van Pelt AA, Gaemers IC, de Rooij DG, de Boer P, Offenbergh HH, Dietrich AJJ, Heyting C. (1995) A change in the phosphorylation pattern of the 30000-33000 M_r synaptonemal complex proteins of the rat between early and mid-pachytene. *Chromosoma* 104:154-163.
- Latos-Bielenska A, Vogel W. (1992) Demonstration of replication patterns in the last premeiotic S-phase of male Chinese hamsters after BrdU pulse labeling. *Chromosoma* 101:279-283.
- Laurie DA, Hultén MA. (1985) Further studies on bivalent chiasma frequency in human males with normal karyotypes. *Ann Hum Genet* 49:189-201.
- Leflon M, Grandont L, Eber F, Huteau V, Coriton O, Chelysheva LA, Jenczewski E, Chevre AM. (2010) Crossovers Get a Boost in Brassica Allotriploid and Allotetraploid Hybrids. *THE PLANT CELL* tpc.
- Lhuissier FGP, Offenbergh HH, Wittich PE, Vischer NOE, Heyting C. (2007) The mismatch repair protein MLH1 marks a subset of strongly interfering crossovers in tomato. *Plant Cell* 19:862-876.
- Li, J, Harper, LC, Golubovskaya, I, Wang, CR, Weber, Det al. (2007) Functional analysis of maize RAD51 in meiosis and double-strand break repair. *Genetics* 176:1469-1482.
- Li W, Chen C, Markmann-Mulisch U, Timofejeva L, Schmelzer E, Ma H, Reiss B. (2004) The *Arabidopsis AtRad51* gene is dispensable for vegetative development but required for meiosis. *Proc Natl Acad Sci USA* 101:10596-10601.
- Li XC, Schimenti JC. (2007) Mouse pachytene checkpoint 2 (*Trip13*) is required for completing meiotic recombination but not synapsis. *PLoS Genet* 3:3130.
doi:10.1371/journal.pgen.0030130.
- Lian J, Yin Y, Oliver-Bonet M, Liehr T, Ko E, Turek P, Sun F, Martin RH. (2008) Variation in crossover interference levels on individual chromosomes from human males. *Human Molecular Genetics* 17:2583-2594.
- Lichten M. (2001) Meiotic recombination: breaking the genome to save it. *Curr Biol* 11:R253-R256.

- Liebe B, Alsheimer M, Höög C, Benavente R, Scherthan H. (2004) Telomere attachment, meiotic chromosome condensation, pairing, and bouquet stage duration are modified in spermatocytes lacking axial elements. *Mol Biol Cell* 15:827-837.
- Lim K-B, Wennekes J, de Jong JH, Jacobsen E, van Tuyl JM. (2001) Karyotype analysis of *Lilium longiflorum* and *Lilium rubellum* by chromosome banding and fluorescence in situ hybridization. *Genome* 44:911-918.
- Lima-De-Faria A. (1965) Labeling of the cytoplasm and the meiotic chromosomes of *Agapanthus* with H³-thymidine. *Hereditas* 53:1-11.
- Lin FM, Lai YJ, Shen HJ, Cheng YH, Wang TF. (2010) Yeast axial-element protein, Red1, binds SUMO chains to promote meiotic interhomologue recombination and chromosome synapsis. *EMBO J* 29:586-596.
- Lipkin SM, Moens PB, Wang V, Lenzi M, Shanmugarajah D, Gilgeous A, Thomas J, Cheng J, Touchman JW, Green ED, Schwarzberg P, Collins FS, Cohen PE. (2002) Meiotic arrest and aneuploidy in MLH3-deficient mice. *Nature Genet* 31:385-390.
- Liu JG, Yuan L, Brundell E, Björkroth B, Daneholt B, Höög C. (1996) Localization of the N-terminus of SCP1 to the central element of the synaptonemal complex and evidence for direct interaction between the N-termini of SCP1 molecules organized head-to-head. *Exp Cell Res* 226:11-19.
- Lohmiller LD, De Muyt A, Howard B, Offenbergh HH, Heyting C, Grelon M, Anderson LK. (2008) Cytological analysis of MRE11 protein during early meiotic prophase I in *Arabidopsis* and tomato. *Chromosoma* 117:277-288.
- Loidl J, Klein F, Scherthan H. (1994) Homologous pairing is reduced but not abolished in asynaptic mutants of yeast. *J Cell Biol* 125:1191-1200.
- Losada A, Hirano T. (2005) Dynamic molecular linkers of the genome: the first decade of SMC proteins. *Genes Devel* 19:1269-1287.
- Lynn A, Soucek R, Börner GV. (2007) ZMM proteins during meiosis: Crossover artists at work. *Chromosome Res* 15:591-605.
- Ma H. (2006) A molecular portrait of *Arabidopsis* meiosis, Somerville CR, Meyerowitz EM (eds): *The Arabidopsis book*, pp doi: 10.1199/tab.0095 (American Society of Plant Biologists, Rockville, MD).
- MacQueen AJ, Colaiácovo MP, McDonald K, Villeneuve AM. (2002) Synapsis-dependent and -independent mechanisms stabilize homolog pairing during meiotic prophase in *C. elegans*. *Genes Devel* 16:2428-2442.
- MacQueen AJ, Phillips CM, Bhalla N, Weiser P, Villeneuve AM. (2005) Chromosome sites play dual roles to establish homologous synapsis during meiosis in *C. elegans*. *Cell* 123:1037-1050.

- Maguire MP. (1966) The relationship of crossing over to chromosome synapsis in a short paracentric inversion. *Genetics* 53:1071-1977.
- Maguire MP. (1978) A possible role for the synaptonemal complex in chiasma maintenance. *Exp Cell Res* 112:297-308.
- Maguire MP. (1995) Is the synaptonemal complex a disjunction machine? *J Heredity* 86:330-340.
- Maguire MP, Riess RW. (1994) The relationship of homologous synapsis and crossing over in a maize inversion. *Genetics* 137:281-288.
- Manheim EA, McKim KS. (2003) The synaptonemal complex component C(2)M regulates meiotic crossing over in *Drosophila*. *Curr Biol* 13:276-285.
- Marcon E, Moens P. (2003) Mlh1p and Mlh3p localize to precociously induced chiasmata of okadaic acid treated mouse spermatocytes. *Genetics* 165:2283-2287.
- Martinez-Perez E, Schvarzstein M, Barroso C, Lightfoot J, Dernburg AF, Villeneuve AM. (2008) Crossovers trigger a remodeling of meiotic chromosome axis composition that is linked to two-step loss of sister chromatid cohesion. *Genes & Development* 22:2886-2901.
- Martini E, Diaz RL, Hunter N, Keeney S. (2006) Crossover homeostasis in yeast meiosis. *Cell* 126:285-295.
- Masson JY, Davies AA, Hajibagheri N, van Dyck E, Benson FE, Stasiak AZ, Stasiak A, West SC. (1999) The meiosis-specific recombinase hDmc1 forms ring structures and interacts with hRad51. *EMBO J* 18:6552-6560.
- Masson JY, West SC. (2001) The Rad51 and Dmc1 recombinases: a non-identical twin relationship. *TIBS* 26:131-136.
- McKee BD. (2004) Homologous pairing and chromosome dynamics in meiosis and mitosis. *Biochim Biophys Acta* 1677:165-180.
- McKim K, Hayashi-Hagihara A. (1998) mei-W68 in *Drosophila melanogaster* encodes a Spo11 homolog: evidence that the mechanism for initiating meiotic recombination is conserved. *Genes & Development* 12:2932-2942.
- McKim KS, Green-Marroquin BL, Sekelsky JJ, Chin G, Steinberg C, Khodosh R, Hawley RS. (1998) Meiotic synapsis in the absence of recombination. *Science* 279:876-878.
- Menda N, Semel Y, Peled D, Eshed Y, Zamir D. (2004) *In silico* screening of a saturated mutation library of tomato. *Plant J* 38:861-872.
- Merino ST, Cummings WJ, Acharya SN, Zolan ME. (2000) Replication-dependent early meiotic requirement for Spo11 and Rad50. *Proc Natl Acad Sci USA* 97:10477-10482.

- Mets DG, Meyer BJ. (2009) Condensins regulate meiotic DNA break distribution, thus crossover frequency, by controlling chromosome structure. *Cell* 139:73-86.
- Miller OL. (1963) Cytological studies in asynaptic maize. *Genetics* 48:1445-1466.
- Moens PB. (1969) Genetic and cytological effects of three desynaptic genes in the tomato. *Can J Genet Cytol* 11:857-869.
- Moens PB, Heyting C, Dietrich AJJ, van Raamsdonk W, Chen Q. (1987) Synaptonemal complex antigen location and conservation. *J Cell Biol* 105:93-103.
- Moens PB, Kolas NK, Tarsounas M, Marcon E, Cohen PE, Spyropoulos B. (2002) The time course and chromosomal localization of recombination-related proteins at meiosis in the mouse are compatible with models that can resolve the early DNA-DNA interactions without reciprocal recombination. *J Cell Sci* 115:1611-1622.
- Moens PB, Marcon E, Shore JS, Kochakpour N, Spyropoulos B. (2007) Initiation and resolution of interhomolog connections: crossover and non-crossover sites along mouse synaptonemal complexes. *J Cell Sci* 120:1017-1027.
- Molnar M, Bahler J, Sipiczki M, Kohli J. (1995) The *rec8* gene of *Schizosaccharomyces pombe* is involved in linear element formation, chromosome pairing and sister-chromatid cohesion during meiosis. *Genetics* 141:61-73.
- Moses M. (1968) Synaptonemal complex. *Ann Rev Genet* 2:363-412.
- Moses MJ. (1956) Chromosome structure in crawfish spermatocytes. *J Biophys Biochem Cytol* 1:215-218.
- Mueller LA, Tanksley S, Giovannoni JJ, Vaneck J, Stack S, Buels R. (2009) A snapshot of the emerging tomato genome sequence. *The Plant Genome* 2:78-92.
- Muller HJ. (1916) The mechanism of crossing-over. II. IV. the manner of occurrence of crossing-over. *Am Natur* 50:284-305.
- Nabeshima K, Villeneuve AM, Hillers KJ. (2004) Chromosome-wide regulation of meiotic crossover formation in *Caenorhabditis elegans* requires properly assembled chromosome axes. *Genetics* 168:1275-1292.
- Nairz K, Klein F. (1997) *mre11S*-a yeast mutation that blocks double-strand-break processing and permits nonhomologous synapsis in meiosis. *Genes Devel* 11:2272-2290.
- Nasmyth K. (2001) Disseminating the genome: joining, resolving, and separating sister chromatids during mitosis and meiosis. *Annu Rev Genet* 35:673-745.
- Nasmyth K. (2002) Segregating sister genomes: the molecular biology of chromosome separation. *Science* 297:559-565.

- Nasmyth K, Haering CH. (2009) Cohesin: Its roles and mechanisms. *Annu Rev Genet* 43:525-558.
- Neale MJ, Pan J, Keeney S. (2005) Endonucleolytic processing of covalent protein-linked DNA double-strand breaks. *Nature* 436:1053-1057.
- Nel PM. (1973) Modifications of crossing over in maize by extraneous chromosomal elements. *Theor Appl Genet* 43:196-202.
- Nel PM. (1979) Effects of the asynaptic factor on recombination in maize. *J Hered* 70:401-406.
- Neyton S, Lespinasse F, Moens PB, Paul R, Gaudray P, Paquis-Flucklinger V, Santucci-Darmanin S. (2004) Association between MSH4 (MutS homologue 4) and the DNA strand-exchange RAD51 and DMC1 proteins during mammalian meiosis. *Mol Hum Reprod* 10:917-924.
- Niu H, Li X, Job E, Park C, Moazed D, Gygi SP, Hollingsworth NM. (2007) Mek1 Kinase Is Regulated To Suppress Double-Strand Break Repair between Sister Chromatids during Budding Yeast Meiosis. *Mol Cell Biol* 27:5456-5467.
- Niu H, Wan L, Baumgartner B, Schaefer D, Loidl J, Hollingsworth NM. (2005) Partner Choice during Meiosis Is Regulated by Hop1-promoted Dimerization of Mek1. *Mol Biol Cell* 16:5804-5818.
- Nonomura K-I, Nakano M, Eiguchi M, Suzuki T, Kurata N. (2006) PAIR2 is essential for homologous chromosome synapsis in rice meiosis I. *J Cell Sci* 119:217-225.
- Nonomura K-I, Nakano M, Murata K, Miyoshi K, Eiguchi M, Miyao A, Hirochika H, Kurata N. (2004) An insertional mutation in the rice *PAIR2* gene, the ortholog of *Arabidopsis ASY1*, results in a defect in homologous chromosome pairing during meiosis. *Molecular Genetics and Genomics* 271:121-129.
- Novak I, Wang H, Revenkova E, Jessberger R, Scherthan H, Höög C. (2008) Cohesin Smc1 β determines meiotic chromatin axis loop organization. *J Cell Biol* 180:83-90.
- Novak JE, Ross-Macdonald PB, Roeder GS. (2001) The budding yeast Msh4 protein functions in chromosome synapsis and regulation of crossover distribution. *Genetics* 158:1013-1025.
- Offenberg HH, Dietrich AJJ, Heyting C. (1991) Tissue distribution of two major components of synaptonemal complexes of the rat. *Chromosoma* 101:83-91.
- Offenberg HH, Schalk JAC, Meuwissen RL, van Aalderen M, Kester HA, Dietrich AJJ, Heyting C. (1998) SCP2: a major protein component of the axial elements of synaptonemal complexes of the rat. *Nucleic Acids Res* 26:2572-2579.
- Ogawa T, Yu X, Shinohara A, Egelman EH. (1993) Similarity of the yeast RAD51 filament to the bacterial RecA filament. *Science* 259:1896-1899.

- Oh SD, Lao JP, Hwang PYH, Taylor AF, Smith GR, Hunter N. (2007) BLM ortholog, Sgs1, prevents aberrant crossing-over by suppressing formation of multichromatid joint molecules. *Cell* 130:259-272.
- Ollinger R, Alsheimer M, Benavente R. (2005) Mammalian Protein SCP1 Forms Synaptonemal Complex-like Structures in the Absence of Meiotic Chromosomes. *Mol Biol Cell* 16:212-217.
- Onn I, Heidinger-Pauli JM, Guacci V, Ünal E, Koshland DE. (2008) Sister chromatid cohesion: A simple concept with a complex reality. *Annu Rev Cell Devel Biol* 24:105-129.
- Page J, de la Fuente R, Gomez R, Calvente A, Viera A, Parra MT, Santos JL, Berríos S, Fernandez-Donoso R, Suja JA, Rufas JS. (2006) Sex chromosomes, synapsis, and cohesins: a complex affair. *Chromosoma* 115:250-259.
- Page SL, Hawley RS. (2003) Chromosome choreography: The meiotic ballet. *Science* 301:785-789.
- Page SL, Hawley RS. (2004) The genetics and molecular biology of the synaptonemal complex. *Annu Rev Cell Dev Biol* 20:525-558.
- Page SL, Khetani RS, Lake CM, Nielsen RJ, Jeffress JK, Warren WD, Bickel SE, Hawley RS. (2008) *corona* is required for higher-order assembly of transverse filaments into full-length synaptonemal complex in *Drosophila* oocytes. *PLoS Genet* 4:e1000194. doi:10.1371/journal.pgen.1000194.
- Parisi S, McKay MJ, Molnar M, Thompson DA, van der Spek PJ, van Drunen-Schoenmaker E, Kanaar R, Lehmann E, Hoeijmakers JHJ, Kohli J. (1999) Rec8p, a meiotic recombination and sister chromatid cohesion phosphoprotein of the Rad21p family conserved from fission yeast to humans. *Mol Cell Biol* 19:3515-3528.
- Pasierbek P, Födermayr M, Jantsch V, Jantsch M, Schweizer D, Loidl J. (2003) The *Caenorhabditis elegans* SCC-3 homologue is required for meiotic synapsis and for proper chromosome disjunction in mitosis and meiosis. *Exp Cell Res* 289:245-255.
- Pasierbek P, Jantsch M, Melcher M, Schleiffer A, Schweizer D, Loidl J. (2001) A *Caenorhabditis elegans* cohesion protein with functions in meiotic chromosome pairing and disjunction. *Genes Devel* 15:1349-1360.
- Passy SI, Yu X, Li Z, Radding CM, Masson JY, West SC, Egelman EH. (1999) Human Dmc1 protein binds DNA as an octameric ring. *Proceedings of the National Academy of Sciences of the United States of America* 96:10684-10688.
- Pawlowski WP, Cande WZ. (2005) Coordinating the events of the meiotic prophase. *Trends in Cell Biology* 15:674-681.

- Pawlowski WP, Golubovskaya IN, Cande WZ. (2003) Altered nuclear distribution of recombination protein RAD51 in maize mutants suggests the involvement of RAD51 in meiotic homology recognition. *Plant Cell* 15:1807-1816.
- Pawlowski WP, Golubovskaya IN, Timofejeva L, Meeley RB, Sheridan WF, Cande WZ. (2004) Coordination of meiotic recombination, pairing, and synapsis by PHS1. *Science* 303:89-92.
- Pelttari J, Hoja M-R, Yuan L, Liu J-G, Brundell E, Moens P, Santucci-Darmanin S, Jessberger R, Barbero JL, Heyting C, Höög C. (2001) A meiotic chromosomal core consisting of cohesin complex proteins recruits DNA recombination proteins and promotes synapsis in the absence of an axial element in mammalian meiotic cells. *Mol Cell Biol* 21:5667-5677.
- Peoples TL, Dean E, Gonzalez O, Lambourne L, Burgess SM. (2002) Close, stable homolog juxtaposition during meiosis in budding yeast is dependent on meiotic recombination, occurs independently of synapsis, and is distinct from DSB-independent pairing contacts. *Genes Dev* 16:1682-1695.
- Peoples-Holst TL, Burgess SM. (2005) Multiple branches of the meiotic recombination pathway contribute independently to homolog pairing and stable juxtaposition during meiosis in budding yeast. *Genes Dev* 19:863-874.
- Peters J-M, Tedeschi A, Schmitz J. (2008) The cohesin complex and its roles in chromosome biology. *Genes Dev* 22:3089-3114.
- Peterson DG, Price HJ, Johnston JS, Stack SM. (1996) DNA content of heterochromatin and euchromatin in tomato (*Lycopersicon esculentum*) pachytene chromosomes. *Genome* 39:77-82.
- Petronczki M, Siomos MF, Nasmyth K. (2003) Un ménage à Quatre: the molecular biology of chromosome segregation in meiosis. *Cell* 112:423-440.
- Pezzi N, Prieto I, Kremer L, del Mazo J, Valero C, del Mazo J, Martínez-A. C, Barbero JL. (2000) *STAG3*, a novel gene encoding a protein involved in meiotic chromosome pairing and location of *STAG3*-related genes flanking the Williams-Beuren syndrome deletion. *FASEB Journal* 14:581-592.
- Phillips D, Mikhailova EI, Timofejeva L, Mitchell JL, Osina O, Sosnikhina SP, Jones RN, Jenkins G. (2008) Dissecting Meiosis of Rye using Translational Proteomics. *Ann Bot* 101:873-880.
- Pigozzi MI, Solari AJ. (2003) Differential immunolocalization of a putative Rec8p in meiotic autosomes and sex chromosomes of triatomine bugs. *Chromosoma* 112:38-47.
- Pittman DL, Cobb J, Schimenti KJ, Wilson LA, Cooper DM, Brignull E, Handel MA, Schimenti JC. (1998) Meiotic prophase arrest with failure of chromosome synapsis in mice deficient for *Dmcl*, a germline-specific RecA homolog. *Mol Cell* 1:697-705.

- Plug AW, Peters AHFM, Keegan KS, Hoekstra MF, de Boer P, Ashley T. (1998) Changes in protein composition of meiotic nodules during mammalian meiosis. *J Cell Sci* 111:413-423.
- Prieto I, Pezzi N, Buesa JM, Kremer L, Barthelemy I, Carreiro C, Roncal F, Martínez A, Gómez L, Fernández R, Martínez-A. C, Barbero JL. (2002) STAG2 and Rad21 mammalian mitotic cohesins are implicated in meiosis. *EMBO Rep* 3:543-550.
- Prieto I, Suja JA, Pezzi N, Kremer L, Martinez-A C, Rufas JS, Barbero JL. (2001) Mammalian STAG3 is a cohesin specific to sister chromatid arms in meiosis I. *Nature Cell Biology* 3:761-766.
- Puizina J, Siroky J, Mokros P, Schweizer D, Riha K. (2004) Mre11 deficiency in Arabidopsis is associated with chromosomal instability in somatic cells and Spo11-dependent genome fragmentation during meiosis. *Plant Cell* 16:1968-1978.
- Revenkova E, Eijpe M, Heyting C, Gross B, Jessberger R. (2001) Novel meiosis-specific isoform of mammalian SMC1. *Mol Cell Biol* 21:6984-6998.
- Revenkova E, Jessberger R. (2006) Shaping meiotic prophase chromosomes: cohesins and synaptonemal complex proteins. *Chromosoma* 115:235-240.
- Reyes-Valdés MH, Ji Y, Crane CF, Taylor JF, Islam-Faridi MN, Price HJ, Stelly DM. (1996) ISH-facilitated analysis of meiotic bivalent pairing. *Genome* 39:784-792.
- Rhoades, MM. (1947) Crossover chromosomes in unreduced gametes of asynaptic maize. *Genetics* 32:101. Abstracts of papers presented at the 1946 meeting of the Genetics Society of America.
- Rhoades MM, Dempsey E. (1949) (none). *MNL* 23:56-57.
- Rockmill B, Roeder GS. (1988) *RED1*: A yeast gene required for the segregation of chromosomes during the reductional division of meiosis. *Proc Natl Acad Sci USA* 85:6057-6061.
- Rockmill B, Roeder GS. (1990) Meiosis in asynaptic yeast. *Genetics* 126:563-574.
- Rockmill B, Roeder GS. (1991) A meiosis-specific protein kinase homolog required for chromosome synapsis and recombination. *Genes Devel* 5:2392-2404.
- Roeder GS. (1997) Meiotic chromosomes: it takes two to tango. *Genes Devel* 11:2600-2621.
- Roig I, Dowdle JA, Toth A, de Rooij DG, Jasin M, Keeney S. (2010) Mouse TRIP13/PCH2 is required for recombination and normal higher-order chromosome structure during meiosis. *PLoS Genet* 6:e1001062. doi:10.1371/journal.pgen.1001062.

- Romanienko PJ, Camerini-Otero RD. (2000) The mouse *spo11* gene is required for meiotic chromosome synapsis. *Mol Cell* 6:975-987.
- Ronceret A, Doutriaux M-P, Golubovskaya I, Pawlowski WP. (2009) PHS1 regulates meiotic recombination and homologous chromosome pairing by controlling the transport of RAD50 to the nucleus. *Proc Natl Acad Sci USA* 106:20121-20126.
- Ross KJ, Fransz PF, Jones GH. (1996) A light microscopic atlas of meiosis in *Arabidopsis thaliana*. *Chrom Res* 4:507-516.
- Ross-Macdonald P, Roeder GS. (1994) Mutation of a meiosis-specific MutS homolog decreases crossing over but not mismatch correction. *Cell* 79:1069-1080.
- San-Segundo PA, Roeder GS. (1999) Pch2 links chromatin silencing to meiotic checkpoint control. *Cell* 97:313-324.
- Sanchez-Moran E, Santos JL, Jones GH, Franklin FCH. (2007) ASY1 mediates AtDMC1-dependent interhomolog recombination during meiosis in *Arabidopsis*. *Genes Devel* 21:2220-2233.
- Santos JL, Jimenez MM. (1994) Meiosis in haploid rye: extensive synapsis and low chiasma frequency. *Heredity* 73:580-588.
- Santucci-Darmanin S, Walpita D, Lespinasse F, Desnuelle C, Ashley T, Paquis-Flucklinger V. (2000) MSH4 acts in conjunction with MLH1 during mammalian meiosis. *FASEB Journal* 14:1539-1547.
- Schalk JAC, Dietrich AJJ, Vink ACG, Offenberger HH, van Aalderen M, Heyting C. (1999) Localization of SCP2 and SCP3 protein molecules within synaptonemal complexes of the rat. *Chromosoma* 107:540-548.
- Schermelleh L, Carlton PM, Haase S, Shao L, Winoto L, Kner P, Burke B, Cardoso MC, Agard DA, Gustafsson MGL, Leonhardt H, Sedat JW. (2008) Subdiffraction multicolor imaging of the nuclear periphery with 3D structured illumination microscopy. *Science* 320:1332-1336.
- Scherthan H, Schönborn I. (2001) Asynchronous chromosome pairing in male meiosis of the rat (*Rattus norvegicus*). *Chromosome Res* 9:273-282.
- Scherthan H, Wang H, Adelfalk C, White EJ, Cowan C, Cande WZ, Kaback DB. (2008) Chromosome mobility during meiotic prophase in *Saccharomyces cerevisiae*. *PNAS USA* 104:16934-16939.
- Scherthan H, Weich S, Schwegler H, Heyting C, Harle M, Cremer T. (1996) Centromere and telomere movements during early meiotic prophase of mouse and man are associated with the onset of chromosome pairing. *J Cell Biol* 134:1109-1125.

- Schleiffer A, Kaitna S, Maurer-Stroh S, Glotzer M, Nasmyth K, Eisenhaber F. (2003) Kleisins: A superfamily of bacterial and eukaryotic SMC protein partners. *Mol Cell* 11:571-575.
- Schmekel K, Daneholt B. (1995) The central region of the synaptonemal complex revealed in three dimensions. *Trends in Cell Biology* 5:239-242.
- Schmekel K, Meuwissen RL, Dietrich AJJ, Vink ACG, van Marle J, van Veen H, Heyting C. (1996) Organization of SCP1 protein molecules within synaptonemal complexes of the rat. *Exp Cell Res* 226:20-30.
- Schubert V. (2009) SMC proteins and their multiple functions in higher plants. *Cytogenet Genome Res* 124:202-214.
- Schwacha A, Kleckner N. (1997) Interhomolog bias during meiotic recombination: Meiotic functions promote a highly differentiated interhomolog-only pathway. *Cell* 90:1123-1135.
- Severson AF, Ling L, van Zuylen V, Meyer BJ. (2009) The axial element protein HTP-3 promotes cohesin loading and meiotic axis assembly in *C. elegans* to implement the meiotic program of chromosome segregation. *Genes & Development* 23:1763-1778.
- Sherman JD, Herickhoff LA, Stack SM. (1992) Silver staining two types of meiotic nodules. *Genome* 35:907-915.
- Sherman JD, Stack SM. (1992) Two-dimensional spreads of synaptonemal complexes from solanaceous plants. V. Tomato (*Lycopersicon esculentum*) karyotype and idiogram. *Genome* 35:354-359.
- Sherman JD, Stack SM. (1995) Two-dimensional spreads of synaptonemal complexes from solanaceous plants. VI. High-resolution recombination nodule map for tomato (*Lycopersicon esculentum*). *Genetics* 141:683-708.
- Shinohara A, Ogawa H, Ogawa T. (1992) Rad51 protein involved in repair and recombination in *S. cerevisiae* is a RecA-like protein. *Cell* 69:457-470.
- Shinohara A, Shinohara M. (2004) Roles of RecA homologues Rad51 and Dmc1 during meiotic recombination. *Cytogenet Genome Res* 107:201-207.
- Shinohara M, Oh SD, Hunter N, Shinohara A. (2008) Crossover assurance and crossover interference are distinctly regulated by the ZMM proteins during yeast meiosis. *Nature Genet* 40:399-209.
- Shinohara M, Sakai K, Shinohara A, Bishop DK. (2003) Crossover interference in *Saccharomyces cerevisiae* requires a *TID1/RDH54*- and *DMC1*-dependent pathway. *Genetics* 163:1273-1286.
- Skibbens RV. (2009) Establishment of sister chromatid cohesion. *Curr Biol* 19:R1126-R1132.

- Smith A, Benavente R. (1992) Identification of a structural protein component of rat synaptonemal complexes. *Exp Cell Res* 198:291-297.
- Smith AV, Roeder GS. (1997) The yeast Red1 protein localizes to the cores of meiotic chromosomes. *J Cell Biol* 136:957-967.
- Smolikov S, Eizinger A, Schild-Prufert K, Hurlburt A, McDonald K, Engebrecht J, Villeneuve AM, Colaiácovo MP. (2007) SYP-3 restricts synaptonemal complex assembly to bridge paired chromosome axes during meiosis in *Caenorhabditis elegans*. *Genetics* 176:2015-2025.
- Soost RK. (1951) Comparative cytology and genetics of asynaptic mutants in *Lycopersicon esculentum* Mill. *Genetics* 36:410-434.
- Sosnikhina SP, Fedotova YS, Smirnov VG, Mikhailova EI, Kolomiets OL, Bogdanov YS. (1992) Meiotic mutants of rye *Secale cereale* L. I. Synaptic mutant *sy-1*. *Theor Appl Genet* 84:979-985.
- Sosnikhina SP, Kirillova GA, Mikhailova EI, Smirnov VG, Fedotova YS, Bogdanov YS. (1999) Genetic control of synapsis in rye *Secale cereale* L.: the *sy9* asynaptic gene. *Russian J Genet* 34:1278-1285.
- Spooner DM, Peralta IE, Knapp S. (2005) Comparison of AFLPs with other markers for phylogenetic inference in wild tomatoes [*Solanum* L. section *Lycopersicon* (Mill.) Wettst.]. *Taxon* 54:43-61.
- Stacey NJ, Kuromori T, Azumi Y, Roberts G, Breuer C, Wada T, Maxwell A, Roberts K, Sugimoto-Shirasu K. (2006) Arabidopsis SPO11-2 functions with SPO11-1 in meiotic recombination. *Plant J* 48:206-216.
- Stack S, Anderson LK. (1986a) Two-dimensional spreads of synaptonemal complexes from solanaceous plants. III. Recombination nodules and crossing over in *Lycopersicon esculentum* (tomato). *Chromosoma* 94:253-258.
- Stack S, Roelofs D. (1996) Localized chiasmata and meiotic nodules in the tetraploid onion *Allium porrum*. *Genome* 39:770-783.
- Stack SM, Anderson LK. (1986b) Two-dimensional spreads of synaptonemal complexes from solanaceous plants. II. Synapsis in *Lycopersicon esculentum*. *Am J Bot* 73:264-281.
- Stack SM, Anderson LK. (2002) Crossing over as assessed by late recombination nodules is related to the pattern of synapsis and distribution of early recombination nodules in maize. *Chromosome Res* 10:329-345.
- Stack SM, Anderson LK. (2009) Electron microscopic immunogold localization of recombination-related proteins in spreads of synaptonemal complexes from tomato microsporocytes, Keeney S (ed): *Meiosis Volume 2 Cytological Methods*, pp 147-169 (Humana Press, Inc., Totowa, NJ).

- Stack SM, Royer SM, Shearer LA, Chang S-B, Giovannoni JJ, Westfall DH, White RA, Anderson LK. (2009) Role of fluorescence in situ hybridization in sequencing the tomato genome. *Cytogenet Genome Res* 124:339-350.
- Stack SM, Sherman JD, Anderson LK, Herickhoff LS. (1993) Meiotic nodules in vascular plants, Sumner AT, Chandley AC (eds): *Chromosomes Today*, pp 301-311 (Chapman & Hall, London).
- Stahl FW, Foss HM, Young LS, Borts RH, Abdullah MFF, Copenhaver GP. (2004) Does crossover interference count in *Saccharomyces cerevisiae*? *Genetics* 168:35-48.
- Suja JA, Barbero JL. (2009) Cohesin complexes and sister chromatid cohesion in mammalian meiosis, Benavente R, Volff J-N (eds): *Meiosis*, pp 94-116 (Karger, Basel).
- Sumara I, Vorlaufer E, Gieffers C, Peters BH, Peters J-M. (2000) Characterization of vertebrate cohesin complexes and their regulation in prophase. *J Cell Biol* 151:749-761.
- Sung P, Trujillo KM, Komen SV. (2000) Recombination factors of *Saccharomyces cerevisiae*. *Mutation Research* 451:257-275.
- Surcel A, Koshland D, Ma H, Simpson RT. (2008) Cohesin interaction with centromeric minichromosomes shows a multi-complex rod-shaped structure. *PLoS One* 3:e2453.
- Svetlanov A, Cohen PE. (2004) Mismatch repair proteins, meiosis, and mice: understanding the complexities of mammalian meiosis. *Exp Cell Res* 296:71-79.
- Sym M, Roeder GS. (1996) Zip1-induced changes in synaptonemal complex structure and polycomplex assembly. *J Cell Biol* 128:455-466.
- Tanksley SD, McCouch SR. (1997) Seed banks and molecular maps: Unlocking genetic potential from the wild. *Science* 277:1063-1066.
- Tarsounas M, Morita T, Pearlman RE, Moens PB. (1999a) RAD51 and DMC1 form mixed complexes associated with mouse meiotic chromosome cores and synaptonemal complexes. *J Cell Biol* 147:207-219.
- Tarsounas M, Pearlman RE, Gasser PJ, Park MS, Moens PB. (1997) Protein-protein interactions in the synaptonemal complex. *Mol Biol Cell* 8:1405-1414.
- Tarsounas M, Pearlman RE, Moens PB. (1999b) Meiotic activation of rat pachytene spermatocytes with okadaic acid: the behaviour of synaptonemal complex components SYN1/SCP1 and COR1/SCP3. *J Cell Sci* 112:423-434.
- Terasawa M, Shinohara A, Hotta Y, Ogawa H, Ogawa T. (1995) Localization of RecA-like recombination proteins on chromosomes of the lily at various stages. *Genes Devel* 9:925-934.

- The Arabidopsis Genome Initiative. (2000) Analysis of the genome sequence of the flowering plant *Arabidopsis thaliana*. *Nature* 408:796-815.
- Trelles-Sticken E, Adelfalk C, Loidl J, Scherthan H. (2005) Meiotic telomere clustering requires actin for its formation and cohesin for its resolution. *The Journal of Cell Biology* 170:213-223.
- Trelles-Stricken E, Dresser M, Scherthan H. (2000) Meiotic telomere protein Ndj1p is required for meiosis-specific telomere distribution, bouquet formation and efficient homologue pairing. *J Cell Biol* 151:95-106.
- Tsai CJ, Mets DG, Albrecht MR, Nix P, Chan A, Meyer BJ. (2008) Meiotic crossover number and distribution are regulated by a dosage compensation protein that resembles a condensin subunit. *Genes Devel* 22:194-211.
- Tung K-S, Roeder GS. (1998) Meiotic chromosome morphology and behavior in *zip1* mutants of *Saccharomyces cerevisiae*. *Genetics* 149:817-832.
- Uhlmann F. (2009) A matter of choice: the establishment of sister chromatid cohesion. *EMBO Rep* 10:1095-1102.
- Usui T, Ohta T, Oshiumi H, Tomizawa J, Ogawa H, Ogawa T. (1998) Complex formation and functional versatility of Mre11 of budding yeast in recombination. *Cell* 95:705-716.
- Valdeolmillos AM, Viera A, Page J, Prieto I, Santos JL, Parra MT, Heck MMS, Martinez-A C, Barbero JL, Suja JA, Rufas JS. (2007) Sequential loading of cohesin subunits during the first meiotic prophase of grasshoppers. *PLoS Genetics* 3:e28-
doi:10.1371/journal.pgen.0030028.
- van Heemst D, Heyting C. (2000) Sister chromatid cohesion and recombination in meiosis. *Chromosoma* 109:10-26.
- Villeneuve AM, Hillers KJ. (2001) Whence meiosis. *Cell* 106:647-650.
- Waizenegger IC, Hauf S, Meinke A, Peters J-M. (2000) Two distinct pathways remove mammalian cohesin from chromosome arms in prophase and from centromeres in anaphase. *Cell* 103:410.
- Wang C-JR, Carlton PM, Golubovskaya IN, Cande WZ. (2009) Interlock formation and coiling of meiotic chromosome axes during synapsis. *Genetics* 183:905-915.
- Wang M, Wang K, Tang D, Wei C, Li M, Shen Y, Chi Z, Gu M, Cheng Z. (2010) The central element protein ZEP1 of the synaptonemal complex regulates the number of crossovers during meiosis in rice. *Plant Cell*.
- Wang TF, Kleckner N, Hunter N. (1999) Functional specificity of MutL homologs in yeast: Evidence for three Mlh1-based heterocomplexes with distinct roles during meiosis in recombination and mismatch correction. *Proc Natl Acad Sci USA* 96:13914-13919.

- Watanabe Y. (2005) Sister chromatid cohesion along arms and at centromeres. *Trends Genet* 21:405-412.
- Watanabe Y, Nurse P. (1999) Cohesin Rec8 is required for reductional chromosome segregation at meiosis. *Nature* 400:461-464.
- Waterworth WM, Altun C, Armstrong SJ, Roberts N, Dean PJ, Young K, Weil CF, Bray CM, West CE. (2007) NBS1 is involved in DNA repair and plays a synergistic role with ATM in mediating meiotic homologous recombination in plants. *Plant J* 52:41-52.
- West SC. (1992) Enzymes and molecular mechanisms of genetic recombination. *Ann Rev Biochem* 61:603-640.
- Wiltzius JJ, Hohl M, Fleming JC, Petrini JH. (2005) The Rad50 hook domain is a critical determinant of Mre11 complex functions. *Nat Struct Mol Biol* 12:403-407.
- Winkel K, Alsheimer M, Öllinger R, Benavente R. (2009) Proteins SYCP2 provides a link between transverse filaments and lateral elements of mammalian synaptonemal complexes. *Chromosoma* 118:259-267.
- Wojtasz L, Daniel K, Roig I, Bolcun-Filas E, Xu H, Boonsanay V, Eckmann CR, Cooke HJ, Jasin M, Keeney S, McKay MJ, Toth A. (2009) Mouse HORMAD1 and HORMAD2, two conserved meiotic chromosomal proteins, are depleted from synapsed chromosome axes with the help of TRIP13 AAA-ATPase. *PLoS Genet* 5:e1000702. doi:10.1371/journal.pgen.1000702.
- Wood AJ, Severson AF, Meyer BJ. (2010) Condensin and cohesin complexity: the expanding repertoire of functions. *Nature Reviews Cancer* 11:391-404.
- Wu H-Y, Burgess SM. (2006) Ndj1, a Telomere-Associated Protein, Promotes Meiotic Recombination in Budding Yeast. *Mol Cell Biol* 26:3683-3694.
- Xu H, Beasley MD, Warren WD, van der Horst GTJ, McKay MJ. (2005) Absence of mouse REC8 cohesin promotes synapsis of sister chromatids in meiosis. *Devel Cell* 8:949-961.
- Yang F, De Le Fuente R, Leu NA, Baumann C, McLaughlin KJ, Wang PJ. (2006) Mouse SYCP2 is required for synaptonemal complex assembly and chromosomal synapsis during male meiosis. *J Cell Biol* 173:497-507.
- Yoshida K, Kondoh G, Matsuda Y, Habu T, Nishimune Y, Morita T. (1998) The mouse *RecA-A* like gene *Dmc1* is required for homologous chromosome synapsis during meiosis. *Mol Cell* 1:707-718.
- Yuan L, Liu J, Zhao J, Brundell E, Daneholt B, Höög C. (2000) The murine *SCP3* gene is required for synaptonemal complex assembly, chromosome synapsis, and male fertility. *Mol Cell* 5:73-83.

- Yuan L, Liu J-G, Hoja M-R, Wilbertz J, Nordqvist K, Höög C. (2002) Female germ cell aneuploidy and embryo death in mice lacking the meiosis-specific protein SCP3. *Science* 296:1115-1118.
- Yuan L, Pelttari J, Brundell E, Björkroth B, Zhao J, Liu JG, Brismar H, Daneholt B, Höög C. (1998) The Synaptonemal complex protein SCP3 can form multistranded, cross-striated fibers in vivo. *J Cell Biol* 142:331-339.
- Zanders S, Alani E. (2009) The *pch2Δ* mutation in baker's yeast alters meiotic crossover levels and confers a defect in crossover interference. *PLoS Genetics* 5:e1000571-
doi:10.1371/journal.pgen.1000571.
- Zetka MC, Kawasaki I, Strome S, Muller F. (1999) Synapsis and chiasma formation in *Caenorhabditis elegans* require HIM-3, a meiotic chromosome core component that functions in chromosome segregation. *Genes Devel* 13:2258-2270.
- Zhang L, Tao J, Wang S, Chong K, Wang T. (2006) The rice OsRad21-4, an orthologue of yeast Rec8 proteins, is required for efficient meiosis. *Plant Mol Biol* 60:533-554.
- Zickler D, Kleckner N. (1998) The leptotene-zygotene transition of meiosis. *Ann Rev Genet* 32:619-697.
- Zickler D, Kleckner N. (1999) Meiotic chromosomes: Integrating structure and function. *Ann Rev Genet* 33:603-754.
- Zink D. (2006) The temporal program of DNA replication: new insights into old questions. *Chromosoma* 115:273-287.